NASA TR R-118

NATIONAL AERONAUTICS AND SPACE ADMINISTRATION

TECHNICAL REPORT
R-118

BOUNDARY-LAYER SIMILAR SOLUTIONS AND CORRELATION EQUATIONS FOR LAMINAR HEAT-TRANSFER DISTRIBUTION IN EQUILIBRIUM AIR AT VELOCITIES UP TO 41,100 FEET PER SECOND

By NATHANIEL B. COHEN

1961

For sale by the Superintendent of Documents, U.S. Government Printing Office, Washington, D.C., 20402. Yearly subscription, $15: foreign, $19 single copy price varies according to size. --------- Price 55 cents

TECHNICAL REPORT R-118

BOUNDARY-LAYER SIMILAR SOLUTIONS AND CORRELATION EQUATIONS FOR LAMINAR HEAT-TRANSFER DISTRIBUTION IN EQUILIBRIUM AIR AT VELOCITIES UP TO 41,100 FEET PER SECOND

By NATHANIEL B. COHEN

Langley Research Center
Langley Air Force Base, Va.

CONTENTS

TECHNICAL REPORT R–118

BOUNDARY-LAYER SIMILAR SOLUTIONS AND CORRELATION EQUATIONS FOR LAMINAR HEAT-TRANSFER DISTRIBUTION IN EQUILIBRIUM AIR AT VELOCITIES UP TO 41,100 FEET PER SECOND

By Nathaniel B. Cohen

SUMMARY

Locally similar solutions of the laminar boundary-layer equations are obtained for air at chemical equilibrium for static enthalpies up to $1{,}000\overline{R}T_{ref}$ (corresponding to the free-stream stagnation enthalpy for atmospheric flight at velocities up to 41,100 feet per second). Correlation of the transport property estimates of NASA TR R-50 are employed in the solutions.

Exact solutions for flat-plate flow, axisymmetric stagnation flow, and stagnation flow for a yawed infinite cylinder are obtained and correlating formulas for the appropriate heat-transfer functions are developed. A correlation formula for the heat-transfer distribution function for an arbitrary favorable pressure gradient on a body of revolution or yawed infinite cylinder is determined for application to various local similarity methods. Pertinent equations are collected in a single section for convenience. Extension to three-dimensional flows with small cross flow is briefly described.

INTRODUCTION

A knowledge of the expected aerodynamic heat-transfer distribution on a body in high-speed flight is essential to proper design of thermal-protection systems. In reference 1 a method for computing the laminar heat-transfer distribution to yawed infinite cylinders of arbitrary cross section and to bodies of revolution at zero angle of attack was presented. This method employed the concept of satisfying the general integrated energy equation with locally similar boundary-layer profiles. Although the method of reference 1 was derived for air in dissociation equilibrium, the similar profiles used therein were obtained from boundary-layer solutions for a perfect gas with viscosity proportional to temperature and with unit Prandtl number. Such an approximation was assumed to be reasonable for determining the ratio of local to reference heat-transfer rates on blunt bodies of practical concern, although insufficient for the calculation of the reference value itself. Experimental heat-transfer distributions obtained at Mach numbers from 3 to 6 on an unyawed circular cylinder and on a flat-faced body of revolution were used in reference 1 to show that the theory gave satisfactory predictions for the perfect-gas case even for large favorable pressure gradients. It was also shown that the simple local similarity technique of reference 2 (which itself is a more approximate form of the integral method of ref. 1) was sufficiently accurate for most design purposes.

Because the use of unit Prandtl number in the similar solutions of reference 1 restricts that analysis to the computation of heat-transfer distribution, a need exists for methods to determine the effect of gas properties upon the heat-transfer distribution and to establish accurately the reference heat-transfer rates for real air (e.g., the stagnation heat-transfer rate). The purpose of the present analysis is to provide a sufficiently large number of similar solutions of the laminar boundary-layer equations for air in chemical equilibrium in order to fulfill this requirement. A brief survey of some of the present results is included in reference 3. The present solutions are computed by use of the transport-property approximations of reference 4, as correlated in

reference 5, and these results are valid for flight up to a velocity of about 29,000 feet per second with zero yaw and to higher velocities with a sufficient degree of yaw. Additional transport property correlations are deduced from reference 4 and used in obtaining a representative group of similar solutions valid for flight at speeds up to 41,100 feet per second with zero yaw. Correlation formulas for the heat-transfer parameters are obtained and their application to the integral and simple local similarity methods of reference 1 is shown.

The results for the body of revolution have application to the more general problem of computing heat-transfer distribution along the inviscid surface streamlines on a three-dimensional body provided that the boundary-layer cross flow is small (refs. 6, 7, and 8). Application of the present solutions to these problems is briefly described.

SYMBOLS

C mass concentration

c_f skin-friction coefficient, $\dfrac{\tau_w}{\frac{1}{2}\rho_e u_e^2}$

$c_{f,x,w}$ skin-friction coefficient, $\dfrac{\tau_w}{\frac{1}{2}\rho_w u_e^2}$

$c_{f,y,w}$ skin-friction coefficient, $\dfrac{\tau_w}{\frac{1}{2}\rho_w u_e v_e}$

c_p specific heat at constant pressure

D binary diffusion coefficient

E_{tr} transformed mixed momentum thickness, $\int_0^\infty \frac{\partial f}{\partial \eta}(1-g)d\eta$

F diffusion function, eq. (6)

F_1, F_2, F_3 three different approximations to the diffusion function for dissociated air

f similar stream function, eq. (12)

G_{tr} transformed thickness function, $\int_0^\infty (1-g^2)d\eta$

G_1 high-enthalpy correlation function for heat transfer, eqs. (75) and (78)

g spanwise velocity ratio, v/v_e

H total enthalpy, $h+\dfrac{u^2+v^2}{2}$

h static enthalpy

h_E reference enthalpy, $250\overline{R}T_{ref}=2.119\times10^8$ ft²/sec²=8,465 Btu/lb

h^* reference enthalpy, eq. (35c)

$\overline{h}$ similarity heat-transfer coefficient, eq. (64)

j exponent ($j=0$ for yawed infinite cylinder; $j=1$ for body of revolution)

k thermal conductivity

L arbitrary reference length

M Mach number

m exponent, equation (82)

N_{Lc} Lewis number, $\dfrac{\rho c_{p,f} D}{k_f}$

$N_{Nu,w}$ Nusselt number, $\dfrac{-q_w c_{p,w} x}{k_w(h_{aw}-h_w)}$

N_{Pr} Prandtl number, $\mu c_p/k$

N_{Re} Reynolds number, $\rho_e u_e x/\mu_e$

$N_{Re,w}$ Reynolds number, $\rho_w u_e x/\mu_w$

N_{St} Stanton number, $\dfrac{-q_w}{\rho_e u_e(h_{aw}-h_w)}$

P, Q, R, N parameters in equation (52)

P_1, Q_1, R_1, N_1 parameters from reference 1 in equation (66)

p pressure

p_{ref} reference pressure, 1 atmosphere =2,117 lb/sq ft abs

q heat flux normal to surface at a point in the boundary layer

$\overline{R}$ gas constant per unit mass of undissociated air, 1,724 ft²/sec²-°R =0.0689 Btu/lb-°R

r radius of body of revolution

$\overline{r}$ enthalpy recovery factor

r_N nose radius

T absolute temperature

T_{ref} reference temperature, 273.16° K =491.69° R

t dimensionless static enthalpy, h/H_e

u, v, w velocity components in x, y, and z directions, respectively

V_∞ free-stream velocity

x, y, z chordwise, spanwise, and normal boundary-layer coordinates in physical system

β pressure gradient parameter, eqs. (19) and (25)

Γ heat-transfer function, eq. (24)

γ ratio of specific heats

Δ^*_{tr} transformed displacement thickness, $\int_0^\infty \left(\frac{\rho_e}{\rho}-\frac{\partial f}{\partial \eta}\right)d\eta$

δ^*_{tr} transformed displacement thickness, $\int_0^\infty \left(1-\frac{\partial f}{\partial \eta}\right) d\eta$

ζ total enthalpy ratio, H/H_e

Θ_{tr} transformed convection thickness, $\int_0^\infty \frac{\partial f}{\partial \eta}\left(\frac{1-\zeta}{1-\zeta_w}\right) d\eta$

Θ^*_{tr} transformed enthalpy thickness, $\int_0^\infty \left(\frac{1-\zeta}{1-\zeta_w}\right) d\eta$

θ^*_{tr} transformed momentum thickness, $\int_0^\infty \frac{\partial f}{\partial \eta}\left(1-\frac{\partial f}{\partial \eta}\right) d\eta$

Λ yaw angle

μ viscosity coefficient

μ_o arbitrary reference viscosity coefficient

ξ, η similarity variables, eqs. (9) and (10)

$\bar{\xi}$ function of x or ξ

ρ mass density

τ shear stress

φ density viscosity product ratio, $\rho\mu/\rho_w\mu_w$

ψ stream function, eq. (11)

Subscripts:

A, M atoms, molecules, constituents of a binary mixture

aw adiabatic wall

E evaluated at reference enthalpy h_E and local pressure

e local value external to boundary layer

f, eff frozen, effective, for specific heat and transport properties

i ith species of gas mixture

s stagnation point or line

w local value at surface

x, y chordwise, spanwise

Superscripts:

$*$ evaluated at reference enthalpy h^*

$'$ differentiation with respect to η

RÉSUMÉ OF INTEGRAL METHOD OF REFERENCE 1

TRANSFORMATION OF BOUNDARY-LAYER EQUATIONS TO SIMILARITY VARIABLES

The Prandtl boundary-layer equations expressing the conservation of mass, momentum, and energy for the steady flow of an equilibrium reacting mixture of "air molecules" and "air atoms" on a body of revolution at zero angle of attack or on an infinite cylinder in yaw are (refs. 1 and 9):

$$\frac{\partial}{\partial x}(\rho u r^j)+\frac{\partial}{\partial z}(\rho w r^j)=0 \tag{1}$$

$$\rho u\frac{\partial u}{\partial x}+\rho w\frac{\partial u}{\partial z}=\rho_e u_e\frac{du_e}{dx}+\frac{\partial}{\partial z}\left(\mu\frac{\partial u}{\partial z}\right) \tag{2}$$

$$\rho u\frac{\partial v}{\partial x}+\rho w\frac{\partial v}{\partial z}=\frac{\partial}{\partial z}\left(\mu\frac{\partial v}{\partial z}\right) \qquad \left(\frac{\partial p}{\partial y}=0\right) \tag{3}$$

$$\frac{\partial p}{\partial z}=0 \tag{4}$$

$$\rho u\frac{\partial H}{\partial x}+\rho w\frac{\partial H}{\partial z}=\frac{\partial}{\partial z}\left[\frac{\mu}{N_{Pr,f}}(1+F)\frac{\partial H}{\partial z}+\frac{\mu}{N_{Pr,f}}(N_{Pr,f}-1-F)\left(u\frac{\partial u}{\partial z}+v\frac{\partial v}{\partial z}\right)\right] \tag{5}$$

where for the yawed infinite cylinder, $j=0$, $v=\text{Constant}=v_e$ outside the boundary layer, and $\partial v/\partial y=0$ within the boundary layer. For a body of revolution, $j=1$ and $v=0$. The coordinate systems are shown in figure 1. Because of the assumption of equilibrium dissociation, the continuity equations of the individual species, in this case air atoms and air molecules, need not be considered because the local species concentrations are functions only of the state of the gas. In equation (5), thermal diffusion has been neglected.

The function F is defined for the equilibrium binary mixture by

$$F(p,h)=(N_{Le}-1)(h_A-h_M)\left(\frac{\partial C_A}{\partial h}\right)_{p=Const.} \tag{6}$$

and is a function of the state of the gas, as are the following properties:

μ viscosity

$N_{Pr,f}$ frozen Prandtl number, $\frac{\mu c_{p,f}}{k_f}$

$c_{p,f}$ frozen specific heat at constant pressure, $\sum_i C_i c_{p,i}$

k_f frozen conductivity

The simulation of equilibrium dissociated air by

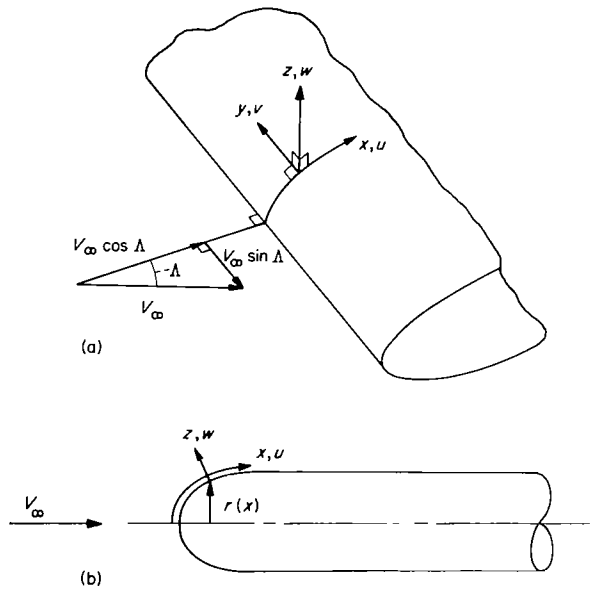

(a) Coordinates for the yawed infinite cylinder.
(b) Coordinates for the body of revolution.

FIGURE 1.—Boundary-layer coordinate systems.

a binary mixture of air atoms and molecules in chemical equilibrium is based upon the similar properties of oxygen and nitrogen atoms and oxygen and nitrogen molecules and the fact that ionization of the atoms is not important until dissociation of the molecules is complete. (See, for example, refs. 4 and 9.) As shown in reference 5, this binary mixture representation should be valid up to enthalpies of $500\bar{R}T_{ref}$, corresponding to the stagnation enthalpy for flight up to about 29,000 feet per second. All subsequent derivations and numerical results based upon the energy equation in the form of equation (5) are restricted to enthalpies below this limit. Higher enthalpies are considered in a subsequent section.

Boundary conditions for equations (1) through (5) are:

At $z=0$,

$$u=v=w=0 \tag{7a}$$

and, with heat transfer

$$H=H_w(x) \tag{7b}$$

or, for an insulated wall

$$\frac{\partial H}{\partial y}=0 \tag{7c}$$

As $z\to\infty$

$$\left.\begin{aligned} u&=u_e(x)\\ v&=v_e=\text{Constant}\\ H&=H_e=\text{Constant}\end{aligned}\right\} \tag{8}$$

Transformation of the boundary-layer equations is afforded by the definitions of the similarity coordinates (refs. 1, 2, and 9, for example)

$$\xi=\frac{1}{\mu_o^2}\int_0^x \rho_w\mu_w u_e\left(\frac{r}{L}\right)^{2j}dx=\xi(x) \tag{9}$$

$$\eta=\frac{u_e\left(\frac{r}{L}\right)^j}{\mu_o\sqrt{2(\xi-\bar{\xi})}}\int_0^z \rho dz=\eta(x,z) \tag{10}$$

the stream function (satisfying eq. (1))

$$\frac{\partial\psi}{\partial z}=\rho u\left(\frac{r}{L}\right)^j \tag{11a}$$

$$\frac{\partial\psi}{\partial x}=-\rho w\left(\frac{r}{L}\right)^j \tag{11b}$$

and the similarity-type dependent variables

$$f(\xi,\eta)=\frac{\psi}{\mu_o\sqrt{2(\xi-\bar{\xi})}} \tag{12}$$

$$g(\xi,\eta)=\frac{v}{v_e} \tag{13}$$

$$\zeta(\xi,\eta)=\frac{H}{H_e} \tag{14}$$

From equations (9) to (12), the chordwise velocity profile is

$$\frac{\partial f}{\partial\eta}=\frac{u}{u_e} \tag{15}$$

The function $\bar{\xi}=\bar{\xi}(x)$ is yet to be determined.

Transformation of equations (2), (3), and (5) to the similarity coordinate system yields

$$\begin{aligned}\frac{\partial}{\partial\eta}\left(\varphi\frac{\partial^2 f}{\partial\eta^2}\right)+\left(1-\frac{d\bar{\xi}}{d\xi}\right)f\frac{\partial^2 f}{\partial\eta^2}&\\ =\beta\left[\left(\frac{\partial f}{\partial\eta}\right)^2-\frac{\zeta}{t_s}+\left(\frac{1-t_s}{t_s}\right)g^2-\frac{t_e}{t_s}\left(\frac{\rho_e}{\rho}-\frac{t}{t_e}\right)\right]&\\ +2(\xi-\bar{\xi})\left(\frac{\partial f}{\partial\eta}\frac{\partial^2 f}{\partial\eta\partial\xi}-\frac{\partial f}{\partial\xi}\frac{\partial^2 f}{\partial\eta^2}\right)&\end{aligned} \tag{16}$$

$$\frac{\partial}{\partial\eta}\left(\varphi\frac{\partial g}{\partial\eta}\right)+\left(1-\frac{d\bar{\xi}}{d\xi}\right)f\frac{\partial g}{\partial\eta}=2(\xi-\bar{\xi})\left(\frac{\partial f}{\partial\eta}\frac{\partial g}{\partial\xi}-\frac{\partial f}{\partial\xi}\frac{\partial g}{\partial\eta}\right) \tag{17}$$

$$\frac{\partial}{\partial\eta}\left[\frac{\varphi}{N_{Pr,f}}(1+F)\frac{\partial\zeta}{\partial\eta}\right]+\left(1-\frac{d\bar{\xi}}{d\xi}\right)f\frac{\partial\zeta}{\partial\eta}$$
$$=\frac{\partial}{\partial\eta}\left\{\frac{\varphi}{N_{Pr,f}}(1-N_{Pr,f}+F)\left[(t_s-t_e)\frac{\partial}{\partial\eta}\left(\frac{\partial f}{\partial\eta}\right)^2+(1-t_s)\frac{\partial}{\partial\eta}(g^2)\right]\right\}$$
$$+2(\xi-\bar{\xi})\left(\frac{\partial f}{\partial\eta}\frac{\partial\zeta}{\partial\xi}-\frac{\partial f}{\partial\xi}\frac{\partial\zeta}{\partial\eta}\right) \tag{18}$$

where the pressure gradient parameter β is defined by

$$\beta=\frac{2(\xi-\bar{\xi})}{u_e}\frac{t_s}{t_e}\frac{du_e}{d\xi} \tag{19}$$

and the static enthalpy ratio t by

$$t=\frac{h}{H_e}=\zeta-(1-t_s)g^2-(t_s-t_e)\left(\frac{\partial f}{\partial\eta}\right)^2 \tag{20}$$

On the infinite cylinder in yaw, t_s is a constant given by

$$t_s=1-\frac{v_e^2}{2H_e}=1-\frac{V_\infty^2\sin^2\Lambda}{2H_e}$$

and is thus the static enthalpy ratio outside the boundary layer on the stagnation line ($u_e=0$). For the body of revolution at zero angle of attack, $t_s\equiv1$ and $g\equiv0$. The function φ is defined by

$$\varphi=\frac{\rho\mu}{\rho_w\mu_w}$$

Boundary conditions in the similarity coordinate system are, at $\eta=0$,

$$f(0,\xi)=\frac{\partial f}{\partial\eta}(0,\xi)=g(0,\xi)=0 \tag{21a}$$

and with heat transfer,

$$\zeta(0,\xi)=\zeta_w(\xi)=t_w(\xi) \tag{21b}$$

or for an insulated wall,

$$\frac{\partial\zeta}{\partial\eta}(0,\xi)=0 \tag{21c}$$

As $\eta\to\infty$,

$$\frac{\partial f}{\partial\eta}(\infty,\xi)=g(\infty,\xi)=\zeta(\infty,\xi)=1 \tag{22}$$

Equations (16) to (18) and the boundary conditions are general within the boundary-layer assumptions for the assumed flow geometry, and the only requirement is that the air be in dissociation equilibrium in order that the binary mixture approximations are applicable.

INTEGRAL METHOD FOR COMPUTING HEAT-TRANSFER DISTRIBUTION FROM REFERENCE 1

The partial differential equations in the similarity coordinates, equations (16) to (18), are in general difficult to solve. For exactly similar flow, all variation with ξ disappears and the resulting ordinary differential equations may be solved numerically. However, exactly similar flows are the exception rather than the rule; their occurrence is discussed, for example, in references 1, 10, and 11.

One method of attack for the more general nonsimilar flows is to integrate the equations of motion and energy across the boundary layer to obtain ordinary differential equations which may be solved after suitable approximations are made for the velocity and enthalpy profiles. In the method of reference 1, it is assumed that the profiles are those of the similar type, that is, profiles which are solutions of the ordinary differential equations that result from equations (16) to (18) when all derivatives with respect to ξ are set equal to zero. These solutions are applied at each x (or ξ) station in the nonsimilar flow by using the appropriate values of t_s and the local values of the parameters t_e, ζ_w, and β. Only one function $\bar{\xi}(\xi)$ is unknown, and thus only one of the three conservation laws may be utilized. In reference 1 it is assumed that the heat transfer is generally of most interest; thus, the integrated energy equation is satisfied in preference to the two integrated momentum equations.

The results of these assumptions for the heat-transfer distribution on blunt yawed cylinders or bodies of revolution are embodied in the following equation:

$$\frac{q_w}{q_{w,s}}=\sqrt{\frac{\frac{\rho_w\mu_w}{\beta t_e}\frac{du_e}{dx}}{\left(\frac{\rho_w\mu_w}{\beta t_e}\right)_s\left(\frac{du_e}{dx}\right)_s}}\Gamma \tag{23}$$

where

$$\Gamma=\frac{\frac{1+F_w}{N_{Pr,w}}\zeta'_w}{\left(\frac{1+F_w}{N_{Pr,w}}\zeta'_w\right)_s} \tag{24}$$

$$\beta=\frac{2t_s\left(\frac{du_e}{dx}\right)}{\rho_w\mu_w u_e^2 t_e\left(\frac{r}{L}\right)^{2j}}\Gamma^2\int_0^x\rho_w\mu_w u_e\left(\frac{r}{L}\right)^{2j}\Gamma^2dx \quad (25)$$

and where $\zeta_w'=\zeta_w'(t_s, t_e, \zeta_w, \beta)$ as determined from solutions of the locally similar boundary-layer equations. The complete integral method of reference 1 is represented by equations (23) to (25) and requires an iterative solution. The simple local similarity method of reference 1 results when Γ is set equal to unity in equation (25) only; this result is essentially the method of reference 2 and does not require iteration because β is then a function only of inviscid flow and wall conditions. With $\Gamma\equiv1$ in both equations (23) and (25), a method essentially equivalent to that of Lees (ref. 11) is obtained; this last method was proposed therein for blunt unyawed cylinders on bodies of revolution with highly cooled walls and is independent of the boundary-layer similar solutions.

LOCALLY SIMILAR SOLUTIONS FOR EQUILIBRIUM DISSOCIATED AIR

In the integral method for computing heat-transfer distribution just described, the dependence of the heat-transfer distribution function, $\zeta_w'/\zeta_{w,s}'$, upon the various parameters for the case of locally similar flows is required. In reference 1, unit Prandtl number solutions provided an approximation for this parameter. Evaluation of this parameter for real air in dissociation equilibrium is now described.

THE COMPUTATION PROGRAM

The equations governing locally similar profiles are, from equations (16) to (18) with $\frac{\partial}{\partial\xi}=0$

$$(\varphi f'')'+ff''=\beta\left[(f')^2-\frac{\zeta}{t_s}+\left(\frac{1-t_s}{t_s}\right)g^2-\frac{t_e}{t_s}\left(\frac{\rho_e}{\rho}-\frac{t}{t_e}\right)\right] \quad (26)$$

$$(\varphi g')'+fg'=0 \quad (27)$$

$$\left[\frac{\varphi}{N_{Pr,f}}(1+F)\zeta'\right]'+f\zeta'=\left\{\frac{\varphi}{N_{Pr,f}}(1-N_{Pr,f}+F)[(t_s-t_e)(f')^{2\prime}+(1-t_s)(g^2)']\right\}' \quad (28)$$

with the boundary conditions

$$f(0)=f'(0)=g(0)=0 \quad (29a)$$

and with heat transfer,

$$\zeta(0)=\zeta_w \quad (29b)$$

or for an insulated wall

$$\zeta'(0)=0 \quad (29c)$$

$$f'(\infty)=g(\infty)=\zeta(\infty)=1 \quad (30)$$

where β, t_s, t_e, and ζ_w are parameters evaluated locally. Solutions of equations (26) to (28) determine the functional dependence of ζ_w' upon the parameters as required by the equations for heat-transfer distribution (eqs. (23) to (25)).

Equations (26) to (28), subject to boundary conditions (29) and (30), were programed on the IBM type 704 electronic data processing machine and solved for wide ranges of the various parameters. Integration was carried out in much the same manner as described in appendix B of reference 12. The variable gas properties ρ_e/ρ, φ, $N_{Pr,f}$, and F, obtained from reference 5, were incorporated in the program as tabular functions of static enthalpy, and are described in the following section.

Thermodynamic and transport properties of equilibrium dissociated air.—From reference 5, equations governing ρ_e/ρ and φ at constant pressure are

$$\frac{\rho_e}{\rho}=\frac{\rho_E/\rho}{\rho_E/\rho_e}=\frac{1.0477\left(\frac{t}{t_E}\right)^{0.6123}-0.0477}{1.0477\left(\frac{t_e}{t_E}\right)^{0.6123}-0.0477} \quad (31a)$$

$$\varphi=\frac{\rho\mu}{\rho_w\mu_w}=\frac{\rho_E\mu_E/\rho_w\mu_w}{\rho_E\mu_E/\rho\mu}=\frac{1.0213\left(\frac{\zeta_w}{t_E}\right)^{0.3329}-0.0213}{1.0213\left(\frac{t}{t_E}\right)^{0.3329}-0.0213} \quad (31b)$$

where $t/t_E=h/h_E$ and where h_E is a reference enthalpy, $h_E=250\overline{K}T_{ref}$.

The frozen Prandtl number was obtained from table I of reference 5. Most of the cases were computed with $F=0$, which is appropriate for unit Lewis number. The effect of nonunit Lewis number was investigated for a few cases by using three different estimates for the diffusion function, F_1, F_2, and F_3, discussed in a subsequent section. Tables of $N_{Pr,f}$, F_1, F_2, and F_3 are given in table I.

These functions are assumed valid for the ranges

$$0.0152 \leqq \frac{h}{h_E} \leqq 2$$

$$10^{-4} \leqq p/p_{ref} \leqq 10$$

as in reference 5. Note that use of these gas properties introduces another parameter ($t_E = h_E/H_e$, representing the level of the total enthalpy outside the boundary layer) which must be specified in order to obtain locally similar solutions.

Limitations on parameters.—The primary limitation on the local enthalpy in the boundary layer is determined by the validity of the gas property correlations as

$$0.0152 \leqq \frac{h}{h_E} = \frac{t}{t_E} \leqq 2 \tag{32}$$

The lower limit represents the enthalpy at a temperature of 300° K; the upper limit is equal to the free-stream total enthalpy in atmospheric flight at a velocity of about 29,000 feet per second. Values of the yaw parameter, t_s, of 1, ⅓, 1/10, and 1/30 were chosen, and values of t_e were assumed to be within

$$0.2 \leqq \frac{t_e}{t_s} \leqq 1$$

The lower limit should include isentropic expansion from a stagnation line to free-stream pressure for most practical conditions.

Consistent with the limits in equation (32), values of the enthalpy-level parameter t_E were chosen corresponding to free-stream velocities up to 29,000 ft/sec ($t_E \geqq 0.5$) for zero yaw ($t_s = 1$). For finite yaw the stagnation-line enthalpy is less than the free-stream total enthalpy and values of the enthalpy-level parameter may be so chosen that the maximum velocity is $\frac{29{,}000}{\cos \Lambda}$ feet per second. A limit was arbitrarily set for these cases such that

$$H_e \leqq 3h_E \left(t_E \geqq \frac{1}{3},\ V_\infty \leqq 35{,}600 \text{ ft/sec} \right)$$

For heat-transfer cases the wall temperature was restricted to the range from 300° K to about 1,750° K, or more specifically

$$0.0152 \leqq \frac{h_w}{h_e} \leqq 0.1$$

for all enthalpy levels. For this wall enthalpy range, F_w was always zero and hence any nonunit Lewis number effects were secondary effects caused by boundary-layer profile distortions away from the wall. These effects were expected to be small. Insulated wall cases were computed only for certain conditions where the total enthalpy outside the boundary layer did not exceed $2h_E$ even for large yaw.

Values of β from zero to about 3.5 were used. Above this limit, solutions of equations (26) to (28) were not generally obtained because of numerical difficulties.

Solutions obtained.—Tables II, III, and IV are a compilation of the results of the program for equilibrium dissociated air. Table II lists all the cases and serves as a key to the solutions given in tables III and IV. The values of flight velocity shown in table II were computed by using a nominal free-stream static enthalpy of $3.8\overline{R}T_{ref} = 0.0152h_E$. Shown in tables III and IV are only selected results at a few pertinent values of β; solutions actually were obtained at up to 20 different values of β between 0 and 3.5. For the special case of $t_s = t_e$, $F = 0$, solutions of the outer limit equations for $\beta \to \infty$ (see appendix B of ref. 1) were obtained with the dissociated air properties to aid in obtaining heat-transfer correlation formulas; these are displayed in the appropriate locations in table III. Listed (for $F = 0$) are the values of f_w'', g_w', ζ_w' (or $\overline{r}$) and, for heat-transfer cases, the displacement thickness, $\Delta_{t'}^*$. Other pertinent thicknesses may be found from these values and equations (A9) to (A11) of the appendix. For nonunit Lewis number (table IV), only ζ_w' or $\overline{r}$ are shown.

The discussions that follow center primarily on results for the heat transfer, that is, ζ_w'. Discussions regarding recovery factor and skin-friction functions are limited to certain special cases.

EXACT SIMILAR FLOWS

For flow on an isothermal flat plate, axisymmetric stagnation flows, and stagnation flows for the yawed infinite cylinder, solutions of equations (26) to (28) yield the corresponding exact boundary-layer profiles because, in these cases, no variation with ξ is present. First to be discussed are solutions for the cases for which unit Lewis number ($F = 0$) is assumed. The effect of nonunit Lewis number is then discussed.

Flat-plate flow ($F=0$).—Flat-plate flow is represented by equations (26) to (28) with $\beta=0$ because, for a flat plate, $\frac{du_e}{dx}=0$. From equations (26), (27), (29), and (30), it is apparent that $g(\eta)=f'(\eta)$ and thus the system of equations for this case is independent of the yaw parameter t_s. For an isothermal wall, ζ_w is constant and the requirements for similarity are satisfied. Solutions of these equations are found in tables III(a) and III(b) for a wide variety of cases. Skin-friction and heat-transfer coefficients were computed from the transformation equations as

$$c_f\sqrt{N_{Re}}=\sqrt{2}f''_w\left(\frac{\rho_w\mu_w}{\rho_e\mu_e}\right)^{1/2} \tag{33}$$

$$N_{St}\sqrt{N_{Re}}=\frac{1}{\sqrt{2}N_{Pr,f,w}}-\frac{\zeta'_w}{\zeta_{aw}-\zeta_w}\left(\frac{\rho_w\mu_w}{\rho_e\mu_e}\right)^{1/2} \tag{34}$$

The skin-friction coefficient as computed from the similar solutions is shown in figure 2 plotted against $\rho_e\mu_e/\rho_w\mu_w$ for a few values of t_e, the parameter indicating the effect of local Mach number. For a perfect gas with constant specific heats

$$M_e^2=\frac{2}{\gamma-1}\left(\frac{1}{t_e}-1\right)$$

and the values of the local Mach number for $\gamma=1.4$ are also listed in figure 2.

For each value of t_e, the numerical data plot as a single curve, independent of total enthalpy level t_E and surface cooling ratio ζ_w. Shown for comparison in figure 2 are results obtained by using the reference enthalpy method of reference 13 applied with the properties of equilibrium dissociated air from reference 5. The equations for this approximation are

$$c_f\sqrt{N_{Re}}=0.664\sqrt{\frac{\rho^*\mu^*}{\rho_e\mu_e}} \tag{35a}$$

$$\frac{\rho^*\mu^*}{\rho_e\mu_e}=\frac{1.0213\left(\frac{t_e}{t_E}\right)^{0.3329}-0.0213}{1.0213\left(\frac{t^*}{t_E}\right)^{0.3329}-0.0213} \tag{35b}$$

$$\frac{h^*}{h_E}=\frac{t^*}{t_E}=\frac{t_e}{t_E}\left[0.5\left(1+\frac{\zeta_w}{t_e}\right)-0.22\bar{r}\left(1-\frac{1}{t_e}\right)\right] \tag{35c}$$

where $\bar{r}$ is the enthalpy recovery factor taken here as a constant equal to $\sqrt{0.7}$ for simplicity. (See fig. 3(a).) Results of the reference enthalpy method are also essentially independent of t_E and ζ_w and give lower skin-friction coefficients than the exact solution by at most 5 percent. A modified form of the reference enthalpy method which might have slightly improved accuracy is given in reference 14.

Shown also in figure 2 are a few points computed for a perfect gas with the Sutherland viscosity-temperature relation (ref. 15); these latter points

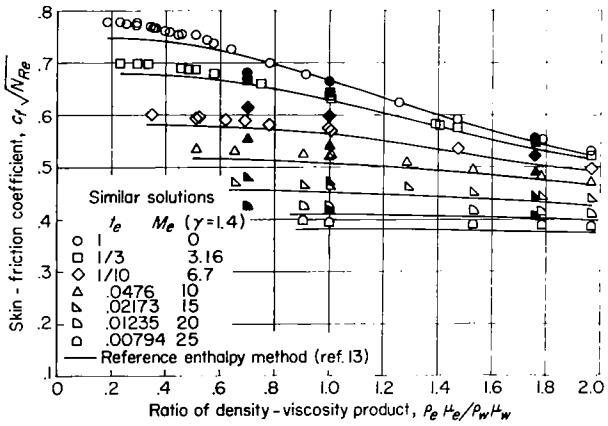

FIGURE 2.—Laminar flat-plate skin-friction coefficient as a function of $\frac{\rho_e\mu_e}{\rho_w\mu_w}$ for equilibrium dissociated air. $N_{Le}=1$. Open symbols represent present solutions; filled symbols represent perfect-gas solution of reference 15.

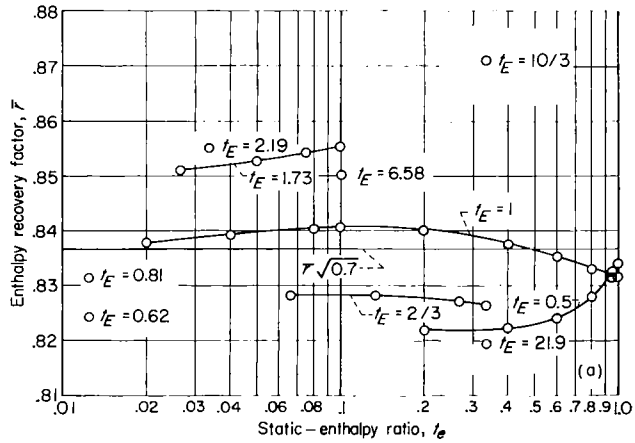

(a) Recovery-factor dependence upon static-enthalpy ratio.

FIGURE 3.—Flat-plate enthalpy recovery factor for equilibrium dissociated air. $N_{Le}=1$.

were appropriate only for a free-stream temperature of −67° F, but the results should be independent of free-stream temperature when plotted as a function of $\rho_e\mu_e/\rho_w\mu_w$. Significant differences occur only for low speed, high-enthalpy-level boundary layers $\left(t_e \to 1, \frac{\rho_e\mu_e}{\rho_w\mu_w} \ll 1\right)$. Elsewhere the real-gas effect is less than 5 percent on the skin-friction coefficient.

The enthalpy recovery factor was investigated for a few cases picked at random and the results (from table III(b)) are shown in figure 3. From figure 3(a) there appears to be no simple correlation function for recovery factor directly in terms of t_E and t_e. However, $\bar{r}$ never deviates far from the nominal low-speed value, $\sqrt{0.7}$ (for a perfect gas with a constant Prandtl number of 0.7). For a variable Prandtl number, the approximation $\bar{r} \approx \sqrt{N^*_{Pr,f}}$ has been proposed (ref. 13). Most of the data are within two percent of the values predicted by this approximation as may be seen in figure 3(b).

Flat-plate heat-transfer coefficients were investigated in terms of the Reynolds analogy factor N_{St}/c_f, a ratio which is very closely approximated by the function $\frac{1}{2}(N_{Pr})^{-2/3}$ for a gas with constant Prandtl number. The accuracy of the variable Prandtl number counterpart of this relation,

$$\frac{N_{St}}{c_f} = \frac{1}{2}(N^*_{Pr,f})^{-2/3} \tag{36}$$

is shown on figure 4 where this relation is compared to the results of the flat-plate similar solutions. In computing the Stanton number from the similar enthalpy derivative (eq. (34)), approximate values of $\bar{r} = \sqrt{N^*_{Pr,f}}$ were used. For most cases, the ratio of wall enthalpy to free-stream stagnation enthalpy (ζ_w) was far from unity and the error introduced by this approximation should be very small. Those cases with $0.2 < \zeta_w < 2$ are shown as the flagged points in figure 4, and for these points, use of an approximate recovery factor could possibly introduce a large error. Two points in this group are particularly far from the correlation. For five of these cases (with $0.2 < \zeta_w < 2$), the exact recovery factors were available and were used in recomputing the Stanton number. The results are shown in the figure as the filled

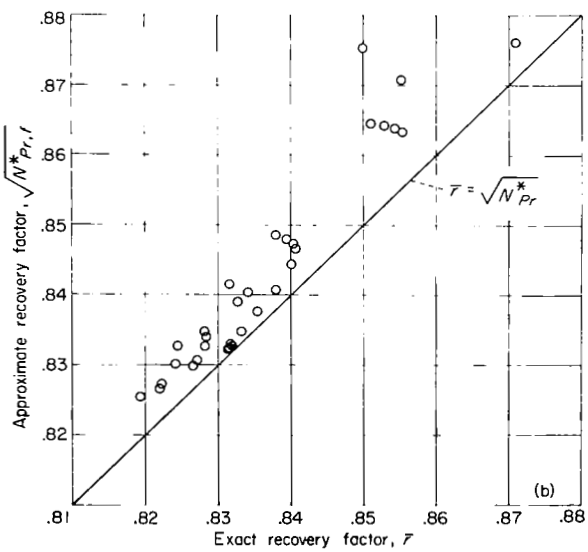

(b) Comparison of approximate and exact recovery factors.

FIGURE 3.—Concluded.

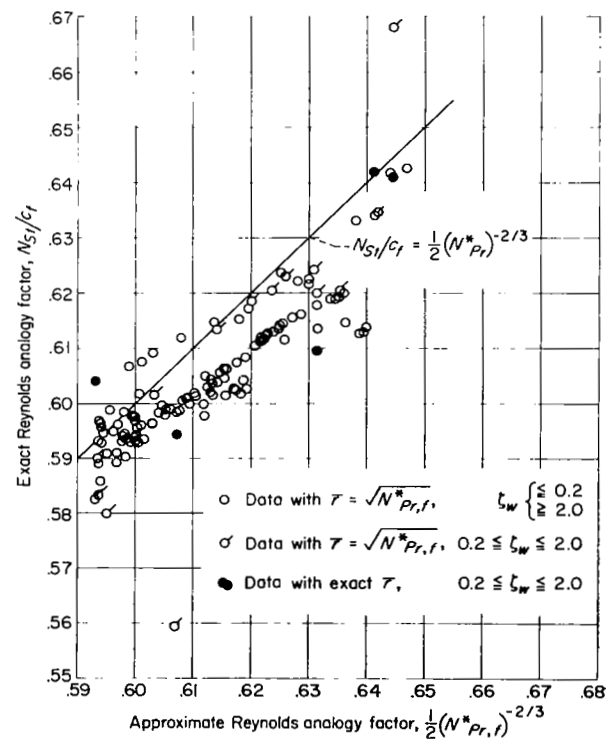

FIGURE 4.—Comparison of exact and approximate Reynolds analogy factors for flat-plate flow of equilibrium dissociated air. $N_{Le} = 1$.

points, each corresponding to the flagged point at the same value of $\frac{1}{2}(N^*_{Pr,f})^{-2/3}$; this correction improves the correlation of the two worst points significantly. Thus, use of equation (36) should generally give results within about 4 percent of the exact solutions for N_{St}/c_f, and for the most part would overestimate this ratio. When equations (35) and (36) are combined to yield N_{St}, the values predicted should be very accurate for most cases because the errors in c_f and N_{St}/c_f are generally compensating.

Axisymmetric stagnation flow ($F=0$).—The boundary-layer flow at the stagnation point of a body of revolution at zero angle of attack $\left(\frac{u_e}{x}=\frac{du_e}{dx}=\text{Constant},\ j=1\right)$ is described by solutions of equations (26) and (28) with $t_s=t_e=1$ and $\beta=\frac{1}{2}$. The heat transfer for this case is conveniently described by the Nusselt number, given by (see appendix)

$$\left[\frac{N_{Nu,w}}{(N_{Re,w})^{1/2}}\right]_s=\frac{\sqrt{2}\zeta'_w}{1-\zeta_w}(1+F_w) \tag{37}$$

Correlations of the numerical results (table III(a)) were sought in the form of $[N_{Nu,w}/(N_{Pr,f,w})^{0.4}(N_{Re,w})^{0.5}]_s$ as a function of the $\rho\mu$ ratio across the boundary layer and the results are shown in figure 5 along with the correlating function

$$\left[\frac{N_{Nu,w}}{(N_{Pr,f,w})^{0.4}(N_{Re,w})^{0.5}}\right]_s=0.767\left(\frac{\rho_e\mu_e}{\rho_w\mu_w}\right)^{0.43}_s \tag{38}$$

which fits the numerical data within about ± 5 percent. The Prandtl number dependence was assumed to have the same form as that for a

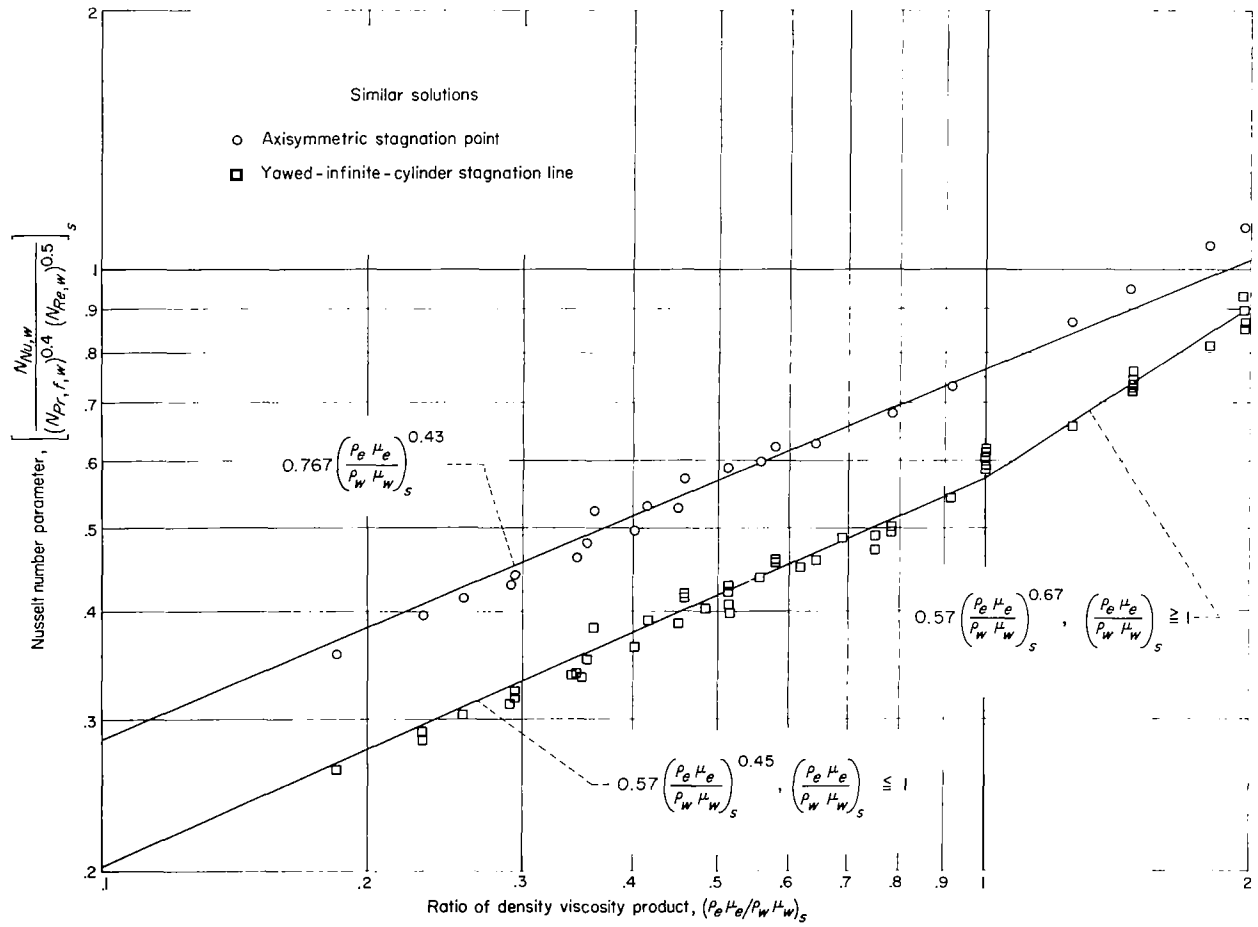

FIGURE 5.—Stagnation-flow heat-transfer parameter as a function of $\left(\frac{\rho_e\mu_e}{\rho_w\mu_w}\right)_s$ for equilibrium dissociated air. $N_{Le}=1$.

constant Prandtl number gas and its inclusion in the correlation function resulted in a slightly smaller scatter of the data than if it were omitted. Such a dependence upon Prandtl number would not be expected to apply if the Prandtl number variation across the boundary layer were more extreme than that for the frozen Prandtl number used herein.

It is noteworthy that the coefficient and exponent on the right-hand side of equation (38) appear to be very little dependent upon the gas properties used in solutions of the differential equations, at least up to the onset of ionization. For example, for the case of constant fluid properties (incompressible fluid), the coefficient and exponent obtained are 0.763 and 0.5, respectively (ref. 16). Corresponding values of 0.768 and 0.4, respectively, were obtained for equilibrium dissociated air with unit Lewis number (ref. 9) and for a perfect gas with constant specific heats (ref. 17), where in both cases the assumption of the Sutherland viscosity relation and a constant Prandtl number were employed. Although the Nusselt number parameter of equation (38) is little influenced by fluid properties, the heat-transfer rate may be more strongly affected. For the correlation of equation (38), the heat-transfer rate may be written

$$-q_{w,s}=0.767(N_{Pr,f,w})_s^{-0.6}(H_e-h_w)_s (\rho_e\mu_e)_s^{0.43}(\rho_w\mu_w)_s^{0.07}\sqrt{\left(\frac{du_e}{dx}\right)_s} \quad (39)$$

For two different estimates of the high-temperature transport properties of air, the corresponding stagnation-point heat-transfer rates will be in proportion to the 0.43 power of the stagnation viscosity, all other quantities being equal. For example, the ratio of Hansen's viscosity to the Sutherland viscosity at 29,000 feet/second is as much as about 1.35, depending upon pressure level. If each of these viscosity estimates is used, the computed heat-transfer rates would be different by as much as 15 percent. As better estimates of the transport properties of equilibrium dissociated air become available, a correspondingly better estimate of stagnation point heat-transfer rates should be possible through the use of equation (39) without modification of the coefficient and exponent arising in equation (38) provided that the frozen Prandtl number does not vary greatly about a mean value.

Stagnation flow for yawed infinite cylinder ($F=0$).—With $\beta=1$ and $t_s=t_e\leqq 1$, equations (26) to (28) represent the stagnation line boundary layer on a yawed infinite cylinder $\left(\frac{u_e}{x}=\frac{du_e}{dx}=\text{Constant},\ j=0\right)$. With $F=0$, solutions for 49 heat-transfer cases were computed with values of the yaw parameter t_s of 1, 1/3, 1/10, and 1/30 (table III(a)). From the appendix, the Nusselt number function is given by

$$\left[\frac{N_{Nu,w}}{(N_{Re,w})^{0.5}}\right]_s=\frac{\zeta'_w}{\zeta_{aw}-\zeta_w}(1+F_w) \quad (40)$$

In the computation of this function from the similar solutions, a recovery factor of 0.85 was used as an approximation to the exact values which varied from 0.84 to 0.88 for those insulated-wall stagnation-line cases computed in the present program as well as those of reference 17 for a perfect gas. (See table III(b) and fig. 6.)

Results are shown in figure 5 along with the following correlating functions:

For $\left(\frac{\rho_e\mu_e}{\rho_w\mu_w}\right)_s\leqq 1$,

$$\left[\frac{N_{Nu,w}}{(N_{Pr,f,w})^{0.4}(N_{Re,w})^{0.5}}\right]_s=0.57\left(\frac{\rho_e\mu_e}{\rho_w\mu_w}\right)_s^{0.45} \quad (41a)$$

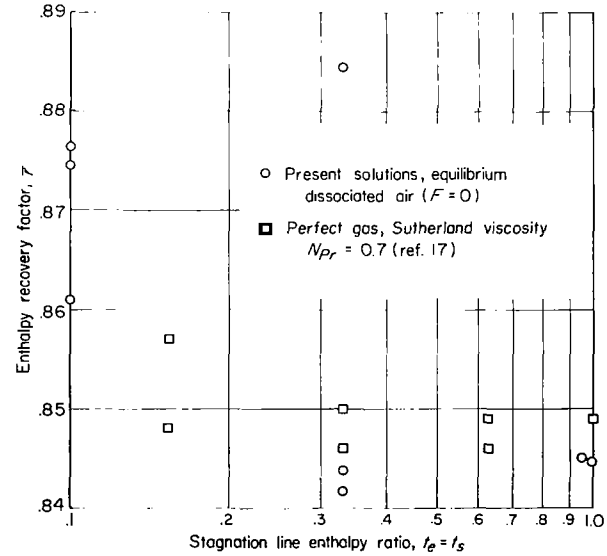

FIGURE 6.—Enthalpy recovery factor for yawed infinite cylinder stagnation line. $N_{Le}=1$.

For $\left(\frac{\rho_e\mu_e}{\rho_w\mu_w}\right)_s \geqq 1$,

$$\left[\frac{N_{Nu,\,w}}{(N_{Pr,\,f,\,w})^{0.4}(N_{Re,\,w})^{0.5}}\right]_s = 0.57\left(\frac{\rho_e\mu_e}{\rho_w\mu_w}\right)_s^{0.67} \quad (41b)$$

which fit the numerical data within about ± 7 percent independent of the enthalpy level. The reason that two functions have been used here to better fit the data is that at large yaw, values of $(\rho_e\mu_e/\rho_w\mu_w)_s$ greater than unity may represent practical high-speed flight conditions with a highly cooled wall, whereas at zero yaw or with axial symmetry, values of $(\rho_e\mu_e/\rho_w\mu_w)_s$ will always be less than unity for highly cooled walls.

Equations (41a) and (41b) may be compared with the results for perfect air with constant specific heats, constant Prandtl number, and the Sutherland viscosity relation (ref. 17), which correlate as

$$\left[\frac{N_{Nu,\,w}}{(N_{Pr,\,w})^{0.4}(N_{Re,\,w})^{0.5}}\right]_s = 0.577\left(\frac{\rho_e\mu_e}{\rho_w\mu_w}\right)_s^{0.44} \quad (42)$$

and little effect of the gas properties is seen for $\left(\frac{\rho_e\mu_e}{\rho_w\mu_w}\right)_s < 1$. For $\left(\frac{\rho_e\mu_e}{\rho_w\mu_w}\right)_s > 1$ the present results and those of reference 17 do not compare as favorably.

Because at the stagnation line of the yawed infinite cylinder moving with velocity V_∞ the local external properties are the same as for an unyawed cylinder at a velocity $V_\infty \cos \Lambda$, equation (41) should be valid for velocities up to $V_\infty = \frac{29{,}000}{\cos \Lambda}$ feet per second.

The effect of nonunit Lewis number.—Before the solutions obtained herein for nonunit Lewis number are discussed, a review of the mechanisms for the transfer of energy in a reacting mixture of gases appears desirable.

At a point in the equilibrium binary boundary layer the heat flux normal to the surface is given by (ref. 5)

$$-q = k_f\frac{\partial T}{\partial z} + \rho D_{AM}(h_A - h_M)\left(\frac{\partial C_A}{\partial h}\right)_{p=Const.}\frac{\partial h}{\partial z} \quad (43)$$

The first term on the right-hand side represents heat transfer by "ordinary" conduction (transfer of energy through collisions of particles) and the second term represents transfer of heat through mass diffusion of the reacting species. The first term may be put in terms of a static-enthalpy gradient (see ref. 5), which yields for the heat flux

$$-q = \frac{\mu}{N_{Pr,\,f}}\left(\frac{\partial h}{\partial z}\right)\left[1 - (h_A - h_M)\left(\frac{\partial C_A}{\partial h}\right)_{p=Const.} + N_{Le}(h_A - h_M)\left(\frac{\partial C_A}{\partial h}\right)_{p=Const.}\right] \quad (44)$$

Now the first two terms in the brackets of equation (44) represent "ordinary" conduction while the third term represents heat transfer by mass diffusion. The two terms containing $\left(\frac{\partial C_A}{\partial h}\right)_{p=Const.}$ are direct functions of the chemistry of the flow and the other term is comparable to the low-speed, perfect-gas result. Equation (44) may be written

$$-q = \frac{\mu}{N_{Pr,\,f}}\left(\frac{\partial h}{\partial z}\right)[1 + F(p, h)] \quad (45)$$

where $F(p, h)$ is given by equation (6).

For equilibrium dissociated air, $h_A - h_M > 0$ and $\left(\frac{\partial C_A}{\partial h}\right)_{p=Const.} > 0$ for the simple binary model of reacting atoms and molecules. Thus, for $N_{Le} > 1$, $F > 0$, and for $N_{Le} < 1$, $F < 0$. For unit Lewis number ($F = 0$), the two terms in equation (44) depending directly upon the concentration derivative, one arising from "ordinary" conduction and one representing mass diffusion, just cancel, and the heat-flux expression takes its low-speed form. When the Lewis number is locally greater than unity ($F > 0$), the effect is to increase the heat flux in the boundary layer relative to the case for $N_{Le} = 1$, whereas for Lewis number less than unity ($F < 0$), the local effect is to decrease the heat transfer.

The effect of diffusion for constant values of N_{Le} of 1.4 and 2.0 was considered in reference 9 for axisymmetric stagnation flow, and it was found that the surface heat transfer was increased a significant amount relative to that for $N_{Le} = 1$, because the function F was equal to or greater than zero throughout the boundary layer. A more realistic estimate of the Lewis number was given in reference 4 and varied from about 1.4 at low enthalpy to about 0.6 at the enthalpy for complete dissociation. In reference 5 it was surmised that the corresponding variation in F across the stagnation-point boundary layer (from $F < 0$ at the edge to $F > 0$ near the surface) would decrease the influence of nonunit Lewis number

from that given in reference 9. It was further estimated in reference 1 that for the diffusion function herein designated F_1, the effect of nonunit Lewis number would be to increase the stagnation-point heat transfer by at most about 6 percent.

The solutions presented herein (tables IV(a) and IV(b)) were obtained by using three different estimates for the diffusion function. The functions F_1 and F_3 represent the diffusion function for equilibrium dissociated air computed in two different ways, where the variable Lewis number as a function of enthalpy from reference 4 is used. The function F_1 is computed from equation (6) and is given in table I of reference 5, while F_3 is given by the relation $F_3=\frac{N_{Pr,f}}{N_{Pr,eff}}-1$ (see table II of ref. 5). These two functions show some similarities (fig. 9 of ref. 5) and are thought to represent the properties of air better than the function F_2, computed from equation (6) with $N_{Le}=1.4$ (fig. 6 of ref. 5). In all cases considered herein (as well as the nonunit Lewis number cases of ref. 9), the surface enthalpy was sufficiently low that $F_w=0$ (no diffusion at the surface). Thus the effect of F upon the surface heat-transfer rate is directly proportional to the effect on the derivative ζ'_w; these effects are dependent upon distortions of the enthalpy profiles in the boundary layer caused by the nonunit Lewis number diffusion function.

Because of the weak coupling between the energy and momentum equations, the effect of nonunit Lewis number upon skin friction was found in the present solutions to be negligible (at most a 1 percent effect upon f''_w and g'_w), regardless of whether F_1, F_2, or F_3 was used. These results are not shown in the tables. Turning to the heat-transfer rate, for the axisymmetric stagnation point, the results obtained by using F_2 agreed with those of reference 9 for $N_{Le}=1.4$ and indicated an increase in heat-transfer rate reaching 15 percent for fully dissociated air $\left(\frac{H_e}{h_E}=2, t_E=0.5\right)$. Because the assumption of $N_{Le}=1.4$ appears incorrect, the results obtained by using F_2 are not considered further.

Plots of $\frac{\zeta'_w(F)}{\zeta'_w(F=0)}$ for $\beta=0$, 1/2, and 1 and of $\frac{\bar{r}(F)}{\bar{r}(F=0)}$ for $\beta=0$ and 1 for $t_e=t_s$ are shown in figures 7(a) and 7(b), respectively, for those cases computed with the diffusion functions F_1 and F_3.

668943—63——3

For the axisymmetric stagnation point problem $\left(\beta=\frac{1}{2}\right)$, the effect of nonunit Lewis number is within the limits

$$\left.\begin{aligned} 0.98 \lessapprox \frac{q_{w,s}(F=F_1)}{q_{w,s}(F=0)} \lessapprox 1.05 \\ 1.0 \lessapprox \frac{q_{w,s}(F=F_3)}{q_{w,s}(F=0)} \lessapprox 1.08 \end{aligned}\right\} \quad (46)$$

and because the Nusselt number is proportional to $q_w/(1-\zeta_w)$, the same relations hold for the Nusselt number function. The influence of the diffusion function upon ζ'_w is very weakly a function of β, so that for the flat-plate ($\beta=0$) and for the yawed-infinite-cylinder stagnation line ($\beta=1$), relations nearly equivalent to equations (46) are valid. In these latter cases, however, heat-transfer coefficients (e.g., Stanton and Nusselt numbers) are proportional to $q_w/(\zeta_{aw}-\zeta_w)$, $\zeta_{aw}\leqq 1$,

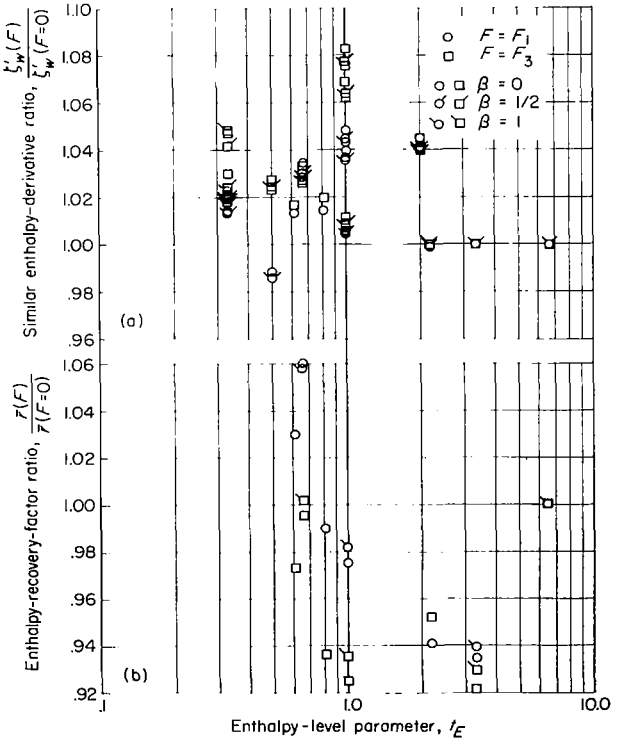

(a) $\frac{\zeta'_w(F)}{\zeta'_w(F=0)}$ for $F=F_1$, F_3.

(b) $\frac{\bar{r}(F)}{\bar{r}(F=0)}$ for $F=F_1$, F_3.

FIGURE 7.—Effect of diffusion for nonunit Lewis number for equilibrium dissociated air. $t_e=t_s$.

so that the diffusion effect upon $\bar{r}$ must be taken into account when the dissipation is large (when $t_e \ll 1$). This dependence is roughly, for those cases computed,

$$\left.\begin{aligned} 0.93 \lessapprox \frac{\bar{r}(F=F_1)}{\bar{r}(F=0)} \lessapprox 1.06 \\ 0.92 \lessapprox \frac{\bar{r}(F=F_3)}{\bar{r}(F=0)} \lessapprox 1.0 \end{aligned}\right\} \tag{47}$$

approximately independent of β. Thus, when a heat-transfer coefficient is computed for highly cooled walls and large dissipation ($\zeta_w \approx 0$, $t_e \ll 1$), the coefficient is proportional roughly to $q_w/\bar{r}$. For those cases where both ζ'_w and $\bar{r}$ were computed by including nonunit Lewis number diffusion, the results are

$$\left.\begin{aligned} 0.97 \lessapprox \frac{\frac{q_w}{\bar{r}}\,(F=F_1)}{\frac{q_w}{\bar{r}}\,(F=0)} \lessapprox 1.07 \\ 1.0 \lessapprox \frac{\frac{q_w}{\bar{r}}\,(F=F_3)}{\frac{q_w}{\bar{r}}\,(F=0)} \lessapprox 1.10 \end{aligned}\right\} \tag{48}$$

The results contained in equations (46) to (48) confirm the estimates made in appendix A of reference 1 and support the assumption that the effect of nonunit Lewis number diffusion may be neglected for equilibrium dissociated air with the transport properties as given in reference 4 and with walls sufficiently cold that no atoms diffuse to the surface. Based upon these results, the effect of nonunit Lewis number is neglected for the discussions that follow, except in the section extending the similar solutions to velocities above the nominal 29,000 feet per second limit for fully dissociated air, where a different method of expressing the gas properties is employed.

LOCALLY SIMILAR SOLUTIONS FOR THE HEAT-TRANSFER-DISTRIBUTION PARAMETER

To determine the heat-transfer distribution for a given configuration and inviscid flow requires the solution of equations (23) to (25), a system of three equations with four unknowns, $q_w/q_{w,s}$, Γ, $\zeta'_w/\zeta'_{w,s}$, and β. The fourth required relation, one between $\zeta'_w/\zeta'_{w,s}$ and β is provided from the locally similar solutions of table III(a) (heat transfer, $F=0$). In general, the surface enthalpy derivative ζ'_w may be written in functional form as

$$\zeta'_w = \zeta'_w(\beta, t_s, t_e, t_E, \zeta_w) \tag{49}$$

For a given blunt configuration with given inviscid flow and wall enthalpy, the distribution of the enthalpy gradient is given by

$$\frac{\zeta'_w}{\zeta'_{w,s}} = \frac{\zeta'_w(\beta, t_e, \zeta_w)}{\zeta'_w(\beta_s, t_e=t_s, \zeta_{w,s})} \tag{50}$$

at constant t_s and t_E. Equation (50) may be broken into a product of various factors representing the dependence of $\zeta'_w/\zeta'_{w,s}$ on each of the parameters. Thus

$$\frac{\zeta'_w(\beta, t_e, \zeta_w)}{\zeta'_w(\beta_s, t_e=t_s, \zeta_{w,s})} = \left[\frac{\zeta'_w(\beta, t_e, \zeta_w)}{\zeta'_w(\beta=1, t_e, \zeta_w)}\right]\left[\frac{\zeta'_w(\beta=1, t_e, \zeta_w)}{\zeta'_w(\beta=1, t_e=t_s, \zeta_w)}\right]\left[\frac{\zeta'_w(\beta=1, t_e=t_s, \zeta_w)}{\zeta'_w(\beta=1, t_e=t_s, \zeta_{w,s})}\right]\left[\frac{\zeta'_w(\beta=1, t_e=t_s, \zeta_{w,s})}{\zeta'_w(\beta_s, t_e=t_s, \zeta_{w,s})}\right] \tag{51}$$

The first factor on the right-hand side of equation (51) represents the dependence of $\zeta'_w/\zeta'_{w,s}$ upon β; the second factor gives the effect of chordwise dissipation, the third factor represents the effect of a nonisothermal wall, and the fourth factor is merely the reciprocal of the first evaluated at the stagnation point or line. Detailed analysis of the numerical solutions indicated that each of these factors may be approximated by correlation formulas which are discussed separately in the following paragraphs.

The β-dependence.—The first factor of equation (51) was investigated first for the special case $t_e=t_s$ (no chordwise dissipation). Plotted in figures 8(a) to 8(d) are the data from tables III(a) as functions of β for values of t_s of 1, 1/3, 1/10, and 1/30, and for various constant values of the parameters t_E and ζ_w. For high enthalpy level (low t_E) and highly cooled walls (low ζ_w), all the data correlate as a single curve for each t_s independent of t_E and ζ_w. These data were fitted to a function of the same form as that of reference 1,

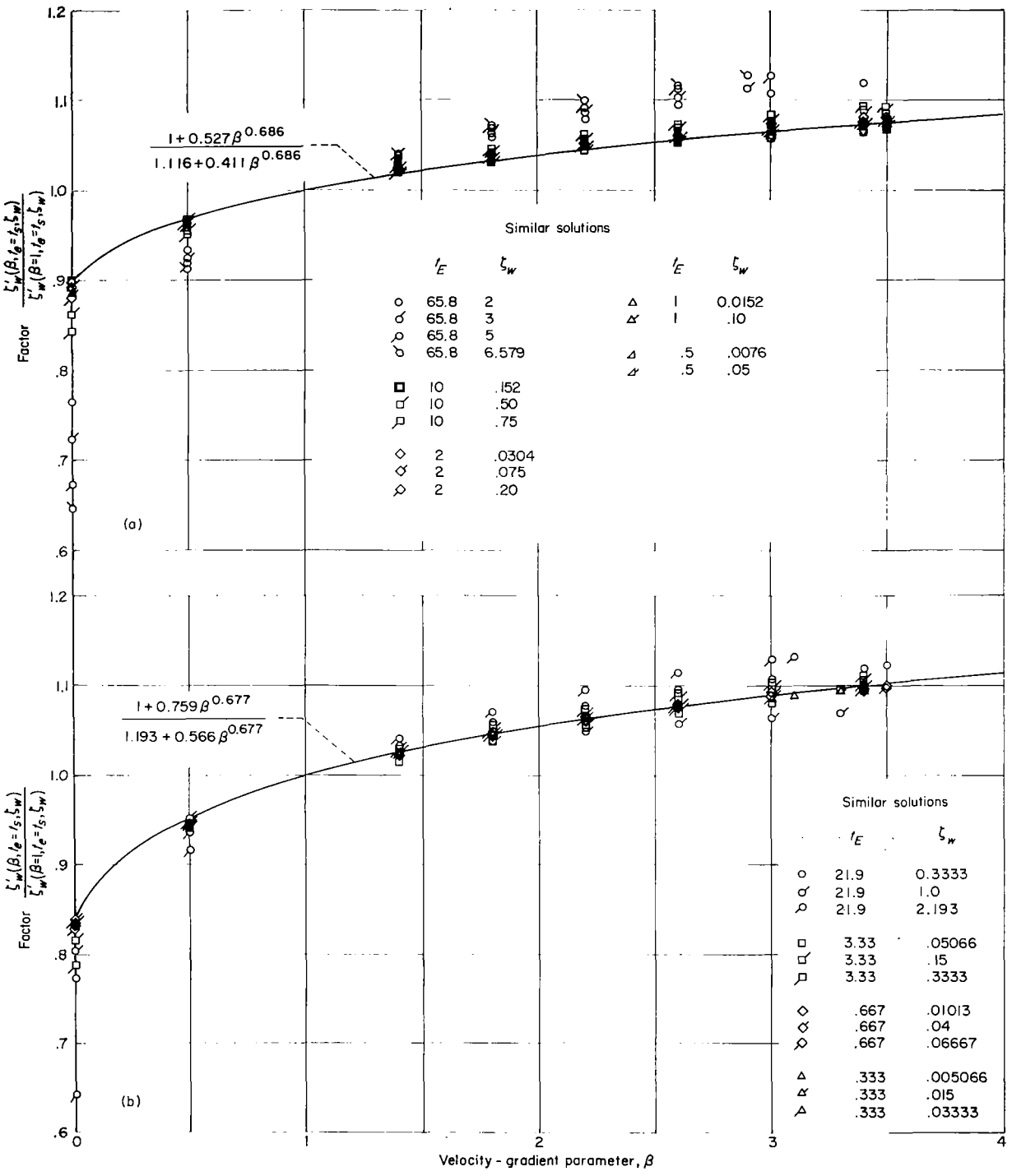

(a) $t_e=t_s=1$.

(b) $t_e=t_s=\frac{1}{3}$.

FIGURE 8.—Dependence of factor $\frac{\zeta'_w(\beta, t_e=t_s, \zeta_w)}{\zeta'_w(\beta=1, t_e=t_s, \zeta_w)}$ upon β for $t_e=t_s$. Equilibrium dissociated air. $N_{Le}=1$.

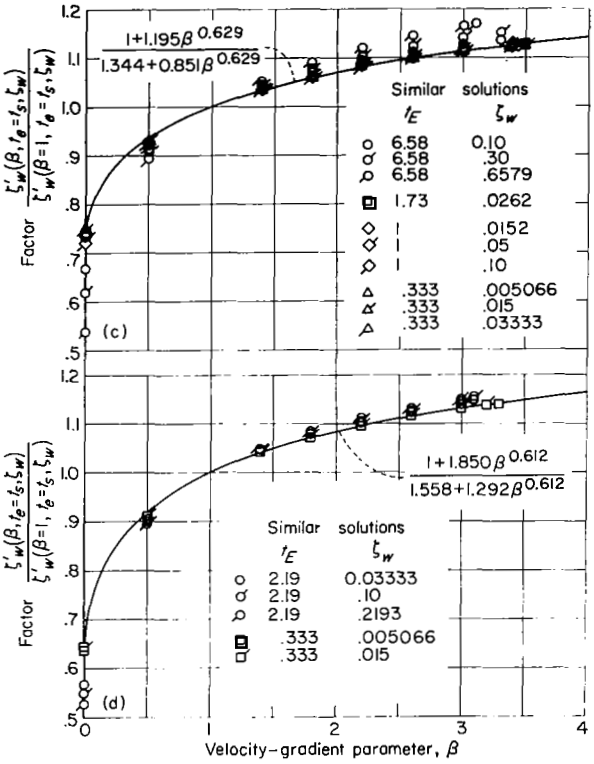

(c) $t_e=t_s=\frac{1}{10}$.

(d) $t_e=t_s=\frac{1}{30}$.

FIGURE 8.—Concluded.

namely

$$\frac{\zeta'_w(\beta, t_e=t_s, \zeta_w)}{\zeta'_w(\beta=1, t_e=t_s, \zeta_w)}=\frac{1+P\beta^N}{Q+R\beta^N} \qquad (52)$$

where the parameters P, Q, R, and N are functions of t_s as given in the following table:

t_s	P	Q	R	N
1	0. 527	1. 116	0. 411	0. 686
1/3	. 759	1. 193	. 566	. 677
1/10	1. 195	1. 344	. 851	. 629
1/30	1. 850	1. 558	1. 292	. 612

Note that $R=1+P-Q$. Solutions as $\beta\to\infty$ were used to aid in determining these parameters. Equation (52) with the appropriate parameters P, Q, R, and N is valid independently of t_E and ζ_w within about 5 percent for $0.5\lessapprox\beta<\infty$ provided that $\frac{\zeta_w}{t_s}\lessapprox 1.0$. For $0\leqq\beta\lessapprox 0.5$, the error may be slightly larger. This function is shown in figures 8(a) to 8(d). Plots of P, Q, and N against t_s for these conditions are given in figure 9 to aid in interpolation. The parameters P and Q plotted as smooth curves in figure 9, but because the choice of points through which to pass the correlating function (eq. (52)) was somewhat arbitrary, the parameter N plotted somewhat irregularly and is shown in figure 9 as a set of discrete points joined by straight lines. Equation (52) should not be sensitive to the value of N.

The effect of $t_e<t_s$ upon the β dependence was next investigated. Shown in figures 10(a) to 10(d) are plots of the parameter $\frac{\zeta'_w(\beta, t_e, \zeta_w)}{\zeta'_w(\beta=1, t_e, \zeta_w)}$ for various constant values of t_e in the range $0.2\leqq\frac{t_e}{t_s}<1.0$ for constant values of t_E and ζ_w and for $t_s=1$, $\frac{1}{3}$, $\frac{1}{10}$, and $\frac{1}{30}$. The correlation relation for $t_e=t_s$ (eq. (52)) is also shown in these figures, and it is evident that an effect of chordwise dissipation appears in the β dependence. For zero yaw ($t_s=1$), this effect is negligible, at least for $0\leqq\beta\lessapprox 3.5$, but as t_s decreases, the data diverge from the $t_e=t_s$ correlation function. It was found that these data could be correlated somewhat better by the modified function

$$\frac{\zeta'_w(\beta, t_e, \zeta_w)}{\zeta'_w(\beta=1, t_e, \zeta_w)}=\frac{\zeta'_w(\beta, t_e=t_s, \zeta_w)}{\zeta'_w(\beta=1, t_e=t_s, \zeta_w)}\left[1+0.050(1-t_s)\left(1-\frac{t_e}{t_s}\right)\left(\frac{\beta-1}{0.2\beta+1}\right)\right] \qquad (53)$$

The form of the correction in brackets was chosen such that it was unity for zero yaw independent of t_e as the data seem to indicate. No numerical results for $\beta\to\infty$ were available and the constants in the correction factor of equation (53) were determined solely from results in the range $0\leqq\beta\lessapprox 3.5$. The accuracy of this function is about 5 percent over this range except again near $\beta=0$, where errors may reach 10 percent. Figure 11 illustrates the correlation for the case $t_s=0.1$.

Although because of program difficulties it was not generally feasible to obtain locally similar solutions for $\beta>3.5$, a few solutions were obtained for values of β to about 4 (these are not shown in the table) and no significant deviations from the correlation of equation (53) were found.

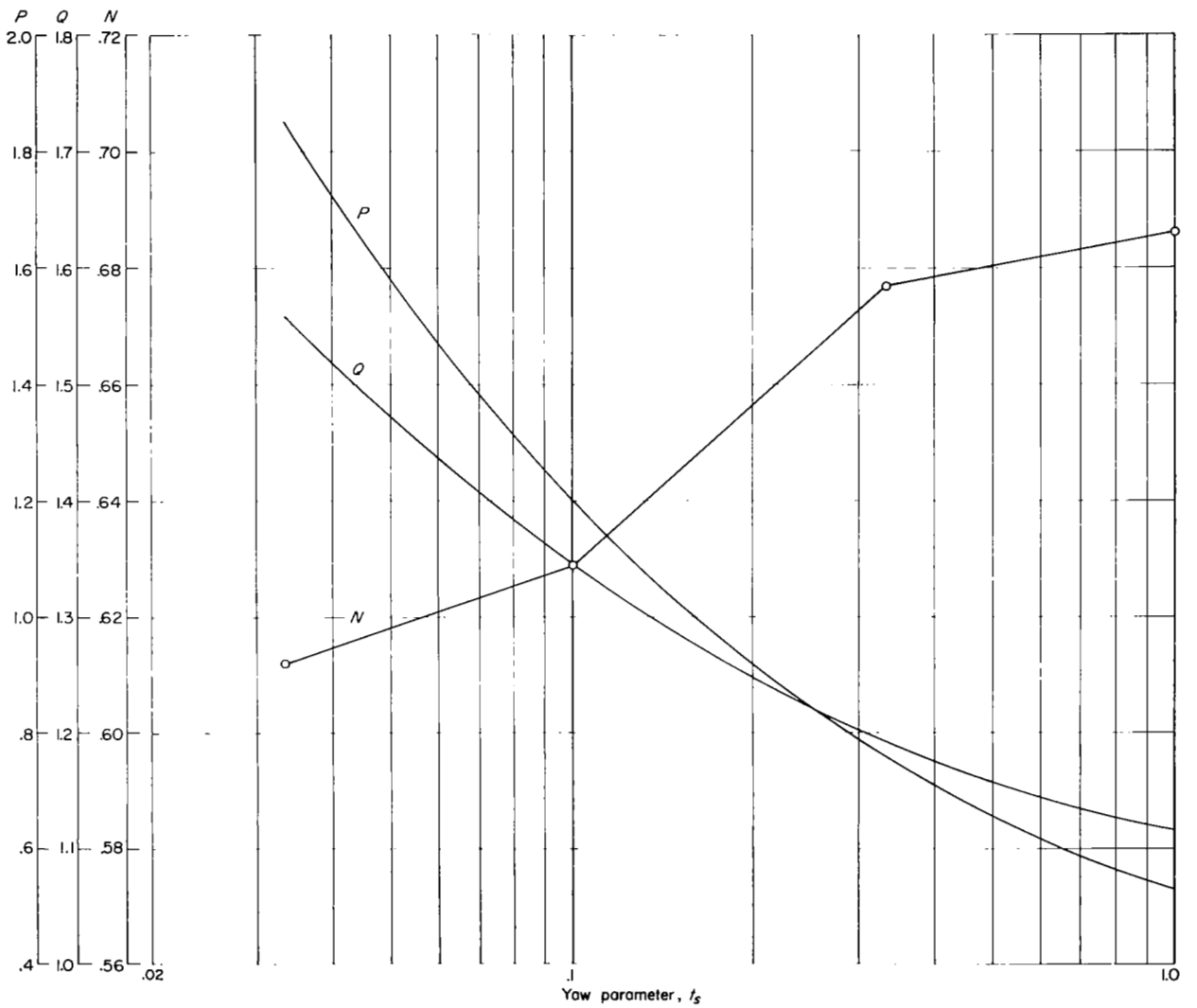

FIGURE 9.—Interpolation plots of parameters P, Q, and N as a function of yaw parameter t_s for $\frac{\zeta_w}{t_s} \lessapprox 1$.

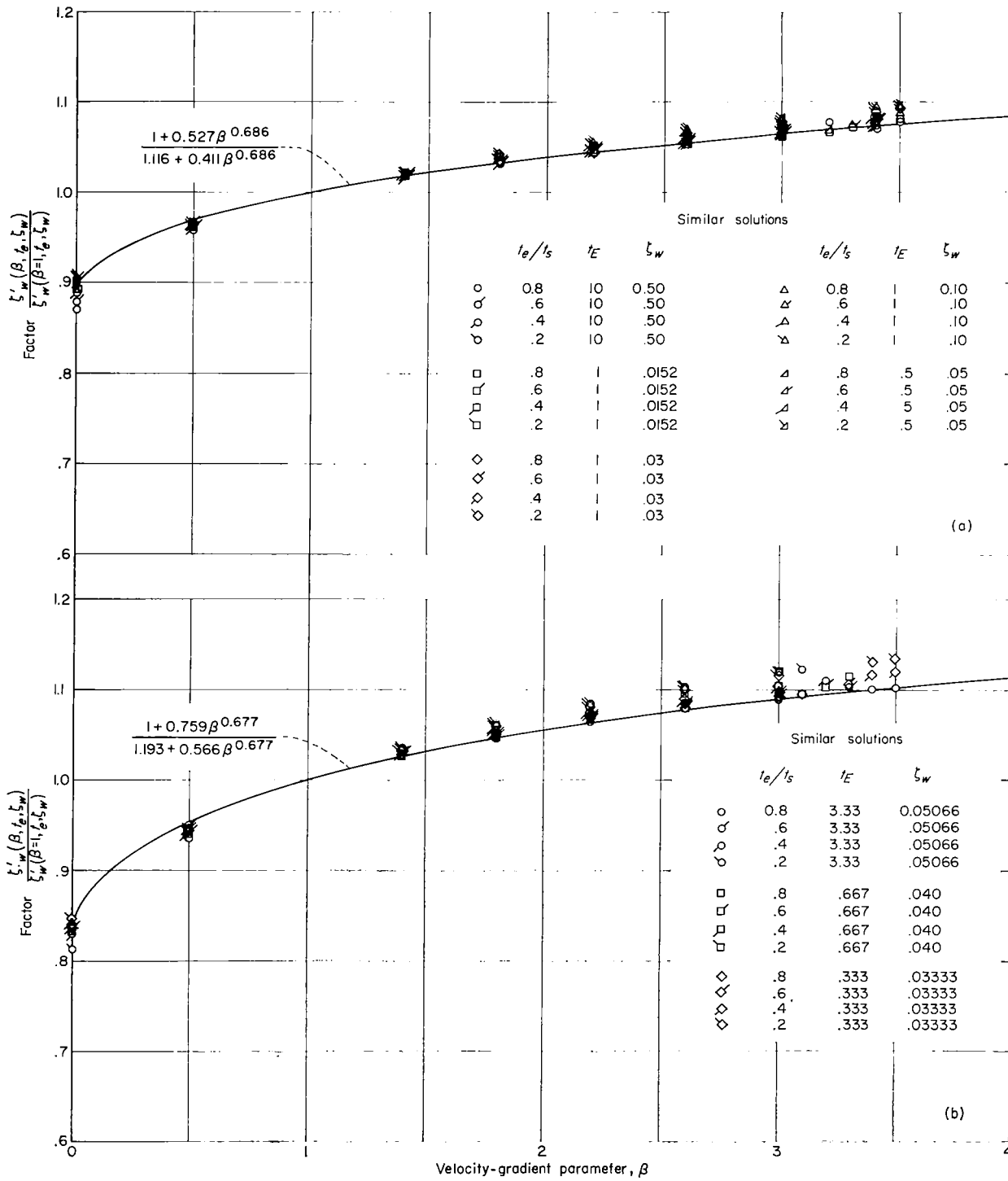

(a) $t_e=1$.

(b) $t_e=\frac{1}{3}$.

FIGURE 10.—Dependence of factor $\frac{\zeta'_w(\beta, t_e, \zeta_w)}{\zeta'_w(\beta=1, t_e, \zeta_w)}$ upon β f $<t_e$. Equilibrium dissociated air; $N_{Le}=1$.

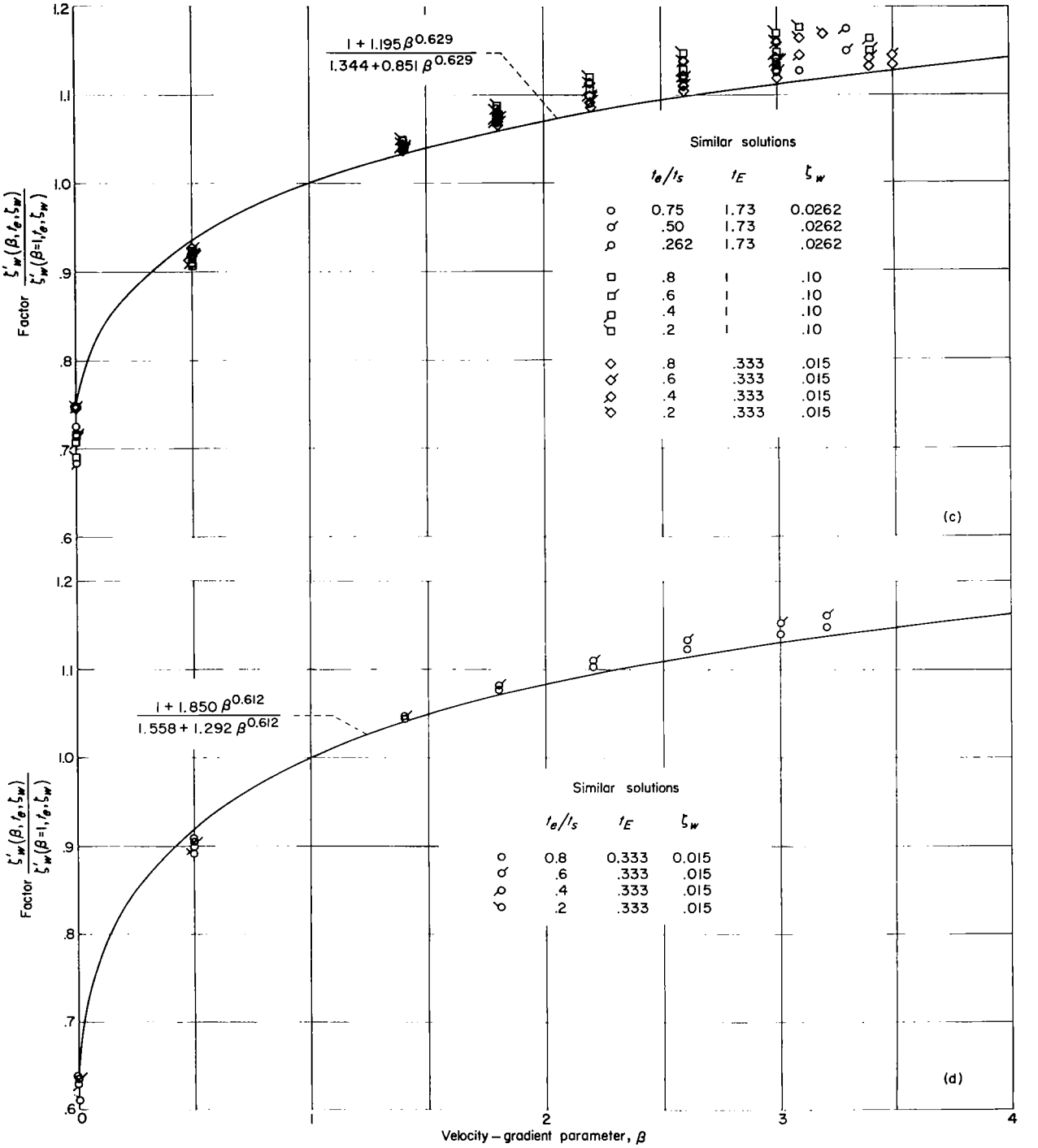

(c) $t_e = \frac{1}{10}$.

(d) $t_e = \frac{1}{30}$.

FIGURE 10.—Concluded.

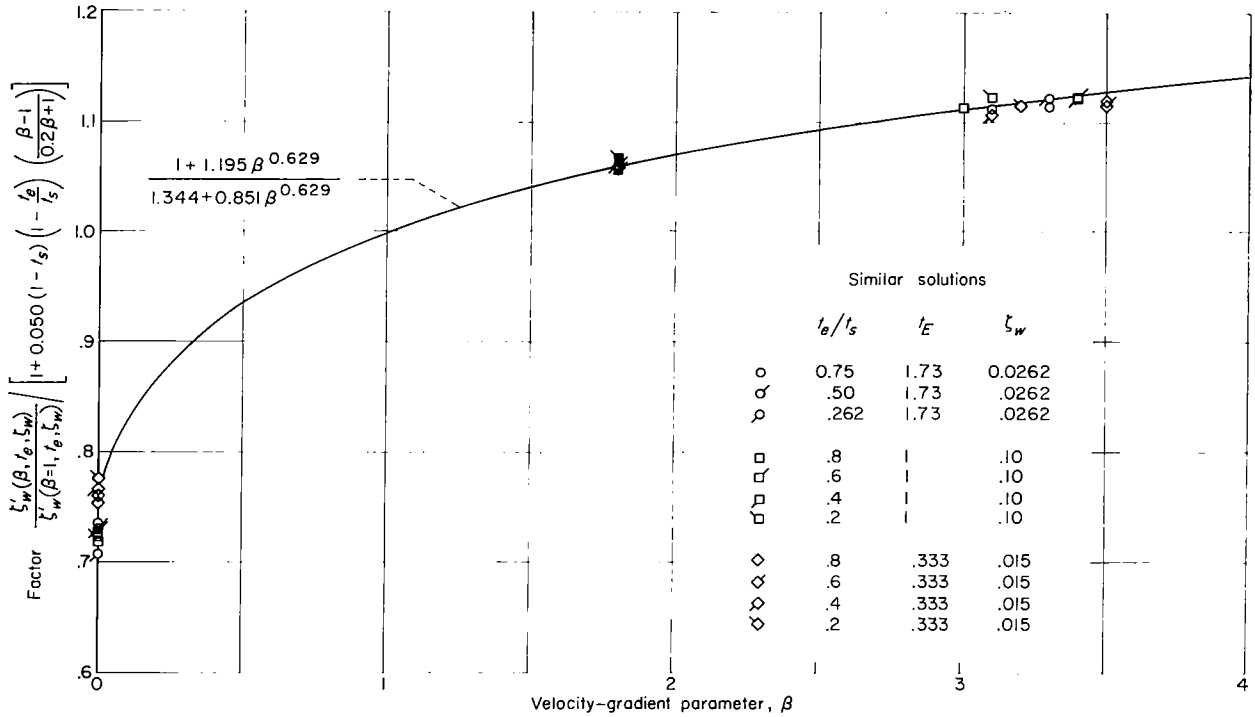

FIGURE 11.—Typical result after elimination of $\frac{t_e}{t_s}<1$ effect from factor $\frac{\zeta'_w(\beta, t_e, \zeta_w)}{\zeta'_w(\beta=1, t_e, \zeta_w)}$. Equilibrium dissociated air; $N_{Le}=1$; $t_s=0.1$.

The final result for the first factor of equation (51) is then

$$\frac{\zeta'_w(\beta, t_e, \zeta_w)}{\zeta'_w(\beta=1, t_e, \zeta_w)}=\left(\frac{1+P\beta^N}{Q+R\beta^N}\right)\left[1+0.050(1-t_s)\left(1-\frac{t_e}{t_s}\right)\left(\frac{\beta-1}{0.2\beta+1}\right)\right] \quad (54)$$

valid for $\frac{\zeta_w}{t_s}\lessapprox 1$ but otherwise independent of t_E and ζ_w. Equation (54) is accurate within about 5 percent for the range $0.5\leqq\beta\lessapprox 4$ except when $t_e=t_s$, where the same accuracy extends to infinite β. For the range $0\leqq\beta<0.5$, accuracy is about 10 percent. Equation (54) may be accepted tentatively for $\beta>4$, $t_e<t_s$.

The effect of t_e at constant β.—The effect of $t_e<t_s$ at constant β (equal to unity as required by the second factor on the right-hand side of eq. (51)) was determined from the numerical solutions as independent of t_s, t_E, and ζ_w when plotted as the ratio

$$\frac{\zeta'_w(\beta=1, t_e, \zeta_w)}{\zeta_{aw}(t_e)-\zeta_w}\Big/\frac{\zeta'_w(\beta=1, t_e=t_s, \zeta_w)}{\zeta_{aw}(t_e=t_s)-\zeta_w}$$

with $\bar{r}$ taken as a constant equal to 0.85 for convenience. All the available numerical data are shown plotted in this form against t_e/t_s in figure 12. Use of the exact recovery factor where possible instead of the nominal value of 0.85 reduced the scatter only slightly and because no convenient correlation formula or plot was found for $\bar{r}$, the correlation using the nominal value was considered to be satisfactory.

Shown also in figure 12 is the function

$$\frac{\dfrac{\zeta'_w(\beta=1, t_e, \zeta_w)}{\zeta_{aw}(t_e)-\zeta_w}}{\dfrac{\zeta'_w(\beta=1, t_e=t_s, \zeta_w)}{\zeta_{aw}(t_e=t_s)-\zeta_w}}=1.1-0.1625\,\frac{t_e}{t_s}+0.0625\left(\frac{t_e}{t_s}\right)^2 \quad (55)$$

which correlates the data within about ± 5 percent. The second factor of equation (51) may be found from equation (55) as

$$\frac{\zeta'_w(\beta=1, t_e, \zeta_w)}{\zeta'_w(\beta=1, t_e=t_s, \zeta_w)}=\frac{0.85+0.15t_e-\zeta_w}{0.85+0.15t_s-\zeta_w}\left[1.1-0.1625\,\frac{t_e}{t_s}+0.0625\left(\frac{t_e}{t_s}\right)^2\right] \quad (56)$$

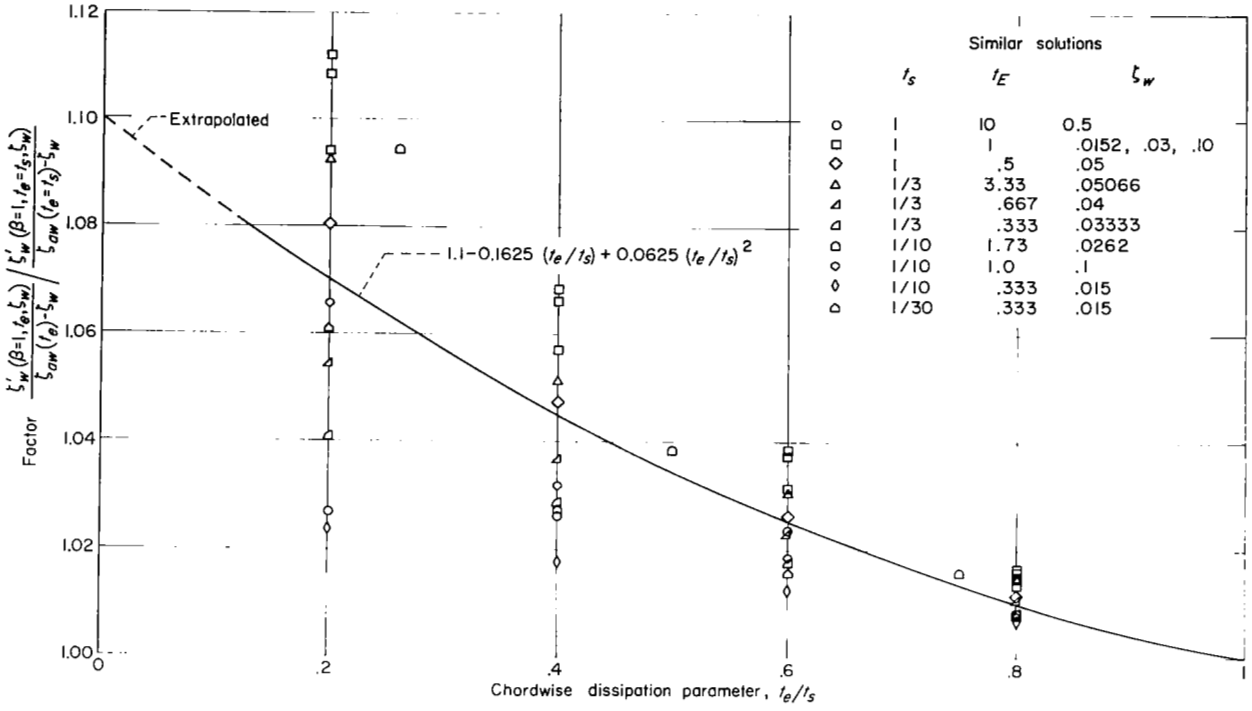

FIGURE 12.—Dependence of the factor $\dfrac{\zeta'_w(\beta=1, t_e, \zeta_w)}{\zeta_{aw}(t_e)-\zeta_w} \Big/ \dfrac{\zeta'_w(\beta=1, t_e=t_s, \zeta_w)}{\zeta_{aw}(t_e=t_s)-\zeta_w}$ upon t_e/t_s.

Correlations for the nonisothermal wall term.—Because the third factor of equation (51) is evaluated at $\beta=1$ and $t_e=t_s$, the yawed infinite cylinder results (eq. (41)) provide a correlation. Equations (40) and (41) may be combined, the assumption again being made that $\bar{r}=0.85$, to yield the ratio

$$\frac{\zeta'_w(\beta=1, t_e=t_s, \zeta_w)}{\zeta'_w(\beta=1, t_e=t_s, \zeta_{w,s})}=\left(\frac{0.85+0.15t_s-\zeta_w}{0.85+0.15t_s-\zeta_{w,s}}\right)\left[\frac{N_{Pr,f,w}}{(N_{Pr,f,w})_s}\right]^{0.4}\frac{[\varphi(t_E, t=t_s, \zeta_w)]^{0.45 \text{ or } 0.67}}{[\varphi(t_E, t=t_s, \zeta_{w,s})]^{0.45 \text{ or } 0.67}} \tag{57}$$

where the values of φ are given by equation (31b) and the choice of exponents depends upon φ as in equation (41); that is, 0.45 for $\varphi \leqq 1$ and 0.67 for $\varphi \geqq 1$. If the correlation is restricted to cases in which $\frac{\zeta_w}{t_s} \lessapprox 1$ (as for the other factors in eq. (51)), then from equation (31b) $\varphi<1$, and equation (57) may be simplified, for $\frac{\zeta_w}{t_s} \lessapprox 1$, to

$$\frac{\zeta'_w(\beta=1, t_e=t_s, \zeta_w)}{\zeta'_w(\beta=1, t_e=t_s, \zeta_{w,s})}=\left(\frac{0.85+0.15t_s-\zeta_w}{0.85+0.15t_s-\zeta_{w,s}}\right)\left[\frac{N_{Pr,f,w}}{(N_{Pr,f,w})_s}\right]^{0.4}\left[\frac{1.0213\left(\frac{\zeta_w}{t_E}\right)^{0.3329}-0.0213}{1.0213\left(\frac{\zeta_{w,s}}{t_E}\right)^{0.3329}-0.0213}\right]^{0.45} \tag{58}$$

Relation for dependence of heat-transfer parameter $\zeta'_w/\zeta'_{w,s}$ upon β_s.—The fourth factor of equation (51) is merely the reciprocal of the first evaluated at β_s, $t_e=t_s$, and $\zeta_{w,s}$. Using equation (52) $\left(\text{valid for } \frac{\zeta_w}{t_s} \lessapprox 1\right)$ yields for axisymmetric flow $\left(\beta_s=\frac{1}{2}, t_s=1\right)$, with $\zeta_{w,s} \lessapprox 1$,

$$\frac{\zeta'_w(\beta=1, t_e=t_s=1, \zeta_{w,s})}{\zeta'_w(\beta=\frac{1}{2}, t_e=t_s=1, \zeta_{w,s})}=1.033 \tag{59}$$

For the yawed infinite cylinder $\beta_s=1$ and the factor in question is unity independent of t_s and ζ_w. A relation encompassing both of these cases is

$$\frac{\zeta'_w(\beta=1,\ t_e=t_s,\ \zeta_{w,s})}{\zeta'_w(\beta_s,\ t_e=t_s,\ \zeta_{w,s})}=(1.033)^j \tag{60}$$

with $j=0$ for the yawed infinite cylinder and $j=1$ for a body of revolution.

Complete correlation formula for heat-transfer-distribution function.—The final result for the heat-transfer-distribution function $\zeta'_w/\zeta'_{w,s}$ is obtained by substituting equations (54), (56), (58), and (60) into equation (51), which yields

$$\frac{\zeta'_w}{\zeta'_{w,s}}=(1.033)^j\left(\frac{1+P\beta^N}{Q+R\beta^N}\right)\left[1+0.050(1-t_s)\left(1-\frac{t_e}{t_s}\right)\left(\frac{\beta-1}{0.2\beta+1}\right)\right]\left[1.1-0.1625\,\frac{t_e}{t_s}+0.0625\left(\frac{t_e}{t_s}\right)^2\right]\left(\frac{0.85+0.15t_e-\zeta_w}{0.85+0.15t_s-\zeta_{w,s}}\right)\left[\frac{N_{Pr,f,w}}{(N_{Pr,f,w})_s}\right]^{0.4}\left[\frac{1.0213\left(\frac{\zeta_w}{t_E}\right)^{0.3329}-0.0213}{1.0213\left(\frac{\zeta_{w,s}}{t_E}\right)^{0.3329}-0.0213}\right]^{0.45} \tag{61}$$

This equation is valid for the conditions $\frac{\zeta_w}{t_s}\lessapprox 1$ and $\beta>0$ but is otherwise independent of enthalpy level (t_E) and wall enthalpy (ζ_w). Equation (61) has a maximum possible error of about 15 percent compared with values obtained from locally similar solutions, and when used in conjunction with equations (23) to (25), completes the description of the laminar heat-transfer distribution on a blunt body of revolution or a yawed infinite cylinder.

Comparison with other solutions.—For a blunt body of revolution, the present correlation formula (eq. (61)) may be compared with that for equilibrium dissociated air with unit Lewis number from reference 2. The comparison is restricted here to the case with an isothermal wall with $\zeta_w\ll 1$ for convenience. If it is noted that βt_e of the present report is the β of reference 2 and that $\xi\mu_o^2L^2$ of the present report is ξ of reference 2, the heat-transfer distribution from the reference may be written in the present notation as

$$\frac{\left(\frac{q_w}{q_{w,s}}\right)_{ref.\,2}}{\frac{\rho_w\mu_w u_e r}{\mu_o L\sqrt{2\xi}}\left[2\rho_w\mu_w\left(\frac{du_e}{dx}\right)\right]_s^{-1/2}}=\frac{1+0.096\sqrt{\beta t_e}}{1.068} \tag{62}$$

The equivalent expression for the present solutions is obtained from equations (9), (19), (23), (24), and (61) (with $\bar{\xi}=0$, $t_s=1$, $j=1$, $F_w=0$, and $\zeta_w=\zeta_{w,s}\ll 1$) as

$$\frac{\frac{q_w}{q_{w,s}}}{\frac{\rho_w\mu_w u_e r}{\mu_o L\sqrt{2\xi}}\left[2\rho_w\mu_w\left(\frac{du_e}{dx}\right)\right]_s^{-1/2}}=1.033\left(\frac{1+0.527\beta^{0.686}}{1.116+0.411\beta^{0.686}}\right)(0.85+0.15t_e)\,(1.10-0.1625t_e+0.0625t_e^2) \tag{63}$$

Equation (62) was derived in reference 2 for values of β no larger than 2. Equation (63), on the other hand, is valid for all positive values of β if $t_e=t_s$. For $t_e<t_s$, equation (63) was derived by using numerical data for values of β up to 3.5 and is thought to be a reasonable approximation up to values of β of about 20. Equations (62) and (63) are compared in figure 13 for various values of t_e over a range of β from 0 to 20. The two sets of curves show qualitative differences arising because of the character of the dependence upon β. Equation (62) (ref. 2) tends to infinity as β approaches infinity whereas the present result remains finite. For values of t_e of 1 and 0.6, this is seen in the divergence of the corresponding curves in figure 13 as β increases above 10.

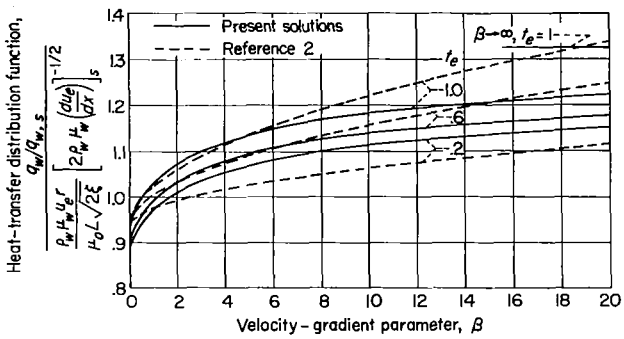

FIGURE 13.—Dependence of heat-transfer distribution function upon β and t_e for a blunt body of revolution. $\zeta_w=0$.

However, for $t_e=0.2$, this divergence must occur at values of β larger than 20. In the range of β between 0 and 10, the two equations differ by at most 5 percent for $t_e=0.2$ and are in much better agreement for the larger values of t_e. The present correlation (eq. (63)) should provide a better representation of the numerical data than that of reference 2 (eq. (62)). However, over the range of β usually encountered (roughly that shown in fig. 13), the two equations will yield results very much in agreement.

The present correlations may also be compared with those for a perfect gas with $\mu\propto T$ and unit Prandtl number from reference 1. For this comparison it is convenient to define a similarity heat-transfer coefficient $\bar{h}$ as

$$\bar{h}=\frac{\zeta'_w}{\zeta_{aw}-\zeta_w} \tag{64}$$

Then, for a comparison of the present results with those of reference 1, it is necessary only to compare the ratios $\bar{h}/\bar{h}_s$. The comparison is here restricted to the yawed infinite cylinder with an isothermal wall. For the present correlations, from equations (61) and (64)

$$\frac{\bar{h}}{\bar{h}_s}=\left(\frac{1+P\beta^N}{Q+R\beta^N}\right)\left[1+0.050(1-t_s)\left(1-\frac{t_e}{t_s}\right)\left(\frac{\beta-1}{0.2\beta+1}\right)\right]\left[1.1-0.1625\left(\frac{t_e}{t_s}\right)+0.0625\left(\frac{t_e}{t_s}\right)^2\right] \tag{65}$$

where $\bar{r}$ is assumed equal to 0.85.

The corresponding expression from reference 1 is

$$\frac{\bar{h}}{\bar{h}_s}=\frac{1+P_1\beta^{N_1}}{Q_1+R_1\beta^{N_1}} \tag{66}$$

where P_1, Q_1, R_1, and N_1 are given in the reference as functions of t_s and ζ_w. The only qualitative difference in the form of equations (65) and (66) is caused by dissipation (excluded in the numerical solutions of reference 1 through the assumption that $N_{Pr}=1$), that is, the terms proportional to $(1-t_s)$ and t_e/t_s in equation (65). These effects are primarily functions of the deviation of the real-air frozen Prandtl number from unity and are not necessarily a result of dissociation.

Equations (65) and (66) are compared in figure 14(a) ($t_s=1$) and figure 14(b) ($t_s=0.1$) for the case $\zeta_w=0$ in equation (66) (which satisfies the condition $\frac{\zeta_w}{t_s}\lessapprox 1$ required by equation (65) for all values of t_s). For $t_e=t_s=1$ in figure 14(a) (no dissipation), the effect of real-air properties is to increase the ratio $\bar{h}/\bar{h}_s$ (compared with that for a perfect gas with $N_{Pr}=1$) by a small amount, which increases with increasing β and reaches about 7 percent at $\beta=20$. The maximum difference, as β

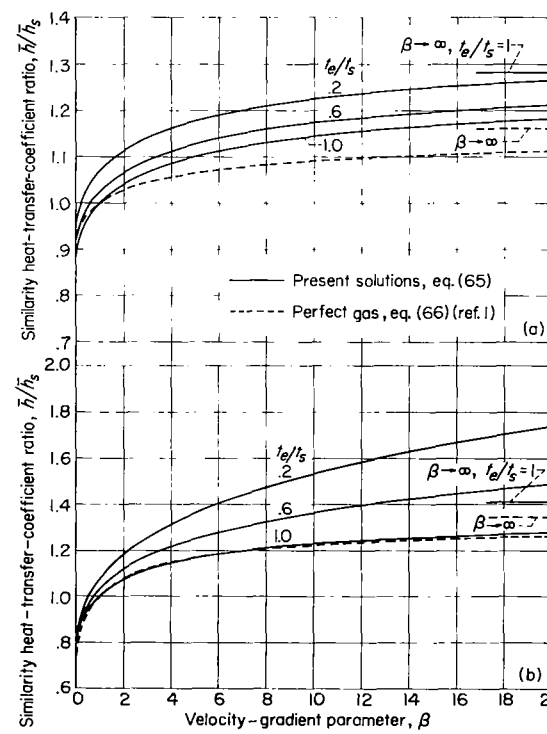

(a) $t_s=1$.
(b) $t_s=0.1$.

FIGURE 14.—Comparison of the similarity heat-transfer-coefficient ratio for the present solutions with that for a perfect gas with $N_{Pr}=1$ and $\mu\propto T$. $\zeta_w=0$.

approaches infinity, is about 12 percent. For increasing chordwise dissipation (decreasing t_e/t_s), the real-air curves depart farther from the perfect-gas curve, with a difference of as much as about 12 percent for $\frac{t_e}{t_s}=0.2$ at $\beta=20$. The same trends are evident at large yaw ($t_s=0.1$, fig. 14(b)), except that for no chordwise dissipation $\left(\frac{t_e}{t_s}=1\right)$ the real-air and perfect-gas curves are extremely close (except for $\beta=0$ where the difference is about 5 percent). A maximum difference of about 12 percent is predicted for infinite β with $t_e=t_s=0.1$. For large chordwise dissipation $\left(\frac{t_e}{t_s}=0.2\right)$ real-air effects are again relatively large; the real-air parameter $\bar{h}/\bar{h}_s$ exceeds that for the $N_{Pr}=1$ gas for this case by about 25 percent for $\beta=20$. Note that large β and $\frac{t_e}{t_s}\lessapprox 0.6$ will generally occur only in regions of relatively low heat-transfer rate.

For high-temperature flight conditions, the present solutions supersede the perfect-gas correlations of reference 1 so long as $\frac{\zeta_w}{t_s}\lessapprox 1$. In situations where the wall is relatively hot and this condition is not met, the present correlations are not valid; in such cases the correlations of reference 1 should give reasonably accurate results judging from the comparison for the highly cooled wall in figures 14(a) and 14(b). However, the effect of dissipation has not been established for such cases.

SIMILAR SOLUTIONS APPLICABLE AT HIGHER ENTHALPY LEVELS

Thus far, the similarity boundary-layer equations, and hence the solutions presented, have been restricted to a binary mixture of atoms and molecules, appropriate for dissociated air up to a nominal static enthalpy level $\frac{h}{h_E}=2.0$. These solutions are appropriate to flight velocities up to 29,000 feet per second for zero yaw, and to higher velocities with finite yaw. When the static enthalpy exceeds about $2h_E$, ionization becomes significant and the simplest representation of the air is that of a mixture of atoms, ions, and electrons. The binary-mixture assumption is no longer valid.

An alternate procedure for computing the boundary layer in such situations is to combine the heat transfer by particle collisions with that from mass diffusion to form a so-called effective conductivity k_{eff}. (See refs. 4 and 5.) This approach is valid for multicomponent mixtures but restricted to chemical equilibrium (the present case). The effective Prandtl number is defined by

$$N_{Pr,\,eff}=\frac{\mu c_{p,\,eff}}{k_{eff}}$$

where $c_{p,\,eff}$ is the effective specific heat. In this way the diffusion terms are contained implicitly in the conduction terms and the boundary-layer equations take on their inert gas form. For example, equations (16) to (18) are valid for an equilibrium multicomponent mixture if $N_{Pr,\,f}$ is formally replaced by $N_{Pr,\,eff}$ and if F is set equal to zero. This substitution is valid for all equations given previously for equilibrium dissociated air and generalizes them to account for an equilibrium mixture of more than two species. This approach was used to make a brief numerical computation in which appropriate transport properties were used to extend the present results to higher enthalpy levels. A description of the procedures follows. Thermal radiation is neglected.

LOCALLY SIMILAR BOUNDARY-LAYER EQUATIONS IN TERMS OF EFFECTIVE PROPERTIES

The locally similar boundary-layer equations for an equilibrium multicomponent mixture are, from equations (26) to (28) and with the substitutions just discussed,

$$(\varphi f'')'+f f''=\beta\left[(f')^2-\frac{\zeta}{t_s}+\left(\frac{1-t_s}{t_s}\right)g^2-\frac{t_e}{t_s}\left(\frac{\rho_e}{\rho}-\frac{t}{t_e}\right)\right] \tag{67}$$

$$(\varphi g')'+fg'=0 \tag{68}$$

$$\left(\frac{\varphi}{N_{Pr,\,eff}}\zeta'\right)'+f\zeta'=\left\{\varphi\left(\frac{1-N_{Pr,\,eff}}{N_{Pr,\,eff}}\right)[(t_s-t_e)(f')^2+(1-t_s)(g^2)']\right\}' \tag{69}$$

with the boundary conditions of equations (29) and (30). The computation program on the IBM 704 electronic data processing machine for equilibrium dissociated air was used with $F\equiv 0$ and with tables of the gas properties $\rho_E\mu_E/\rho\mu$, ρ_E/ρ, and $N_{Pr,\,eff}$ as functions of h/h_E appropriate for this case substituted for the properties used in the equilibrium dissociated air program.

The gas properties were obtained from reference 4 and plotted as functions of enthalpy at constant pressure. These results were found to correlate independent of pressure for the ranges

$$0.0152 \leqq \frac{h}{h_E} \leqq 4 \tag{70}$$

$$10^{-4} \leqq \frac{p}{p_{ref}} \leqq 10^2 \tag{71}$$

with reasonable accuracy. (See fig. 15.) The correlating functions (none of them conveniently expressed by an analytic function) were programed as tables, and the functions are shown in figures 15 (a), (b), and (c).

A group of locally similar solutions was obtained using this program for a range of β from zero to 3.5. The program was limited to heat-transfer cases, in most instances with no chordwise dissipation ($t_e=t_s$). Values of t_s of 1, 1/3, 1/10, and 1/30 were employed, and the enthalpy level parameter t_E was restricted to $t_E \geqq 0.25$, which corresponds to $\frac{1}{t_E}=\frac{H_e}{h_E} \leqq 4$ and $V_\infty \leqq 41{,}100$ feet per second. Lastly, the wall enthalpy range for this program was set as

$$0.0152 \leqq \frac{\zeta_w}{t_E}=\frac{h_w}{h_E} \leqq 0.45$$

corresponding to

$$300^\circ K \leqq T_w \lessapprox \begin{cases} 3{,}600^\circ \text{ K for } \dfrac{p}{p_{ref}}=10^{-4} \\ 5{,}200^\circ \text{ K for } \dfrac{p}{p_{ref}}=10^{2} \end{cases}$$

DISCUSSION OF SIMILAR SOLUTIONS

Flat-plate flow.—Solutions for $\beta=0$ were compared with results obtained by the reference enthalpy method of reference 13. For this case equations (35a), (35c), (36), and figures 15(b) and 15(c) were used with $\bar{r}=\sqrt{0.7}$ in equation (35c) and with $\bar{r}=\sqrt{N^*_{Pr,\,eff}}$ in computing ζ_{aw}. Approximate and exact results for $c_f\sqrt{N_{Re}}$ again agreed within about 5 percent; however, no such good agreement was obtained for the Reynolds analogy factor, where discrepancies as large as 25 to 30 percent were evident. Although these comparisons are not presented, the following observations are of interest. The reason for the failure of the reference enthalpy method in computing the heat transfer lies in the extreme, nonmonotonic variation of the effective Prandtl number with enthalpy. As can be seen from figure 15(c), $N^*_{Pr,\,eff}$ may be as large as 0.96 or as small as 0.28, and equation (36) can in no way account for the fact that a particular extreme value of $N^*_{Pr,\,eff}$ is not necessarily representative of the effective Prandtl number throughout the boundary layer. The largest departures from the Reynolds analogy correlation occurred for $N^*_{Pr,\,eff} \approx 0.9$, whereas for $N^*_{Pr,\,eff}$ from 0.5 to 0.8, agreement between exact and approximate Reynolds analogy factors was better (no cases were computed for which h^* was so large that $N^*_{Pr,\,eff}$ approached 0.3). It may be that the reference enthalpy method might be modified through alteration of the constants in equation (35c) to improve its accuracy. This modification was not attempted. Because of the nonmonotonic behavior of $N^*_{Pr,\,eff}$, it appears unlikely that a single set of formulas like equations (35) and (36) would be sufficient, but instead different formulas covering different wall and stream conditions would be necessary.

Axisymmetric stagnation flow.—Solutions for $t_s=t_e=1$, $\beta=\frac{1}{2}$ were obtained and the Nusselt number function

$$\left[\frac{N_{Nu,\,w}}{(N_{Pr,\,eff,\,w})^{0.4}(N_{Re,\,w})^{0.5}}\right]_s=\sqrt{2}\,\frac{\zeta'_w}{1-\zeta_w}\,\frac{1}{(N_{Pr,\,eff,\,w})^{0.4}} \tag{72}$$

was computed and plotted as a function of $(\rho_e\mu_e/\rho_w\mu_w)_s$. In this equation the Nusselt number is defined by the effective conductivity and specific heat. The results are shown in figure 16, where it is apparent that the correlation of equation (38) obtained for the lower speed range is no longer valid. The discrepancy must be again attributed to the effective Prandtl number; in this case use of the surface Prandtl number in the correlation does not account for the extreme variation of local Prandtl number through the boundary layer. Use of the reference enthalpy of equation (35c) to obtain a correlating Prandtl number gave no improvement and this course was not pursued further. It was found, however, that the data could be correlated as a function of total enthalpy level. Shown in figure 17 are the data, where the parameter

$$\left[\frac{N_{Nu,\,w}}{0.767\left(\frac{\rho_e\mu_e}{\rho_w\mu_w}\right)^{0.43}(N_{Pr,\,eff,\,w})^{0.4}(N_{Re,\,w})^{0.5}}\right]_s$$

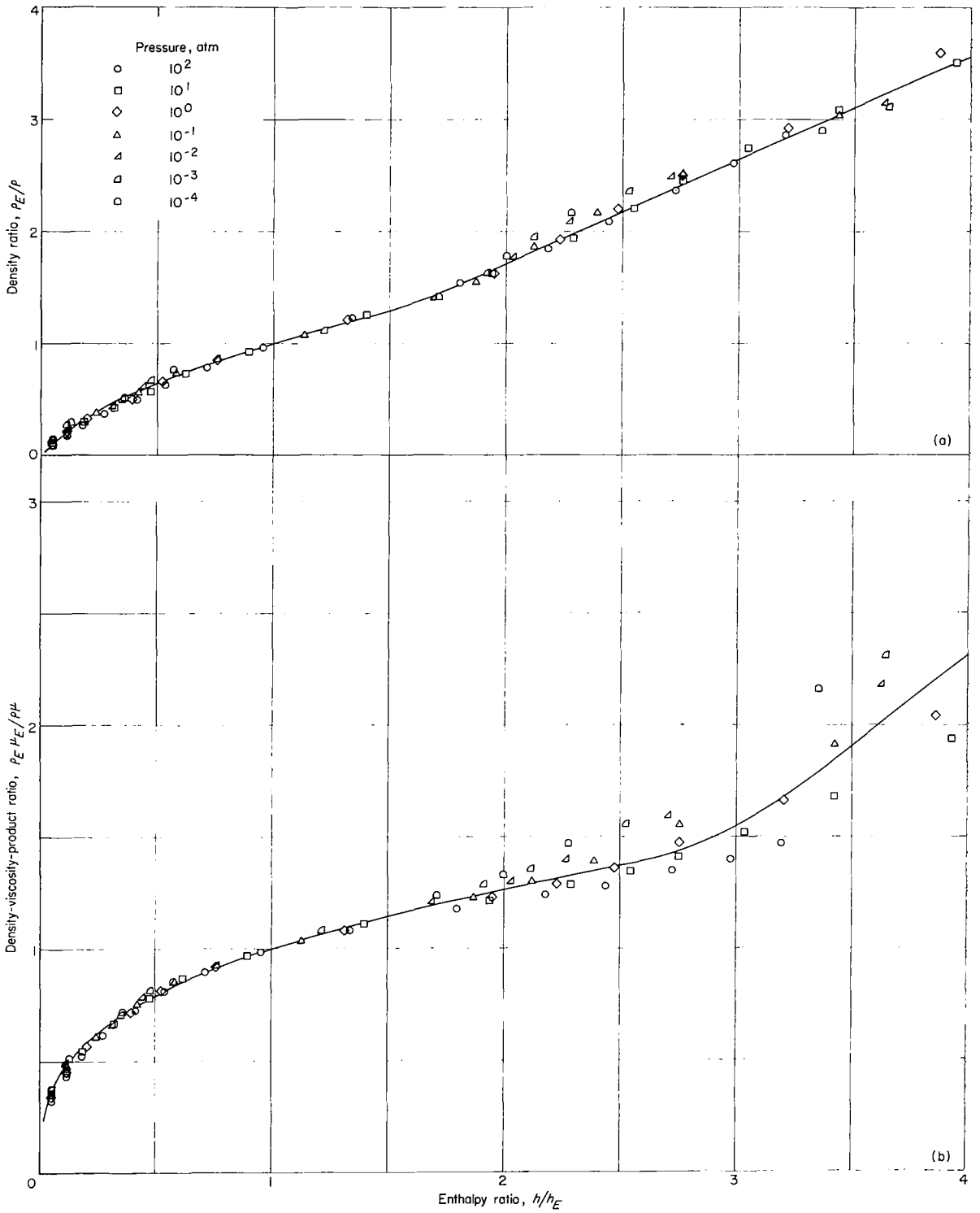

(a) Density.

(b) Density-viscosity product.

FIGURE 15.—Correlations of density, density-viscosity product, and effective Prandtl number for air at enthalpies up to $4h_E = 1{,}000\overline{R}T_{ref}$.

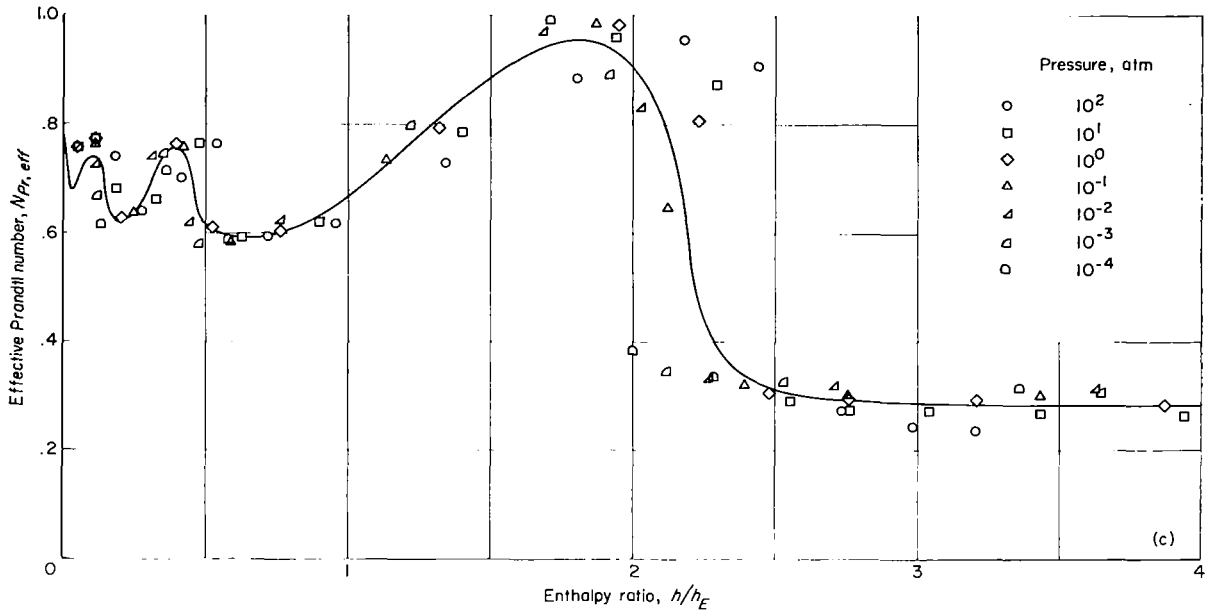

(c) Effective Prandtl number.

FIGURE 15.—Concluded.

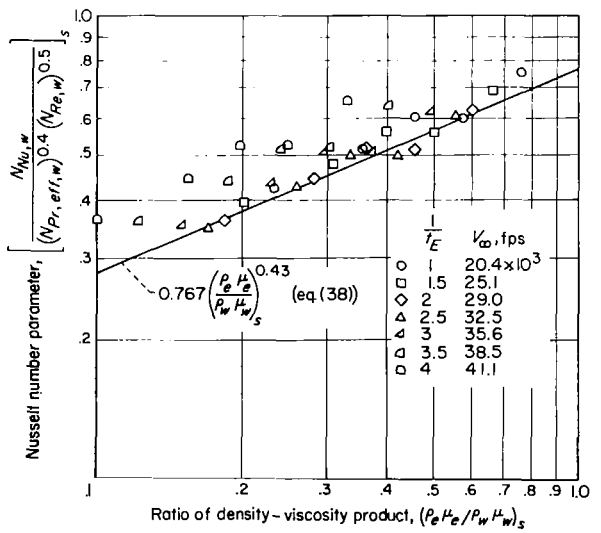

FIGURE 16.—Stagnation-point heat-transfer parameter as a function of $\left(\frac{\rho_e\mu_e}{\rho_w\mu_w}\right)_s$ for a body of revolution at high enthalpy levels.

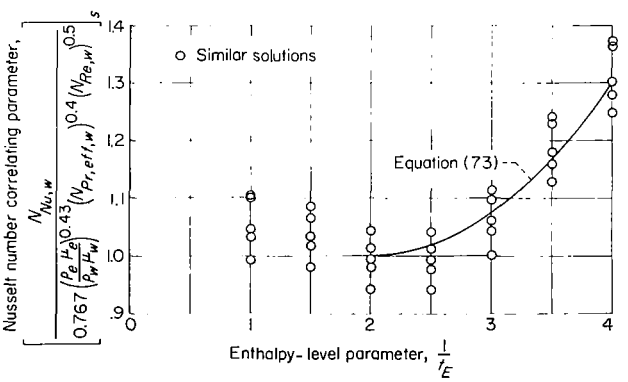

FIGURE 17.—Stagnation-point heat-transfer correlating parameter as a function of enthalpy-level parameter for a body of revolution at high enthalpy levels.

is plotted against $\frac{1}{t_E}=\frac{H_e}{h_E}$. The data correlate within about ±10 percent and are adequately represented by the function, for $2\leqq\frac{1}{t_E}\leqq4$,

$$\left[\frac{N_{Nu,\,w}}{0.767\left(\frac{\rho_e\mu_e}{\rho_w\mu_w}\right)^{0.43}(N_{Pr,\,eff,\,w})^{0.4}(N_{Re,\,w})^{0.5}}\right]_s=1+0.075\left(\frac{1}{t_E}-2\right)^2 \quad (73)$$

For $\frac{1}{t_E}<2$ (the region covered by the equilibrium-dissociated-air calculations), the numerical data

agree reasonably well with equation (38). More scatter is apparent in this lower enthalpy data than was present in the dissociated air calculation; this is attributed to the wider range of surface enthalpy used in the effective property program and also to the fact that for $0.0152 \leqq \frac{1}{t_E} \leqq 2$ the effective property calculations are equivalent to the dissociated air calculations with $F=F_3$, not to $F=0$ for which equation (38) was derived.

The correlations of equations (38) and (73) may be combined to yield a formula for the aerodynamic heat-transfer function covering the entire range of flight velocities to 41,100 feet per second ($t_E \geqq 0.25$). This is

$$\left[\frac{N_{Nu,\,w}}{(N_{Pr,\,eff,\,w})^{0.4}(N_{Re,\,w})^{0.5}}\right]_s = 0.767\left(\frac{\rho_e\mu_e}{\rho_w\mu_w}\right)_s^{0.43} G_1(t_E) \tag{74}$$

where for $0.5 \leqq t_E$,

$$G_1(t_E) = 1 \tag{75a}$$

and for $0.25 \leqq t_E \leqq 0.5$,

$$G_1(t_E) = 1 + 0.075\left(\frac{1}{t_E} - 2\right)^2 \tag{75b}$$

which are valid for the stagnation point of a body of revolution at zero angle of attack within about ± 10 percent.

From equation (74), together with the definitions of the Nusselt, Reynolds, and Prandtl numbers and the assumption of a Newtonian stagnation velocity gradient, a heat-transfer coefficient may be derived as

$$\frac{-q_{w,s}\sqrt{r_N}}{(H_e - h_w)_s} = 0.767\,(N_{Pr,\,eff,\,w})_s^{-0.6}(\rho_e\mu_e)_s^{0.43}(\rho_w\mu_w)_s^{0.07}\left(2\frac{p_e}{\rho_e}\right)_s^{1/4} G_1(t_E) \tag{76}$$

Equation (76) was evaluated for a range of velocities and altitudes of interest and the results are shown in figure 18. Argon-free air was assumed and the thermodynamic properties were taken from reference 18. Normal-shock relations were obtained from unpublished work of Paul W. Huber of the Langley Research Center for argon-free air. These data parallel the data provided by Huber in reference 19 but employ the 1959 ARDC atmosphere (ref. 20) rather than the 1956 atmosphere. Effective transport properties were taken from reference 4. In figure 18(a) the heat-transfer coefficient is plotted against velocity for various altitudes. The circles represent the results of equation (76) for wall temperatures ranging from 300° K to 3,600° K and the results are essentially independent of this parameter. The curves represent a rough correlating plot for each altitude. Because interpolation to intermediate altitudes is awkward, a cross plot of the curves, as shown in figure 18(b), may be used to obtain an engineering approximation for the computation of the stagnation point heat-transfer coefficient. Interpolation to intermediate velocities and altitudes is straightforward.

Stagnation flow for yawed infinite cylinder.— The stagnation-line local enthalpy outside the boundary layer is related to the free-stream total enthalpy by

$$h_s = t_s H_e$$

and in the present effective-property program, only at zero yaw was any effect of the high-enthalpy effective properties apparent. For $t_s = \frac{1}{3}$, $\frac{1}{10}$, and $\frac{1}{30}$, t_s was always less than $2t_E$ and nowhere in the highly cooled boundary layer did the static enthalpy exceed the nominal maximum enthalpy for equilibrium dissociated air. Thus for these cases (with $t_s = t_e < 1$, $\beta = 1$) the results agreed with equation (41) which used $\bar{r} = 0.85$. For zero yaw, a correction factor equal to $G_1(t_E)$ must be applied to equation (41) as in the axisymmetric case. Because the stagnation-line local external properties for a yawed infinite cylinder with free-stream stagnation enthalpy H_e are equivalent to those for another cylinder at zero yaw with a lower stagnation enthalpy equal to h_s, the high-enthalpy correction factor may be generalized for arbitrary yaw by substituting t_s/t_E for $1/t_E$. Thus, the correlating function for the

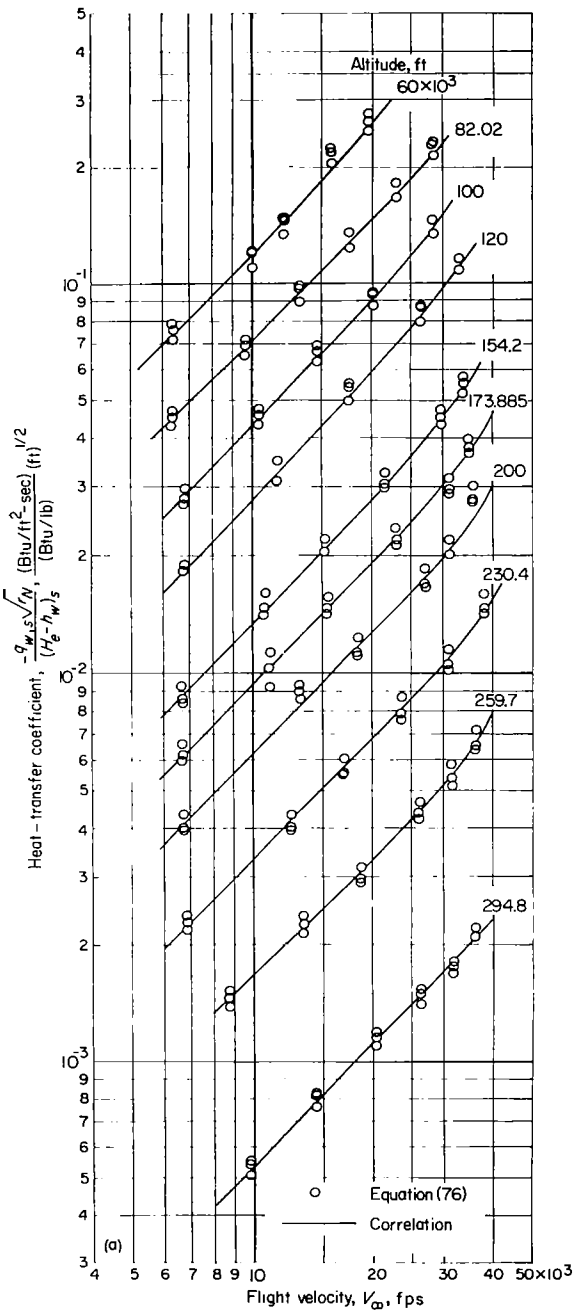

(a) Heat transfer plotted against velocity at various altitudes.

FIGURE 18.—Stagnation-point heat-transfer coefficient for a body of revolution.

Nusselt number parameter is, when $\left(\frac{\rho_e\mu_e}{\rho_w\mu_w}\right)_s<1$,

$$\left[\frac{N_{Nu,\,w}}{(N_{Pr,\,eff,\,w})^{0.4}(N_{Re,\,w})^{0.5}}\right]_s=0.57\left(\frac{\rho_e\mu_e}{\rho_w\mu_w}\right)_s^{0.45}G_1\left(\frac{t_E}{t_s}\right) \tag{77a}$$

and when $\left(\frac{\rho_e\mu_e}{\rho_w\mu_w}\right)_s>1$

$$\left[\frac{N_{Nu,\,w}}{(N_{Pr,\,eff,\,w})^{0.4}(N_{Re,\,w})^{0.5}}\right]_s=0.57\left(\frac{\rho_e\mu_e}{\rho_w\mu_w}\right)_s^{0.67}G_1\left(\frac{t_E}{t_s}\right) \tag{77b}$$

where, for $0.5\leqq\frac{t_E}{t_s}$,

$$G_1\left(\frac{t_E}{t_s}\right)=1 \tag{78a}$$

and for $0.25\leqq\frac{t_E}{t_s}\leqq 0.5$,

$$G_1\left(\frac{t_E}{t_s}\right)=1+0.075\left(\frac{t_s}{t_E}-2\right)^2 \tag{78b}$$

For large yaw the results are valid to velocities in excess of 41,100 feet per second so long as $V_\infty \cos\Lambda\lessapprox$41,100 feet per second.

For the case $\frac{\zeta_w}{t_s}\lessapprox 1\left[\left(\frac{\rho_e\mu_e}{\rho_w\mu_w}\right)_s\lessapprox 1\right]$, the plots in figures 18(a) and 18(b) may be used to give approximate yawed-cylinder stagnation-line heat-transfer coefficients if $V_\infty \cos\Lambda$ is substituted for V_∞, h_{aw} is substituted for H_e in the coefficient, and if the heat-transfer coefficient is multiplied by $\frac{0.57}{0.767}=0.743$. At values of velocity and yaw angle such that $V_\infty \cos\Lambda$ is less than 29,000 feet per second, the use of $\bar{r}=0.85$ should give satisfactory results but at higher velocities this assumption may require modification. However, for $\frac{\zeta_w}{t_s}>1\left[\left(\frac{\rho_e\mu_e}{\rho_w\mu_w}\right)_s>1\right]$, figures 18(a) and 18(b) should not be used for the yawed cylinder unless an additional correction to account for the difference in the exponents of the $\left(\frac{\rho_e\mu_e}{\rho_w\mu_w}\right)_s$ factor in equations (74) and (77) is inserted.

The heat-transfer-distribution parameter.—The effect of β upon the parameter $\frac{\zeta_w'(\beta,\ t_e=t_s,\ \zeta_w)}{\zeta_w'(\beta=1,\ t_e=t_s,\ \zeta_w)}$ was investigated for a range of β from zero to 3.5

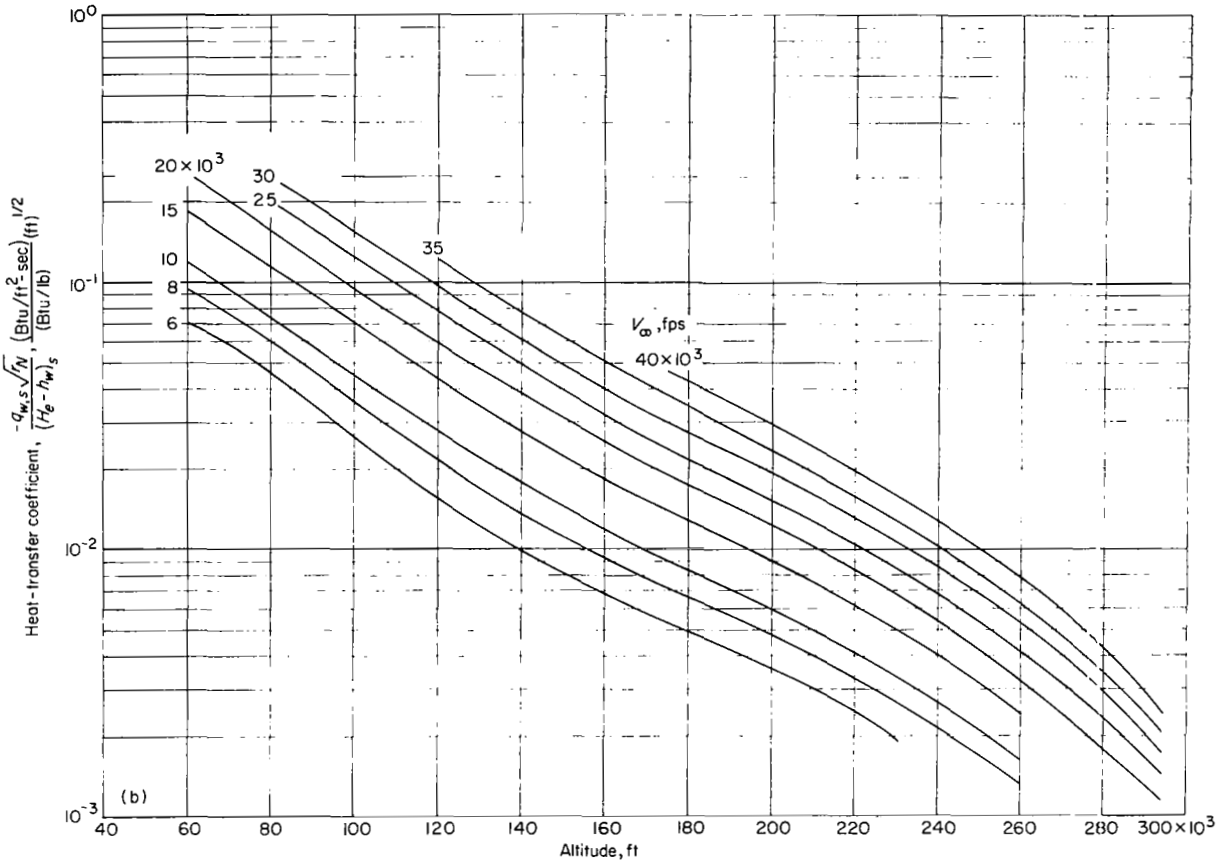

(b) Heat transfer plotted against altitude for various velocities.

FIGURE 18.—Concluded.

and, for $t_e=t_s$, the numerical data were found to be correlated by the same relation as for equilibrium dissociated air, namely by equation (52) with the same values for the parameters P, Q, R, and N. The few solutions obtained for $t_e<t_s$ indicated reasonably good agreement with equation (54) but did not correlate too well with equation (56). The discrepancy was such that use of a lower value of $\bar{r}$ in equation (55) would have accounted for the difference. At very high enthalpy levels the recovery factor would be expected to be lower than 0.85 because of the lower effective Prandtl numbers. If the appropriate values of $\bar{r}$ were known, equation (55) might well be applicable, but because no insulated wall solutions were made in the present program this knowledge is not available. It is suggested that equation (56) be used without modification, inasmuch as, at worst, slightly conservative results will be obtained at very high enthalpy levels. The same comment is appropriate for the recovery factor as it appears in the nonisothermal wall term, equations (57) and (58). Furthermore, so long as the wall enthalpy is such that the condition

$\frac{\zeta_w}{t_s}\lessapprox 1$ (required for the validity of the correlations)

is met, no modification of the φ term in equations (57) and (58) is necessary. As a result, equation (61) may be applied to this very high enthalpy case.

SUMMARY OF EQUATIONS FOR HEAT-TRANSFER CALCULATIONS

For convenience, the correlations obtained from the numerical solutions reported herein are listed in the following sections.

FLAT-PLATE FLOW

The flat-plate skin-friction coefficient is (eq. (35a))

$$c_f\sqrt{N_{Re}}=0.664\sqrt{\frac{\rho^*\mu^*}{\rho_e\mu_e}}$$

and is valid within about 5 percent for velocities up to 41,100 feet per second. The heat-transfer coefficient is (eq. (36))

$$\frac{N_{St}}{c_f}=\frac{1}{2}(N^*_{Pr,f})^{-2/3}$$

and is valid within about 4 percent up to a velocity of 29,000 feet per second. The properties $\rho^*\mu^*/\rho_e\mu_e$ and $N^*_{Pr,f}$ are evaluated at h^*, which is given by equation (35c) as

$$\frac{h^*}{h_E}=\frac{t^*}{t_E}=\frac{t_e}{t_E}\left[0.5\left(1+\frac{\zeta_w}{t_e}\right)-0.184\left(1-\frac{1}{t_e}\right)\right]$$

For $\frac{h^*}{h_E}\leqq 2.0$, $\frac{\rho^*\mu^*}{\rho_e\mu_e}$ is, according to equation (35b),

$$\frac{\rho^*\mu^*}{\rho_e\mu_e}=\frac{1.0213\left(\frac{t_e}{t_E}\right)^{0.3329}-0.0213}{1.0213\left(\frac{t^*}{t_E}\right)^{0.3329}-0.0213}$$

and $N^*_{Pr,f}$ is given in table I.

For $\frac{h}{h_E}>2.0$, $\frac{\rho^*\mu^*}{\rho_e\mu_e}$ must be computed from the correlation of figure 15(b) and the relation

$$\frac{\rho^*\mu^*}{\rho_e\mu_e}=\frac{\left(\frac{\rho_E\mu_E}{\rho_e\mu_e}\right)}{\left(\frac{\rho_E\mu_E}{\rho^*\mu^*}\right)}$$

Because equation (36) is not valid for velocities in excess of 29,000 feet per second, there is no necessity to evaluate $N^*_{Pr,f}$ for $\frac{h^*}{h_E}>2.0$.

AXISYMMETRIC STAGNATION FLOW

The heat-transfer rate for axisymmetric stagnation flow is given (from eq. (74) and the definition of the Nusselt number) by the relation

$$-q_{w,s}=0.767(N_{Pr,w})_s^{-0.6}(H_e-h_w)_s$$
$$(\rho_e\mu_e)_s^{0.43}(\rho_w\mu_w)_s^{0.07}\sqrt{\left(\frac{du_e}{dx}\right)_s}G_1(t_E) \quad (79)$$

where, for velocities up to 29,000 feet per second ($t_E\geqq 0.5$),

$$\left.\begin{aligned}N_{Pr,w}&=N_{Pr,f,w}\\G_1(t_E)&=1\end{aligned}\right\} \quad (80)$$

and for velocities from 29,000 to 41,100 feet per second ($0.25\leqq t_E\leqq 0.5$),

$$\left.\begin{aligned}N_{Pr,w}&=N_{Pr,eff,w}\\G_1(t_E)&=1+0.075\left(\frac{1}{t_E}-2\right)^2\end{aligned}\right\} \quad (81)$$

Equations (79) and (80) were developed from numerical data for wall temperatures from 300° K to about 1,750° K in the lower velocity range where they represent the data within about 5 percent. For the high-velocity range, the maximum wall temperatures permitted ranged from 3,600° K to 5,200° K, and equations (79) and (81) represent the numerical data within about 10 percent. Plots of the coefficient $\frac{-q_{w,s}\sqrt{r_N}}{(H_e-h_w)_s}$ for axisymmetric stagnation flow as functions of velocity and altitude are given in figures 18(a) and 18(b) for a Newtonian stagnation-point velocity gradient.

STAGNATION FLOW FOR YAWED INFINITE CYLINDER

The yawed-infinite-cylinder stagnation-line heat transfer may be expressed, from equation (77), and the definition of the Nusselt number, as

$$-q_{w,s}=0.57(N_{Pr,w})_s^{-0.6}(h_{aw}-h_w)_s$$
$$(\rho_e\mu_e)_s^{m}(\rho_w\mu_w)_s^{\frac{1}{2}-m}\sqrt{\left(\frac{du_e}{dx}\right)_s}G_1\left(\frac{t_E}{t_s}\right) \quad (82)$$

where

$$h_{aw}=h_e+0.85\left(\frac{u_e^2+v_e^2}{2}\right) \quad (83)$$

and $(N_{Pr,w})_s$, m, and $G_1(t_E/t_s)$ are given in the following table:

$V_\infty \cos \Lambda$, fps	$\frac{t_E}{t_s}$	$\frac{\zeta_w}{t_s}$	$\left(\frac{\rho_e \mu_e}{\rho_w \mu_w}\right)_s$	$(N_{Pr,w})_s$	m	$G_1\left(\frac{t_E}{t_s}\right)$	$T_{w,\max}$, °K
$\leqq 29{,}000$	$\geqq 0.5$	$\leqq 1$	$\leqq 1$	Frozen	0.45	1	1,750
$\leqq 29{,}000$	$< .5$	> 1	> 1	Frozen	.67	1	1,750
$\leqq 41{,}100$	$\geqq .25$	$\leqq 1$	$\leqq 1$	Effective	.45	$1+0.075\left(\frac{t_s}{t_E}-2\right)^2$	3,600 to 5,200
$> 29{,}000$	$< .5$						
$\leqq 41{,}100$	$\geqq .25$	> 1	> 1	Effective	.67	$1+0.075\left(\frac{t_s}{t_E}-2\right)^2$	3,600 to 5,200
$> 29{,}000$	$< .5$						

The maximum error inherent in equation (82) is about 10 percent.

HEAT-TRANSFER-DISTRIBUTION PARAMETER

The heat-transfer distribution on blunt yawed cylinders and bodies of revolution at zero angle of attack may be computed from equations (23) to (25) and the correlation equation (eq. (61))

$$\frac{\zeta'_w}{\zeta'_{w,s}} = (1.033)^J \left(\frac{1+P\beta^N}{Q+R\beta^N}\right)\left[1+0.050(1-t_s)\left(1-\frac{t_e}{t_s}\right)\left(\frac{\beta-1}{0.2\beta+1}\right)\right]\left[1.1-0.1625\,\frac{t_e}{t_s}+0.0625\left(\frac{t_e}{t_s}\right)^2\right]$$
$$\left(\frac{0.85+0.15t_e-\zeta_w}{0.85+0.15t_s-\zeta_{w,s}}\right)\left[\frac{N_{Pr,f,w}}{(N_{Pr,f,w})_s}\right]^{0.4}\left[\frac{1.0213\left(\frac{\zeta_w}{t_E}\right)^{0.3329}-0.0213}{1.0213\left(\frac{\zeta_{w,s}}{t_E}\right)^{0.3329}-0.0213}\right]^{0.45}$$

which is valid for $V_\infty \cos \Lambda \leqq 29{,}000$ feet per second, $\frac{\zeta_w}{t_s} \lessapprox 1$, and $0 \leqq \beta \lessapprox 4$ and represents numerical data within 15 percent. Extension to larger values of β should not introduce significant additional error. Values of P, Q, and N are plotted in figure 9 and $R=1+P-Q$. Lastly, for 29,000 feet per second $< V_\infty \cos \Lambda \leqq 41{,}100$ feet per second, equation (61) should give reasonable, although somewhat conservative, results.

DISCUSSION

VALIDITY OF ASSUMPTION OF CHEMICAL EQUILIBRIUM

Although the present calculations are restricted to the case of chemical equilibrium, the results for dissociated air, $\frac{h}{h_E} \leqq 2$, should be useful for nonequilibrium situations provided that the wall is catalytic and that the flow outside the boundary layer is in equilibrium. This conclusion follows from the results for dissociated air with arbitrary recombination rates in reference 9. Even for a nonequilibrium external flow, it is believed that the heat transfer will be little influenced by finite rate processes so long as equilibrium concentrations exist at the surface.

Those results computed herein for the higher enthalpy levels characterized by significant ionization, however, may very possibly not be independent of reaction rates for catalytic walls. The reason is that for nonequilibrium chemistry, diffusion of electrons and ions may tend to set up significant electric and magnetic fields which can no longer be neglected in the boundary-layer equations. The equilibrium assumption, on the other hand, requires a gas electrically neutral at every point by definition, and therefore the inclusion of these terms is unnecessary. It is of interest that calculations of the stagnation-point heat transfer at velocities to above 40,000 feet per second in reference 21 for frozen chemistry agree substantially with the present results, but in reference 21 the electrical terms were neglected. If it is found that charge separation is negligible when recombination rates are low, the present results may then be used to give reasonably accurate predictions for the nonequilibrium case (provided again that the walls are catalytic). These aspects of aerodynamic heating at velocities characteristic of lunar and planetary reentries warrant further study.

UNCERTAINTY IN TRANSPORT-PROPERTY APPROXIMATIONS OF REFERENCE 4

The transport property values of reference 4 are admittedly only approximations, but should

be reasonable for equilibrium dissociated air. It has been shown here that the stagnation point Nusselt number function for this case is a very weak function of the transport properties. Furthermore, calculations of the stagnation-point heat-transfer rate from equation (39) and the transport properties of reference 4 generally agree with the large body of experimental data available about as well as do calculations obtained by the widely used formula of reference 9 in which the Sutherland viscosity relation and $N_{Le}=1.4$ (a nominal constant) are used. Also, heat-transfer distribution will normally be a very weak function of transport properties as illustrated in figures 13 and 14. On this basis, the transport properties of reference 4 may be accepted for heat-transfer calculations for equilibrium dissociated air.

For the case with appreciable ionization characterized by the enthalpy range $2\lessapprox\frac{h}{h_E}\lessapprox 4$, the uncertainty in the validity of the transport properties is greater. The present solutions in this range indicate somewhat greater dependence upon the transport properties than in the dissociated air range, particularly upon the behavior of the effective Prandtl number. Further comment must await experimental or more advanced theoretical efforts in this enthalpy range.

APPLICATION OF THE PRESENT RESULTS TO THREE-DIMENSIONAL FLOWS

The application of the heat-transfer results for a body of revolution to three-dimensional flows with small cross flow is discussed thoroughly in references 3, 6, 7, and 8. The present results may be applied to such problems by replacing r/L in equation (25) by the inviscid streamline spacing at the surface and by integrating this equation along the inviscid surface streamlines. The correlation formula for $\zeta'_w/\zeta'_{w,s}$ (eq. (61)) is applied for $t_s=1$ and the factor $(1.033)^j$ in this equation is replaced by the factor

$$\frac{\zeta'_w(\beta=1, t_e=1, \zeta_{w,s})}{\zeta'_w(\beta_s, t_e=1, \zeta_{w,s})}=\frac{1.116+0.411\beta_s^{0.686}}{1+0.527\beta_s^{0.686}}$$

which is the inverse of equation (52) for $t_s=1$ applied at β_s. The stagnation value of β (that is, β_s) may be computed from the method in reference 8. The stagnation point heat-transfer function is determined by applying the perfect-gas method of reference 22 to the present results.

CONCLUDING REMARKS

Locally similar solutions of the laminar boundary-layer equations have been obtained for air at chemical equilibrium at static enthalpies from $3.8\overline{R}T_{ref}$ (corresponding to a temperature of 300° K) to $1{,}000\overline{R}T_{ref}$ (corresponding to a temperature of from about 8,500° K to about 15,000° K, depending upon pressure level), where $\overline{R}$ is the gas constant for undissociated air and T_{ref} is 273.16° K. The upper enthalpy limit corresponds to the free-stream stagnation enthalpy for atmospheric flight at a velocity of about 41,100 feet per second. For the range of enthalpy up to $500\overline{R}T_{ref}$, which was herein treated extensively, the air was assumed to be an equilibrium mixture of atoms and molecules (equilibrium dissociated air), and the frozen transport properties were taken from the correlations of NASA TN D–194. The upper limit in this enthalpy range corresponds to flight at 29,000 feet per second. For the higher enthalpy range, treated in less detail, the air was assumed to be an equilibrium mixture of atoms, ions, and electrons, and the effective transport properties of NASA TR R–50 were employed.

Exact solutions for flat-plate flow, axisymmetric stagnation flow, and stagnation flow for a yawed infinite cylinder were obtained for equilibrium dissociated air with unit Lewis number. For the flat plate the well-known reference enthalpy approximation gave excellent agreement with the exact solutions. Correlations for the stagnation-flow Nusselt number parameter were determined and found to be little different from previous results obtained by using other estimates of the thermodynamic and transport properties for air. It was shown, however, that the absolute heat-transfer rate would depend more strongly upon the air properties. The effect of nonunit Lewis number was found to be negligible for the enthalpy range characteristic of equilibrium dissociated air.

Locally similar solutions for equilibrium dissociated air were employed to determine a correlating expression for the function used in computing the heat-transfer distribution on a body of revolution at zero angle of attack or on a yawed infinite cylinder with arbitrary favorable pressure gradient. Application of this correlation to the integral and simple local similarity methods of NASA TN D–625 was described. Comparison of this function with previous results based on different gas

property assumptions indicated moderate dependence upon the assumed Prandtl number, although the strongest effect occurred for conditions where the heat transfer would be relatively low.

For the enthalpy range where ionization is important (above $500\overline{R}T_{ref}$) a small group of locally similar solutions was obtained. It was found that the flat-plate and stagnation-flow heat-transfer results were as much as 30 percent higher than a simple extrapolation of the results for equilibrium dissociated air. This behavior is attributed to the low effective Prandtl number predicted in NASA TR R–50 at such high enthalpies. A modified correlation formula to take these results into account for the stagnation point was found and a graph of a stagnation-point heat-transfer function was plotted as a function of flight velocity and altitude. It was also found that the heat-transfer-distribution correlation formula found for equilibrium dissociated air was useful at the higher enthalpy range. A summary of equations for computing heat transfer is included.

Adaptation of the present results to the computation of heat-transfer distribution for three-dimensional flows with small cross flows was briefly described.

LANGLEY RESEARCH CENTER,
NATIONAL AERONAUTICS AND SPACE ADMINISTRATION,
LANGLEY AIR FORCE BASE, VA., *May 22, 1961.*

APPENDIX

SIMILARITY BOUNDARY-LAYER FUNCTIONS FOR EQUILIBRIUM DISSOCIATED AIR

BOUNDARY-LAYER-THICKNESS FUNCTIONS

The boundary-layer integral equations for equilibrium dissociated air may be obtained from equations (16) to (18). First it is convenient to change the form of equation (16) by substitution for the term t/t_e from equation (20). The result is

$$\frac{\partial}{\partial\eta}\left(\varphi\frac{\partial^2 f}{\partial\eta^2}\right)+\left(1-\frac{d\bar{\xi}}{d\xi}\right)f\frac{\partial^2 f}{\partial\eta^2}=\beta\frac{t_e}{t_s}\left[\left(\frac{\partial f}{\partial\eta}\right)^2-\frac{\rho_e}{\rho}\right]+2(\xi-\bar{\xi})\left(\frac{\partial f}{\partial\eta}\frac{\partial^2 f}{\partial\eta\partial\xi}-\frac{\partial f}{\partial\xi}\frac{\partial^2 f}{\partial\eta^2}\right) \quad \text{(A1)}$$

The similarity form of equation (A1) could also have been employed in place of equation (26) in obtaining locally similar solutions. Equations (A1), (17), and (18) are multiplied by $d\eta$ and integrated across the boundary layer from $\eta=0$ to $\eta\to\infty$ using boundary conditions (21) and (22). The results are

$$\frac{d}{d\xi}\left[\sqrt{\xi-\bar{\xi}}(\theta^*_{tr})\right]=\frac{1}{2\sqrt{\xi-\bar{\xi}}}\left[\left(\frac{\partial^2 f}{\partial\eta^2}\right)_w-\beta\frac{t_e}{t_s}(\Delta^*_{tr}+\theta^*_{tr})\right] \quad \text{(A2)}$$

$$\frac{d}{d\xi}\left[\sqrt{\xi-\bar{\xi}}(E_{tr})\right]=\frac{1}{2\sqrt{\xi-\bar{\xi}}}\left(\frac{\partial g}{\partial\eta}\right)_w \quad \text{(A3)}$$

$$\frac{d}{d\xi}\left[\sqrt{\xi-\bar{\xi}}(1-\zeta_w)\Theta_{tr}\right]=\frac{1}{2\sqrt{\xi-\bar{\xi}}}\left(\frac{1+F_w}{N_{Pr,f,w}}\right)\left(\frac{\partial\zeta}{\partial\eta}\right)_w \quad \text{(A4)}$$

where

$$\theta^*_{tr}=\int_0^\infty\frac{\partial f}{\partial\eta}\left(1-\frac{\partial f}{\partial\eta}\right)d\eta \quad \text{(A5)}$$

$$\Delta^*_{tr}=\int_0^\infty\left(\frac{\rho_e}{\rho}-\frac{\partial f}{\partial\eta}\right)d\eta \quad \text{(A6)}$$

$$E_{tr}=\int_0^\infty\frac{\partial f}{\partial\eta}(1-g)d\eta \quad \text{(A7)}$$

$$\Theta_{tr}=\int_0^\infty\frac{\partial f}{\partial\eta}\left(\frac{1-\zeta}{1-\zeta_w}\right)d\eta \quad \text{(A8)}$$

Equations (A2) to (A4) are general within the boundary-layer assumptions and the assumption of an equilibrium binary mixture. Although these equations are cast in the similarity coordinate system, no assumption of local similarity is as yet implied.

For locally similar profiles, equations (A2) to (A4) reduce to

$$\theta^*_{tr}=f''_w-\beta\frac{t_e}{t_s}(\Delta^*_{tr}+\theta^*_{tr}) \quad \text{(A9)}$$

$$E_{tr}=g'_w \quad \text{(A10)}$$

$$\Theta_{tr}=\frac{1+F_w}{N_{Pr,f,w}}\frac{\zeta'_w}{1-\zeta_w} \quad \text{(A11)}$$

In table III(a), listings of the results of the similar solutions include f''_w, g'_w, ζ'_w, and Δ^*_{tr}. The thicknesses θ^*_{tr}, E_{tr}, and Θ_{tr} are not listed, but may be computed from equations (A9) to (A11).

Note that for a perfect gas with constant specific heats, Δ^*_{tr} may be written in terms of other parameters as follows: Since for this special case $\frac{\rho_e}{\rho}=\frac{t}{t_e}$, then

$$\Delta^*_{tr}=\int_0^\infty\left(\frac{t}{t_e}-\frac{\partial f}{\partial\eta}\right)d\eta=\int_0^\infty\left(1-\frac{\partial f}{\partial\eta}\right)d\eta-\int_0^\infty\left(1-\frac{t}{t_e}\right)d\eta$$

and using equation (20) and rearranging gives

$$\Delta^*_{tr}=\frac{t_s}{t_e}\delta^*_{tr}+\frac{t_s-t_e}{t_e}\theta^*_{tr}-\frac{1-\zeta_w}{t_e}\Theta^*_{tr}+\frac{1-t_s}{t_e}G_{tr} \quad \text{(A12)}$$

where

$$\delta^*_{tr}=\int_0^\infty\left(1-\frac{\partial f}{\partial\eta}\right)d\eta \quad \text{(A13)}$$

$$\Theta^*_{tr}=\int_0^\infty\left(\frac{1-\zeta}{1-\zeta_w}\right)d\eta \quad \text{(A14)}$$

$$G_{tr}=\int_0^\infty (1-g^2)d\eta \qquad \text{(A15)}$$

Substitution of equation (A12) into the integrated chordwise momentum equations (eqs. (A2) and (A9)) puts equations (A2) and (A9) in the perfect-gas form used in references 1 and 17.

SKIN-FRICTION AND HEAT-TRANSFER FUNCTIONS

Chordwise and spanwise skin friction are given by

$$\left.\begin{aligned}\tau_{w,x}&=\mu_w\left(\frac{\partial u}{\partial z}\right)_w\\ \tau_{w,y}&=\mu_w\left(\frac{\partial v}{\partial z}\right)_w\end{aligned}\right\} \qquad \text{(A16)}$$

Application of the transformation equations (9) to (15) and the assumption of locally similar profiles gives

$$\left.\begin{aligned}\tau_{w,x}&=\sqrt{\frac{\rho_w\mu_w u_e^2 t_s}{\beta t_e}\frac{du_e}{dx}}\,f''_w\\ \tau_{w,y}&=\sqrt{\frac{\rho_w\mu_w v_e^2 t_s}{\beta t_e}\frac{du_e}{dx}}\,g'_w\end{aligned}\right\} \qquad \text{(A17)}$$

In terms of skin-friction coefficients, equations (A17) may be rewritten

$$\left.\begin{aligned}c_{f,x,w}\sqrt{N_{Re,w}}&=2\sqrt{\frac{t_s}{\beta t_e}\frac{x}{u_e}\frac{du_e}{dx}}\,f''_w\\ c_{f,y,w}\sqrt{N_{Re,w}}&=2\sqrt{\frac{t_s}{\beta t_e}\frac{x}{u_e}\frac{du_e}{dx}}\,g'_w\end{aligned}\right\} \qquad \text{(A18)}$$

The heat-transfer rate at the surface for a gas composed of a reacting mixture of atoms and molecules is (ref. 5, for example)

$$-q_w=\frac{\mu_w}{N_{Pr,f,w}}\left(\frac{\partial h}{\partial z}\right)_w(1+F_w) \qquad \text{(A19)}$$

or, in the similarity coordinate system

$$-q_w=\frac{H_e}{N_{Pr,f,w}}\sqrt{\frac{\rho_w\mu_w t_s}{\beta t_e}\frac{du_e}{dx}}\,\zeta'_w(1+F_w) \qquad \text{(A20)}$$

Definition of the Nusselt number leads to the relation

$$\frac{N_{Nu,w}}{(N_{Re,w})^{1/2}}=\sqrt{\frac{t_s}{\beta t_e}\frac{x}{u_e}\frac{du_e}{dx}}\,\frac{\zeta'_w}{\zeta_{aw}-\zeta_w}(1+F_w) \qquad \text{(A21)}$$

where

$$\zeta_{aw}=t_e+\bar{r}(1-t_e) \qquad \text{(A22)}$$

REFERENCES

1. Beckwith, Ivan E., and Cohen, Nathaniel B.: Application of Similar Solutions to Calculation of Laminar Heat Transfer on Bodies With Yaw and Large Pressure Gradient in High-Speed Flow. NASA TN D-625, 1961.
2. Kemp, Nelson H., Rose, Peter H., and Detra, Ralph W.: Laminar Heat Transfer Around Blunt Bodies in Dissociated Air. Jour. Aero/Space Sci., vol. 26, no. 7, July 1959, pp. 421–430.
3. Cohen, Nathaniel B., and Beckwith, Ivan E.: Boundary-Layer Similar Solutions for Equilibrium Dissociated Air and Application to the Calculation of Laminar Heat-Transfer Distribution on Blunt Bodies in High-Speed Flow. For presentation at the Second International Heat Transfer Conference (Boulder, Colo.), Aug. 28–Sept. 1, 1961.
4. Hansen, C. Frederick: Approximations for the Thermodynamic and Transport Properties of High-Temperature Air. NASA TR R-50, 1959. (Supersedes NACA TN 4150.)
5. Cohen, Nathaniel B.: Correlation Formulas and Tables of Density and Some Transport Properties of Equilibrium Dissociating Air for Use in Solutions of the Boundary-Layer Equations. NASA TN D-194, 1960.
6. Cooke, J. C., and Hall, M. G.: Boundary Layers in Three Dimensions. Rep. No. Aero. 2635, British R.A.E., Feb. 1960.
7. Vaglio-Laurin, Roberto: Laminar Heat Transfer on Three-Dimensional Blunt Nosed Bodies in Hypersonic Flow. ARS Jour., vol. 29, no. 2, Feb. 1959, pp. 123–129.
8. Beckwith, Ivan E.: Similarity Solutions for Small Cross Flows in Laminar Compressible Boundary Layers. NASA TR R-107, 1961.
9. Fay, J. A., and Riddell, F. R.: Theory of Stagnation Point Heat Transfer in Dissociated Air. Jour. Aero. Sci., vol. 25, no. 2, Feb. 1958, pp. 73–85, 121.
10. Hayes, Wallace D., and Probstein, Ronald F.: Hypersonic Flow Theory. Academic Press, Inc. (New York), 1959, pp. 292–294.
11. Lees, Lester: Laminar Heat Transfer Over Blunt-Nosed Bodies at Hypersonic Flight Speeds. Jet Propulsion, vol. 26, no. 4, Apr. 1956, pp. 259–269, 274.
12. Reshotko, Eli, and Beckwith, Ivan E.: Compressible Laminar Boundary Layer Over a Yawed Infinite Cylinder With Heat Transfer and Arbitrary Prandtl Number. NACA Rep. 1379, 1958. (Supersedes NACA TN 3986.)
13. Eckert, Ernst R. G.: Survey on Heat Transfer at High Speeds. WADC Tech. Rep. 54-70, U.S. Air Force, Apr. 1954.
14. Wilson, R. E.: Real Gas Laminar Boundary Layer. Skin Friction and Heat Transfer. U.S. Naval Ord. Lab. (White Oak, Md.), Apr. 11, 1960.

15. Van Driest, E. R.: Investigation of Laminar Boundary Layer in Compressible Fluids Using the Crocco Method. NACA TN 2597, 1952.
16. Sibulkin, M.: Heat Transfer Near the Forward Stagnation Point of a Body of Revolution. Jour. Aero. Sci. (Readers' Forum), vol. 19, no. 8, Aug. 1952, pp. 570–571.
17. Beckwith, Ivan E.: Similar Solutions for the Compressible Boundary Layer on a Yawed Cylinder With Transpiration Cooling. NASA TR R–42, 1959. (Supersedes NACA TN 4345.)
18. Moeckel, W. E., and Weston, Kenneth C.: Composition and Thermodynamic Properties of Air in Chemical Equilibrium. NACA TN 4265, 1958.
19. Huber, Paul W.: Tables and Graphs of Normal-Shock Parameters at Hypersonic Mach Numbers and Selected Altitudes. NACA TN 4352, 1958.
20. Minzner, R. A., Champion, K. S. W., and Pond, H. L.: The ARDC Model Atmosphere, 1959. Air Force Surveys in Geophysics No. 115 (AFCRC–TR–59–267), Air Force Cambridge Res. Center, Aug. 1959.
21. Adams, Mac C.: A Look at the Heat Transfer Problem at Super Satellite Speeds. [Preprint] 1556–60, American Rocket Soc., Dec. 1960.
22. Reshotko, Eli: Heat Transfer to a General Three-Dimensional Stagnation Point. Jet Propulsion, vol. 28, no. 1, Jan. 1958, pp. 58–60.

TABLE I.—GAS PROPERTY CORRELATIONS FOR EQUILIBRIUM DISSOCIATED AIR AT CONSTANT PRESSURE, $10^{-4} \leqq \frac{p}{p_{ref}} \leqq 10$

Low temperature		High temperature				
$\frac{h}{h_E}=\frac{t}{t_E}$	$N_{Pr,f}$	$\frac{h}{h_E}=\frac{t}{t_E}$	$N_{Pr,f}$	F_1	F_2	F_3
0.0005	0.770	0.10	0.768	[a] 0	[a] 0	[b] 0
.010	.739	.20	.771	.190	.236	.231
.015	.708	.30	.755	.171	.269	.112
.020	.689	.40	.742	.087	.168	−.006
.026	.680	.50	.731	.056	.150	.210
.031	.680	.60	.721	.039	.179	.230
.036	.684	.70	.712	.016	.217	.198
.042	.689	.80	.704	−.016	.239	.139
.048	.696	.90	.698	−.052	.257	.075
.053	.702	1.00	.693	−.089	.270	.016
		1.10	.689	−.124	.279	−.040
		1.20	.686	−.159	.287	−.092
		1.30	.684	−.191	.294	−.139
		1.40	.683	−.219	.299	−.181
		1.50	.684	−.244	.304	−.218
		1.60	.686	−.265	.307	−.250
		1.70	.690	−.267	.291	−.270
		1.80	.695	−.259	.270	−.279
		1.90	.700	−.235	.236	−.268
		2.00	.707	−.204	.198	−.235

[a] For $\frac{h}{h_E} \leqq 0.15$, $F_1=F_2=0$.

[b] For $\frac{h}{h_E} \leqq 0.13$, $F_3=0$.

TABLE II.—A KEY TO THE TABLES OF SOLUTIONS FOR EQUILIBRIUM DISSOCIATED AIR

(a) Heat-transfer cases; $F=0$ ($N_{Le}=1$)

l_s	$\frac{l_e}{l_s}$	l_R	V_∞, fps	A, deg	ζ_w	$\frac{h_w}{h_R}$	Range of β	Table	Case
1	1	65.8	0	----------	2	0.0304	0 to 3.4, ∞	III(a)	1
					3	.0456	0 to 2.9		2
					5	.0760	0 to 3.0		3
					6.579	.1000	0 to 2.9		4
1	1	10	6,000	0	.152	.0152	0 to 3.5, ∞		5
					.20	.020	0 to 3.5		6
					.30	.030	0 to 3.5		7
					.50	.050	0 to 3.5, ∞		8
					.75	.075	0 to 3.5, ∞		9
1	.8	10	6,000	0	.50	.05	0 to 3.2		10
	.6						0 to 3.5		11
	.4						0 to 3.5		12
	.2						0 to 3.4		13
1	1	2	14,300	0	.0304	.0152	0 to 3.5, ∞		14
					.05	.025	0 to 3.5		15
					.075	.0375	0 to 3.5		16
					.10	.05	0 to 3.5		17
					.20	.10	0 to 3.5, ∞		18
1	1	1	20,400	0	.0152	.0152	0 to 3.4, ∞		19
					.03	.03	0 to 3.5		20
					.05	.05	0 to 3.5		21
					.075	.075	0 to 3.5		22
					.100	.100	0 to 3.5		23
1	.8	1	20,400	0	.0152	.0152	0 to 3.2		24
	.6						0 to 3.3		25
	.4						0 to 3.4		26
	.2						0 to 3.4		27
1	.8	1	20,400	0	.03	.03	0 to 3.1		28
	.6						0 to 3.0		29
	.4						0 to 3.4		30
	.2						0 to 3.5		31
1	.8	1	20,400	0	.10	.10	0 to 3.3		32
	.6						0 to 3.4		33
	.4						0 to 3.5		34
	.2						0 to 3.5		35
1	1	.5	29,000	0	.0076	.0152	0 to 3.4, ∞		36
					.02	.04	0 to 3.5		37
					.05	.10	0 to 3.5, ∞		38
1	.8	.5	29,000	0	.05	.10	0 to 3.2		39
	.6						0 to 3.4		40
	.4						0 to 3.4		41
	.2						0 to 3.5		42
¼	1	21.9	3,600	90	.3333	.0152	0 to 3.5, ∞		43
					1.0	.0456	0 to 3.3		44
					2.193	.100	0 to 3.1		45
¼	1	3.333	11,000	57	.05066	.0152	0 to 3.3, ∞		46
					.15	.045	0 to 3.4, ∞		47
					.3333	.100	0 to 3.4	↓	48

TABLE II.—A KEY TO THE TABLES OF SOLUTIONS FOR EQUILIBRIUM DISSOCIATED AIR—Continued

(a) Heat-transfer cases; $F=0$ ($N_{Le}=1$)—Concluded

t_s	$\frac{t_s}{t_s}$	t_E	V_∞, fps	Λ, deg	ζ_w	$\frac{h_w}{h_E}$	Range of β	Table	Case
	0.8						0 to 3.5	III(a)	49
	.6						0 to 3.3		50
⅓	.4	3.333	11,000	57	0.05066	0.0152	0 to 3.2		51
	.2						0 to 3.1		52
					.01013	.0152	0 to 3.5, ∞		53
⅓	1	.667	25,100	55	.040	.060	0 to 3.4		54
					.06667	.100	0 to 3.5, ∞		55
	.8						0 to 3.1		56
	.6						0 to 3.2		57
⅓	.4	.667	25,100	55	.040	.060	0 to 3.3		58
	.2						0 to 3.0		59
					.005066	.0152	0 to 3.1, ∞		60
⅓	1	.333	35,600	55	.015	.045	0 to 3.3		61
					.03333	.100	0 to 3.4, ∞		62
	.8						0 to 3.1		63
	.6						0 to 3.3		64
⅓	.4	.333	35,600	55	.03333	.100	0 to 3.5		65
	.2						0 to 3.5		66
					.10	.0152	0 to 3.3, ∞		67
⅓₀	1	6.58	7,600	90	.30	.0456	0 to 3.3, ∞		68
					.6579	.100	0 to 3.1		69
	1						0 to 3.5		70
	.75						0 to 3.1		71
⅓₀	.50	1.73	15,500	74	.0262	.0152	0 to 3.3		72
	.262						0 to 3.3		73
					.0152	.0152	0 to 3.5, ∞		74
⅓₀	1	1	20,400	73	.05	.05	0 to 3.4		75
					.10	.10	0 to 3.4, ∞		76
	.8						0 to 3.0		77
	.6						0 to 3.4		78
⅓₀	.4	1	20,400	73	.10	.10	0 to 3.4		79
	.2						0 to 3.1		80
					.005066	.0152	0 to 3.5, ∞		81
⅓₀	1	.333	35,600	72	.015	.045	0 to 3.5		82
					.03333	.100	0 to 3.5, ∞		83
	.8						0 to 3.5		84
	.6						0 to 3.5		85
⅓₀	.4	.333	35,600	72	.015	.045	0 to 3.1		86
	.2						0 to 3.2		87
					.03333	.0152	0 to 3.0, ∞		88
⅓₀	1	2.19	13,700	90	.10	.0456	0 to 3.1, ∞		89
					.2193	.100	0 to 3.1, ∞		90
					.005066	.0152	0 to 3.3, ∞		91
⅓₀	1	.333	35,600	80	.015	.045	0 to 3.2, ∞		92
	.8						0 to 3.2		93
	.6						0 to 3.2		94
⅓₀	.4	.333	35,600	80	.015	.045	0 to 1.0		95
	.2						0 to 1.0	↓	96
Additional flat-plate solutions ($\beta=0$)									97

TABLE II.—A KEY TO THE TABLES OF SOLUTIONS FOR EQUILIBRIUM DISSOCIATED AIR—Concluded

(b) Insulated wall cases, $F=0$ ($N_{Le}=1$)

t_s	$\frac{t_e}{t_s}$	t_E	V_∞, fps	A, deg	Range of β	Table	Case
1	0.99	1	20,400	0	0 to 1.0	III(b)	1
	.95				0 to 3.0		2
	.8				0 to 3.0		3
	.6				0 to 3.1		4
	.4				0 to 3.1		5
	.2				0 to 3.3		6
1	.99	.5	29,000	0	0 to 1.0		7
	.95				0 to 2.7		8
	.8				0 to 2.7		9
	.6				0 to 3.0		10
	.4				0 to 3.3		11
	.2				0 to 3.4		12
.99	1	1	20,400	5.7	0 to 1		13
.95	1	1	20,400	13	0 to 1		14
1/3	1	21.9	3,600	90	0 to 3.5		15
1/3	1	3.333	11,000	57	0 to 1.0		16
1/3	1	.667	25,100	55	0 to 3.2		17
	.8				0 to 3.2		18
	.4				0 to 3.0		19
	.2				0 to 3.4		20
1/10	1	6.58	7,600	90	0 to 3.0		21
1/10	1	1.73	15,500	74	0 to 3.1		22
	.75				0 to 2.9		23
	.50				0 to 3.0		24
	.262				0 to 3.0		25
1/10	1	1	20,400	73	0 to 3.2		26
	.8				0 to 2.4		27
	.4				0 to 3.0		28
	.2				0 to 2.2		29
1/30	1	2.19			0 to 0.75		30
Additional flat-plate solutions ($\beta=0$)							31

(c) Heat-transfer cases, $N_{Le}\neq 1$

t_s	$\frac{t_e}{t_s}$	t_E	V_∞, fps	A, deg	ζ_w	$\frac{h_w}{h_E}$	Range of β	Table	Case
1	1	2	14,300	0	0.0304	0.0152	0, 1/2, 1	IV(a)	1
		1	20,400	0	.0152	.0152	0, 1/2, 1		2
		1	20,400	0	.10	.10	0 to 3.5		3
		.5	29,000	0	.05	.10	0 to 3.5		4
1/3	1	3.333	11,000	57	.05066	.0152	0, 1/2, 1		5
		3.333	11,000	57	.3333	.10	0, 1/2, 1		6
		.667	25,100	55	.040	.060	0 to 3.5		7
		.667	35,600	55	.03333	.10	0 to 3.5		8
1/10	1	6.58	7,600	90	.6579	.10	0, 1/2, 1		9
		1	20,400	73	.0152	.0152	0, 1/2, 1		10
		.333	35,600	72	.03333	.10	0 to 3.2		11
1/30	1	2.19	13,700	90	.2193	.10	0, 1/2, 1		12
		.333	35,600	80	.005066	.0152	0, 1/2, 1		13
Additional flat-plate solutions ($\beta=0$)									14

(d) Insulated wall cases, $N_{Le}\neq 1$

t_s	$\frac{t_e}{t_s}$	t_E	V_∞, fps	A, deg	Range of β	Table	Case
1/3	1	3.333	11,000	57	0, 1	(IVb)	1
1/3	1	.667	25,100	55	0, 1		2
1/10	1	6.58	7,600	90	0, 1		3
1/10	1	1	20,400	73	0, 1		4
1/30	1	2.19	13,700	90	0, 1		5
Additional flat-plate solutions ($\beta=0$)							6

TABLE III.—TABLES OF SIMILAR SOLUTIONS FOR EQUILIBRIUM DISSOCIATED AIR, $F=0$ ($N_{Le}=1$)

(a) Heat-transfer cases

Case 1:

$t_s=1$; $\frac{t_e}{t_s}=1$; $t_E=65.8$; $V_\infty=0$ fps; $\zeta_w=2$; $\frac{h_w}{h_E}=0.0304$;

$N_{Pr,f,w}=0.680$; $\frac{\rho_e\mu_e}{\rho_w\mu_w}=1.259$

β	g'_w	ζ'_w	f''_w	$\frac{\zeta'_w}{\zeta'_w(\beta=1)}$	Δ^*_{tr}
0	0.4934	−0.4305	0.4934	0.7650	3.017
.5	.6111	−.5253	1.364	.9335	2.041
1.0	.6581	−.5627	1.924	1.0	1.730
1.4	.6822	−.5816	2.289	1.034	1.587
1.8	.7003	−.5958	2.608	1.059	1.488
2.2	.7146	−.6070	2.896	1.079	1.413
2.6	.7265	−.6162	3.160	1.095	1.354
3.0	.7365	−.6239	3.406	1.109	1.306
3.4	.7451	−.6305	3.636	1.121	------
∞	.9600	−.7862	--------	1.397	------

Case 2:

$t_s=1$; $\frac{t_e}{t_s}=1$; $t_E=65.8$; $V_\infty=0$ fps; $\zeta_w=3$; $\frac{h_w}{h_E}=0.0456$;

$N_{Pr,f,w}=0.693$; $\frac{\rho_e\mu_e}{\rho_w\mu_w}=1.475$

β	g'_w	ζ'_w	f''_w	$\frac{\zeta'_w}{\zeta'_w(\beta=1)}$	Δ^*_{tr}
0	0.5076	−0.9048	0.5076	0.7235	4.747
.5	.6614	−1.158	1.721	.9259	3.167
1.0	.7183	−1.251	2.487	1.0	2.717
1.4	.7470	−1.297	2.982	1.037	2.515
1.8	.7684	−1.331	3.416	1.064	2.376
2.2	.7852	−1.358	3.807	1.086	2.272
2.6	.7991	−1.380	4.165	1.103	2.191
2.9	.8080	−1.394	4.416	1.115	------

Case 3:

$t_s=1$; $\frac{t_e}{t_s}=1$; $t_E=65.8$; $V_\infty=0$ fps; $\zeta_w=5$; $\frac{h_w}{h_E}=0.0760$;

$N_{Pr,f,w}=0.737$; $\frac{\rho_e\mu_e}{\rho_w\mu_w}=1.795$

β	g'_w	ζ'_w	f''_w	$\frac{\zeta'_w}{\zeta'_w(\beta=1)}$	Δ^*_{tr}
0	0.5211	−1.945	0.5211	0.6726	7.816
.5	.7258	−2.654	2.276	.9177	5.065
1.0	.7952	−2.892	3.357	1.0	4.383
1.4	.8295	−3.009	4.054	1.040	4.084
1.8	.8550	−3.094	4.663	1.070	3.880
2.2	.8749	−3.161	5.209	1.093	3.729
2.6	.8912	−3.216	5.710	1.112	------
3.0	.9048	−3.261	6.175	1.128	------

Case 4:

$t_s=1$; $\frac{t_e}{t_s}=1$; $t_E=65.8$; $V_\infty=0$ fps; $\zeta_w=6.579$; $\frac{h_w}{h_E}=0.1000$;

$N_{Pr,f,w}=0.768$; $\frac{\rho_e\mu_e}{\rho_w\mu_w}=1.969$

β	g'_w	ζ'_w	f''_w	$\frac{\zeta'_w}{\zeta'_w(\beta=1)}$	Δ^*_{tr}
0	0.5246	−2.799	0.5246	0.6463	9.894
.5	.7575	−3.957	2.613	.9139	6.292
1.0	.8332	−4.330	3.886	1.000	5.460
1.4	.8704	−4.512	4.704	1.042	5.100
1.8	.8978	−4.646	5.418	1.073	4.855
2.2	.9193	−4.749	6.059	1.097	4.674
2.6	.9367	−4.833	6.646	1.116	4.535
2.9	.9479	−4.887	7.057	1.129	4.449

Case 5:

$t_s=1$; $\frac{t_e}{t_s}=1$; $t_E=10$; $V_\infty=6{,}000$ fps; $\zeta_w=0.152$; $\frac{h_w}{h_E}=0.0152$;

$N_{Pr,f,w}=0.709$; $\frac{\rho_e\mu_e}{\rho_w\mu_w}=0.5122$

β	g'_w	ζ'_w	f''_w	$\frac{\zeta'_w}{\zeta'_w(\beta=1)}$	Δ^*_{tr}
0	0.3808	0.2845	0.3808	0.9004	0.1939
.5	.4110	.3055	.5410	.9667	.06330
1.0	.4263	.3160	.6464	1.000	.00552
1.4	.4346	.3217	.7136	1.018	−.02340
1.8	.4410	.3260	.7718	1.032	−.04455
2.2	.4462	.3296	.8235	1.043	−.06092
2.6	.4506	.3325	.8704	1.052	−.07410
3.0	.4544	.3351	.9135	1.060	−.08496
3.4	.4576	.3372	.9536	1.067	−.09419
3.5	.4584	.3377	.9632	1.069	.09628
∞	.5485	.3948	-------	1.249	--------

Case 6:

$t_s=1$; $\frac{t_e}{t_s}=1$; $t_E=10$; $V_\infty=6{,}000$ fps; $\zeta_w=0.20$; $\frac{h_w}{h_E}=0.020$;

$N_{Pr,f,w}=0.690$; $\frac{\rho_e\mu_e}{\rho_w\mu_w}=0.5568$

β	g'_w	ζ'_w	f''_w	$\frac{\zeta'_w}{\zeta'_w(\beta=1)}$	Δ^*_{tr}
0	0.3921	0.2695	0.3921	0.8940	0.2630
.5	.4255	.2909	.5756	.9648	.1143
1.0	.4423	.3015	.6971	1.000	.04927
1.4	.4514	.3072	.7753	1.019	.01686
1.8	.4584	.3116	.8431	1.034	−.00679
2.2	.4642	.3152	.9037	1.045	−.02511
2.6	.4690	.3181	.9589	1.055	−.03983
3.0	.4731	.3207	1.010	1.064	−.05197
3.4	.4766	.3229	1.057	1.071	−.06225
3.5	.4775	.3234	1.069	1.073	--------

Case 7:

$t_s=1$; $\frac{t_e}{t_s}=1$; $t_E=10$; $V_\infty=6{,}000$ fps; $\zeta_w=0.30$; $\frac{h_w}{h_E}=0.030$;

$N_{Pr,f,w}=0.680$; $\frac{\rho_e\mu_e}{\rho_w\mu_w}=0.6419$

β	g'_w	ζ'_w	f''_w	$\frac{\zeta'_w}{\zeta'_w(\beta=1)}$	Δ^*_{tr}
0	0.4113	0.2428	0.4113	0.8819	0.4074
.5	.4510	.2646	.6407	.9613	.2206
1.0	.4706	.2753	.7939	1.000	.1409
1.4	.4812	.2810	.8931	1.021	.1016
1.8	.4893	.2854	.9797	1.037	.07285
2.2	.4960	.2890	1.057	1.050	.05075
2.6	.5015	.2919	1.128	1.060	.03002
3.0	.5063	.2944	1.194	1.070	.01832
3.4	.5104	.2966	1.256	1.077	.00594
3.5	.5114	.2971	1.271	1.079	.00316

Case 8:

$t_s=1$; $\frac{t_e}{t_s}=1$; $t_E=10$; $V_\infty=6{,}000$ fps; $\zeta_w=0.50$; $\frac{h_w}{h_E}=0.050$;

$N_{Pr,f,w}=0.699$; $\frac{\rho_e\mu_e}{\rho_w\mu_w}=0.7833$

β	g'_w	ζ'_w	f''_w	$\frac{\zeta'_w}{\zeta'_w(\beta=1)}$	Δ^*_{tr}
0	0.4379	0.1876	0.4379	0.8627	0.6822
.5	.4885	.2079	.7481	.9560	.4215
1.0	.5126	.2175	.9557	1.000	.3151
1.4	.5255	.2226	1.091	1.023	.2631
1.8	.5355	.2265	1.209	1.041	.2255
2.2	.5435	.2296	1.316	1.056	.1966
2.6	.5503	.2322	1.414	1.068	.1736
3.0	.5560	.2345	1.505	1.078	.1545
3.4	.5610	.2364	1.590	1.087	.1385
3.5	.5621	.2368	1.610	1.089	.1349
∞	.6972	.2864	-------	1.317	------

TABLE III.—TABLES OF SIMILAR SOLUTIONS FOR EQUILIBRIUM DISSOCIATED AIR, $F=0$ ($N_{Le}=1$)—Con.

(a) Heat-transfer cases—Continued

β	g'_w	ζ'_w	f''_w	$\frac{\zeta'_w}{\zeta'_w(\beta=1)}$	Δ^*_{tr}
Case 9: $t_s=1$; $\frac{t_e}{t_s}=1$; $t_E=10$; $V_\infty=6{,}000$ fps; $\zeta_w=0.75$; $\frac{h_w}{h_E}=0.075$; $N_{Pr,f,w}=0.735$; $\frac{\rho_e\mu_e}{\rho_w\mu_w}=0.9149$					
0	0.4580	0.1013	0.4580	0.8444	0.9900
.5	.5194	.1141	.8517	.9512	.6442
1.0	.5478	.1199	1.114	1.000	.5088
1.4	.5629	.1230	1.285	1.026	.4435
1.8	.5745	.1254	1.436	1.046	.3966
2.2	.5838	.1272	1.571	1.061	.3608
2.6	.5915	.1288	1.696	1.074	.3323
3.0	.5981	.1302	1.811	1.085	.3088
3.4	.6039	.1313	1.920	1.095	.2891
3.5	.6052	.1316	1.946	1.097	.2847
∞	.7570	.1608	-------	1.341	----------
Case 10: $t_s=1$; $\frac{t_e}{t_s}=0.8$; $t_E=10$; $V_\infty=6{,}000$ fps; $\zeta_w=0.50$; $\frac{h_w}{h_E}=0.05$; $N_{Pr,f,w}=0.699$; $\frac{\rho_e\mu_e}{\rho_w\mu_w}=0.8468$					
0	0.4442	0.1805	0.4442	0.8706	0.9046
.5	.4954	.1987	.7442	.9582	.5865
1.0	.5205	.2074	.9468	1.000	.4518
1.4	.5342	.2120	1.079	1.022	.3854
1.8	.5448	.2156	1.195	1.040	.3371
2.2	.5534	.2185	1.300	1.053	.3000
2.6	.5606	.2209	1.396	1.065	.2702
3.0	.5667	.2229	1.485	1.075	.2457
3.2	.5695	.2238	1.527	1.079	----------
Case 11: $t_s=1$; $\frac{t_e}{t_s}=0.6$; $t_E=10$; $V_\infty=6{,}000$ fps; $\zeta_w=0.50$; $\frac{h_w}{h_E}=0.05$; $N_{Pr,f,w}=0.699$; $\frac{\rho_e\mu_e}{\rho_w\mu_w}=0.9367$					
0	0.4521	0.1723	0.4521	0.8798	1.251
.5	.5040	.1882	.7411	.9606	.8412
1.0	.5305	.1959	.9387	1.000	.6619
1.4	.5452	.2000	1.068	1.021	.5722
1.8	.5566	.2032	1.182	1.037	.5067
2.2	.5659	.2058	1.284	1.051	.4561
2.6	.5738	.2079	1.379	1.062	.4155
3.0	.5805	.2098	1.466	1.071	.3819
3.4	.5865	.2114	1.548	1.079	.3536
3.5	.5878	.2118	1.568	1.081	.3471
Case 12: $t_s=1$; $\frac{t_e}{t_s}=0.4$; $t_E=10$; $V_\infty=6{,}000$ fps; $\zeta_w=0.5$; $\frac{h_w}{h_E}=0.05$; $N_{Pr,f,w}=0.699$; $\frac{\rho_e\mu_e}{\rho_w\mu_w}=1.081$					
0	0.4620	0.1628	0.4620	0.8892	1.958
.5	.5158	.1763	.7425	.9633	1.360
1.0	.5444	.1830	.9367	1.000	1.091
1.4	.5605	.1866	1.064	1.020	.9549
1.8	.5731	.1895	1.177	1.035	.8549
2.2	.5836	.1917	1.278	1.048	.7774
2.6	.5924	.1936	1.371	1.058	.7147
3.0	.6000	.1953	1.458	1.067	.6633
3.4	.6068	.1967	1.539	1.075	.6195
3.5	.6083	.1978	1.558	1.077	.6096

β	g'_w	ζ'_w	f''_w	$\frac{\zeta'_w}{\zeta'_w(\beta=1)}$	Δ^*_{tr}
Case 13: $t_s=1$; $\frac{t_e}{t_s}=0.2$; $t_E=10$; $V_\infty=6{,}000$ fps; $\zeta_w=0.5$; $\frac{h_w}{h_E}=0.05$; $N_{Pr,f,w}=0.699$; $\frac{\rho_e\mu_e}{\rho_w\mu_w}=1.385$					
0	0.4752	0.1518	0.4752	0.8945	4.812
.5	-------	-------	-------	-------	----------
1.0	.5711	.1697	.9778	1.000	2.738
1.4	.5901	.1729	1.112	1.019	2.421
1.8	.6052	.1753	1.230	1.033	2.188
2.2	.6177	.1773	1.336	1.045	2.008
2.6	.6283	.1790	1.434	1.055	1.863
3.0	.6375	.1804	1.525	1.063	1.744
3.4	.6457	.1817	1.610	1.071	1.643
Case 14: $t_s=1$; $\frac{t_e}{t_s}=1$; $t_E=2$; $V_\infty=14{,}300$ fps; $\zeta_w=0.0304$; $\frac{h_w}{h_E}=0.0152$; $N_{Pr,f,w}=0.709$; $\frac{\rho_e\mu_e}{\rho_w\mu_w}=0.2940$					
0	0.2975	0.2442	0.2975	0.8984	0.1266
.5	.3212	.2625	.4182	.9658	.02830
1.0	.3333	.2718	.4971	1.000	−.01563
1.4	.3400	.2768	.5468	1.019	−.03774
1.8	.3451	.2807	.5894	1.033	−.05391
2.2	.3492	.2839	.6269	1.045	−.06648
2.6	.3527	.2865	.6607	1.054	−.07658
3.0	.3557	.2888	.6916	1.062	−.08494
3.4	.3583	.2907	.7201	1.070	−.09203
3.5	.3589	.2912	.7269	1.071	----------
∞	.4287	.3416	-------	1.257	----------
Case 15: $t_s=1$; $\frac{t_e}{t_s}=1$; $t_E=2$; $V_\infty=14{,}300$ fps; $\zeta_w=0.05$; $\frac{h_w}{h_E}=0.025$; $N_{Pr,f,w}=0.681$; $\frac{\rho_e\mu_e}{\rho_w\mu_w}=0.3448$					
0	0.3195	0.2466	0.3195	0.8957	0.1608
.5	.3457	.2656	.4569	.9650	.05005
1.0	.3591	.2753	.5471	1.000	.000898
1.4	.3664	.2805	.6045	1.019	−.02380
1.8	.3721	.2846	.6539	1.034	−.04189
2.2	.3767	.2878	.6976	1.046	−.05592
2.6	.3805	.2905	.7371	1.055	−.06721
3.0	.3838	.2929	.7733	1.064	−.07655
3.4	.3866	.2949	.8069	1.071	−.08448
3.5	.3873	.2954	.8149	1.073	−.08628
Case 16: $t_s=1$; $\frac{t_e}{t_s}=1$; $t_E=2$; $V_\infty=14{,}300$ fps; $\zeta_w=0.075$; $\frac{h_w}{h_E}=0.0375$; $N_{Pr,f,w}=0.685$; $\frac{\rho_e\mu_e}{\rho_w\mu_w}=0.4014$					
0	0.3414	0.2576	0.3414	0.8925	0.2033
.5	.3705	.2783	.4978	.9640	.07820
1.0	.3853	.2887	.6012	1.000	.02305
1.4	.3933	.2943	.6672	1.020	−.004574
1.8	.3996	.2987	.7244	1.035	−.02481
2.2	.4046	.3022	.7752	1.047	−.04048
2.6	.4089	.3051	.8213	1.057	−.05310
3.0	.4125	.3076	.8636	1.066	−.06353
3.4	.4156	.3098	.9029	1.073	−.07238
3.5	.4164	.3103	.9124	1.075	−.07438

TABLE III.—TABLES OF SIMILAR SOLUTIONS FOR EQUILIBRIUM DISSOCIATED AIR, $F=0$ ($N_{Le}=1$)—Con.

(a) Heat-transfer cases—Continued

Case 17:

$t_s=1$; $\frac{t_e}{t_s}=1$; $t_E=2$; $V_\infty=14{,}300$ fps; $\zeta_w=0.10$; $\frac{h_w}{h_E}=0.05$;

$N_{Pr,f,w}=0.699$; $\frac{\rho_e\mu_e}{\rho_w\mu_w}=0.4497$

β	g'_w	ζ'_w	f''_w	$\frac{\zeta'_w}{\zeta'_w(\beta=1)}$	Δ^*_{tr}
0	0.3584	0.2679	0.3584	0.8894	0.2437
.5	.3900	.2901	.5315	.9631	.1057
1.0	.4059	.3012	.6465	1.000	.04528
1.4	.4146	.3072	.7202	1.020	.01505
1.8	.4214	.3119	.7844	1.036	0
2.2	.4268	.3156	.8413	1.048	−.02417
2.6	.4313	.3187	.8932	1.058	−.03796
3.0	.4352	.3214	.9409	1.067	−.04933
3.4	.4386	.3237	.9854	1.075	−.08799
3.5	.4394	.3243	.9961	1.077	−.06119

Case 18:

$t_s=1$; $\frac{t_e}{t_s}=1$; $t_E=2$; $V_\infty=14{,}300$ fps; $\zeta_w=0.20$; $\frac{h_w}{h_E}=0.10$;

$N_{Pr,f,w}=0.768$; $\frac{\rho_e\mu_e}{\rho_w\mu_w}=0.5790$

β	g'_w	ζ'_w	f''_w	$\frac{\zeta'_w}{\zeta'_w(\beta=1)}$	Δ^*_{tr}
0	0.3965	0.2890	0.3965	0.8796	0.3831
.5	.4352	.3155	.6205	.9603	.2044
1.0	.4545	.3285	.7705	1.000	.1278
1.4	.4649	.3356	.8677	1.021	.08982
1.8	.4729	.3410	.9526	1.038	.06210
2.2	.4795	.3454	1.029	1.051	.04073
2.6	.4848	.3490	1.098	1.062	.02353
3.0	.4896	.3521	1.162	1.072	.009336
3.4	.4937	.3548	1.222	1.080	−.00268
3.5	.4945	.3555	1.237	1.082	−.00537
∞	.6079	.4280	------	1.303	----------

Case 19:

$t_s=1$; $\frac{t_e}{t_s}=1$; $t_E=1$; $V_\infty=20{,}400$ fps; $\zeta_w=0.0152$; $\frac{h_w}{h_E}=0.0152$;

$N_{Pr,f,w}=0.709$; $\frac{\rho_e\mu_e}{\rho_w\mu_w}=0.2322$

β	g'_w	ζ'_w	f''_w	$\frac{\zeta'_w}{\zeta'_w(\beta=1)}$	Δ^*_{tr}
0	0.2652	0.2230	0.2652	0.8977	0.1173
.5	.2867	.2399	.3752	.9654	.02835
1.0	.2978	.2485	.4470	1.000	−.01139
1.4	.3038	.2531	.4924	1.019	−.03142
1.8	.3085	.2567	.5314	1.033	−.04610
2.2	.3123	.2596	.5657	1.045	−.05752
2.6	.3154	.2621	.5966	1.055	−.06670
3.0	.3182	.2641	.6248	1.063	−.07430
3.4	.3205	.2659	.6508	1.070	−.08079
∞	.3847	.3131	------	1.260	----------

Case 20:

$t_s=1$; $\frac{t_e}{t_s}=1$; $t_E=1$; $V_\infty=20{,}400$ fps; $\zeta_w=0.03$; $\frac{h_w}{h_E}=0.03$;

$N_{Pr,f,w}=0.680$; $\frac{\rho_e\mu_e}{\rho_w\mu_w}=0.2909$

β	g'_w	ζ'_w	f''_w	$\frac{\zeta'_w}{\zeta'_w(\beta=1)}$	Δ^*_{tr}
0	0.2948	0.2341	0.2948	0.8957	0.1484
.5	.3193	.2522	.4227	.9649	.04597
1.0	.3318	.2614	.5068	1.000	.00038
1.4	.3386	.2664	.5603	1.019	−.02254
1.8	.3439	.2702	.6063	1.034	−.03936
2.2	.3482	.2733	.6471	1.046	−.05241
2.6	.3518	.2759	.6839	1.056	−.06292
3.0	.3549	.2781	.7176	1.064	−.07163
3.4	.3576	.2801	.7488	1.071	−.07900
3.5	.3582	.2805	.7563	1.073	−.08068

Case 21:

$t_s=1$; $\frac{t_e}{t_s}=1$; $t_E=1$; $V_\infty=20{,}400$ fps; $\zeta_w=0.05$; $\frac{h_w}{h_E}=0.05$;

$N_{Pr,f,w}=0.699$; $\frac{\rho_e\mu_e}{\rho_w\mu_w}=0.3550$

β	g'_w	ζ'_w	f''_w	$\frac{\zeta'_w}{\zeta'_w(\beta=1)}$	Δ^*_{tr}
0	0.3230	0.2580	0.3230	0.8932	0.1869
.5	.3506	.2785	.4705	.9641	.06953
1.0	.3646	.2889	.5682	1.000	.01762
1.4	.3722	.2945	.6306	1.019	−.00844
1.8	.3782	.2988	.6845	1.034	−.02754
2.2	.3830	.3023	.7324	1.047	−.04236
2.6	.3870	.3053	.7758	1.057	−.05429
3.0	.3905	.3078	.8157	1.065	−.06418
3.4	.3935	.3099	.8527	1.073	−.07254
3.5	.3942	.3104	.8616	1.075	----------

Case 22:

$t_s=1$; $\frac{t_e}{t_s}=1$; $t_E=1$; $V_\infty=20{,}400$ fps; $\zeta_w=0.075$; $\frac{h_w}{h_E}=0.075$;

$N_{Pr,f,w}=0.735$; $\frac{\rho_e\mu_e}{\rho_w\mu_w}=0.4146$

β	g'_w	ζ'_w	f''_w	$\frac{\zeta'_w}{\zeta'_w(\beta=1)}$	Δ^*_{tr}
0	0.3461	0.2832	0.3461	0.8904	0.2290
.5	.3765	.3064	.5127	.9634	.09701
1.0	.3920	.3180	.6235	1.000	.03905
1.4	.4004	.3243	.6947	1.020	.01001
1.8	.4069	.3292	.7564	1.035	−.01125
2.2	.4122	.3332	.8114	1.048	−.02773
2.6	.4166	.3364	.8614	1.058	−.04101
3.0	.4204	.3393	.9074	1.067	−.05200
3.4	.4237	.3417	.9502	1.074	−.06126
3.5	.4245	.3423	.9605	1.076	−.06339

Case 23:

$t_s=1$; $\frac{t_e}{t_s}=1$; $t_E=1$; $V_\infty=20{,}400$ fps; $\zeta_w=0.10$; $\frac{h_w}{h_E}=0.10$;

$N_{Pr,f,w}=0.768$; $\frac{\rho_e\mu_e}{\rho_w\mu_w}=0.4571$

β	g'_w	ζ'_w	f''_w	$\frac{\zeta'_w}{\zeta'_w(\beta=1)}$	Δ^*_{tr}
0	0.3607	0.3004	0.3607	0.8880	0.2653
.5	.3933	.3257	.5422	.9627	.1219
1.0	.4098	.3383	.6633	1.000	.05922
1.4	.4187	.3452	.7414	1.020	.02791
1.8	.4257	.3504	.8092	1.036	.005017
2.2	.4313	.3547	.8698	1.048	−.01276
2.6	.4360	.3583	.9249	1.059	−.02704
3.0	.4401	.3613	.9758	1.068	−.03887
3.4	.4436	.3640	1.023	1.076	−.04886
3.5	.4444	.3646	1.035	1.078	−.05114

Case 24:

$t_s=1$; $\frac{t_e}{t_s}=0.8$; $t_E=1$; $V_\infty=20{,}400$ fps; $\zeta_w=0.0152$; $\frac{h_w}{h_E}=0.0152$;

$N_{Pr,f,w}=0.709$; $\frac{\rho_e\mu_e}{\rho_w\mu_w}=0.2505$

β	g'_w	ζ'_w	f''_w	$\frac{\zeta'_w}{\zeta'_w(\beta=1)}$	Δ^*_{tr}
0	0.2703	0.2206	0.2703	0.9008	0.1702
.5	.2916	.2365	.3733	.9658	.06810
1.0	.3030	.2449	.4415	1.000	.02044
1.4	.3093	.2495	.4847	1.019	−.003914
1.8	.3142	.2531	.5218	1.034	−.02190
2.2	.3182	.2560	.5544	1.046	−.03593
2.6	.3216	.2585	.5838	1.056	−.04728
3.0	.3245	.2606	.6107	1.064	−.05672
3.2	.3258	.2616	.6233	1.068	----------

TABLE III.—TABLES OF SIMILAR SOLUTIONS FOR EQUILIBRIUM DISSOCIATED AIR, $F=0$ ($N_{Le}=1$)—Con.

(a) Heat-transfer cases—Continued

Case 25:

$t_s=1$; $\frac{t_e}{t_s}=0.6$; $t_E=1$; $V_\infty=20{,}400$ fps; $\zeta_w=0.0152$; $\frac{h_w}{h_E}=0.0152$;

$N_{Pr,f,w}=0.709$; $\frac{\rho_e\mu_e}{\rho_w\mu_w}=0.2763$

β	g'_w	ζ'_w	f''_w	$\frac{\zeta'_w}{\zeta'_w(\beta=1)}$	Δ^*_{ir}
0	0.2764	0.2189	0.2764	0.9035	0.2577
.5	.2975	.2340	.3718	.9656	.1349
1.0	.3093	.2423	.4360	1.000	.07491
1.4	.3159	.2470	.4768	1.019	.04374
1.8	.3212	.2507	.5119	1.035	.02049
2.2	.3255	.2537	.5428	1.047	.002271
2.6	.3291	.2563	.5707	1.058	−.01251
3.0	.3323	.2585	.5961	1.067	−.02483
3.3	.3344	.2599	.6138	1.073	----------

Case 26:

$t_s=1$; $\frac{t_e}{t_s}=0.4$; $t_E=1$; $V_\infty=20{,}400$ fps; $\zeta_w=0.0152$; $\frac{h_w}{h_E}=0.0152$;

$N_{Pr,f,w}=0.709$; $\frac{\rho_e\mu_e}{\rho_w\mu_w}=0.3174$

β	g'_w	ζ'_w	f''_w	$\frac{\zeta'_w}{\zeta'_w(\beta=1)}$	Δ^*_{ir}
0	0.2840	0.2185	0.2840	0.9055	0.4294
.5	.3049	.2329	.3707	.9652	.2682
1.0	.3172	.2413	.4304	1.000	.1855
1.4	.3244	.2461	.4686	1.020	.1416
1.8	.3301	.2500	.5015	1.036	.1085
2.2	.3348	.2532	.5306	1.050	.08248
2.6	.3388	.2559	.5567	1.061	.06123
3.0	.3423	.2583	.5806	1.071	.04348
3.4	.3454	.2604	.6027	1.080	----------

Case 27:

$t_s=1$; $\frac{t_e}{t_s}=0.2$; $t_E=1$; $V_\infty=20{,}400$ fps; $\zeta_w=0.0152$; $\frac{h_w}{h_E}=0.0152$;

$N_{Pr,f,w}=0.709$; $\frac{\rho_e\mu_e}{\rho_w\mu_w}=0.4028$

β	g'_w	ζ'_w	f''_w	$\frac{\zeta'_w}{\zeta'_w(\beta=1)}$	Δ^*_{ir}
0	0.2941	0.2200	0.2941	0.9065	0.9216
.5	.3149	.2339	.3701	.9638	.6591
1.0	.3281	.2427	.4241	1.000	.5147
1.4	.3360	.2479	.4592	1.022	.4363
1.8	.3424	.2522	.4895	1.039	.3766
2.2	.3479	.2558	.5164	1.054	.3291
2.6	.3526	.2589	.5407	1.067	.2901
3.0	.3567	.2617	.5629	1.078	.2574
3.4	.3604	.2642	.5834	1.089	.2295

Case 28:

$t_s=1$; $\frac{t_e}{t_s}=0.8$; $t_E=1$; $V_\infty=20{,}400$ fps; $\zeta_w=0.03$; $\frac{h_w}{h_E}=0.03$

$N_{Pr,f,w}=0.680$; $\frac{\rho_e\mu_e}{\rho_w\mu_w}=0.3139$

β	g'_w	ζ'_w	f''_w	$\frac{\zeta'_w}{\zeta'_w(\beta=1)}$	Δ^*_{ir}
0	0.3004	0.2313	0.3004	0.8989	0.2107
.5	.3247	.2483	.4203	.9652	.09301
1.0	.3375	.2573	.5002	1.000	.03832
1.4	.3446	.2622	.5511	1.019	.01042
1.8	.3502	.2661	.5950	1.034	−.01018
2.2	.3548	.2692	.6338	1.046	−.02625
2.6	.3586	.2719	.6689	1.057	−.03925
3.0	.3619	.2741	.7010	1.065	−.05005
3.1	.3626	.2746	.7086	1.067	−.05247

Case 29:

$t_s=1$; $\frac{t_e}{t_s}=0.6$; $t_E=1$; $V_\infty=20{,}400$ fps; $\zeta_w=0.03$; $\frac{h_w}{h_E}=0.03$;

$N_{Pr,f,w}=0.680$; $\frac{\rho_e\mu_e}{\rho_w\mu_w}=0.3462$

β	g'_w	ζ'_w	f''_w	$\frac{\zeta'_w}{\zeta'_w(\beta=1)}$	Δ^*_{ir}
0	0.3071	0.2293	0.3071	0.9018	0.2926
.5	.3311	.2454	.4181	.9652	.1717
1.0	.3444	.2543	4933	1.000	.1028
1.4	.3519	.2593	.5415	1.020	.06706
1.8	.3578	.2632	.5830	1.035	.04041
2.2	.3627	.2664	.6198	1.048	.01955
2.6	.3669	.2692	.6531	1.059	.00262
3.0	.3704	.2715	.6835	1.068	−.01148

Case 30:

$t_s=1$; $\frac{t_e}{t_s}=0.4$; $t_E=1$; $V_\infty=20{,}400$ fps; $\zeta_w=0.03$; $\frac{h_w}{h_E}=0.03$;

$N_{Pr,f,w}=0.680$; $\frac{\rho_e\mu_e}{\rho_w\mu_w}=0.3977$

β	g'_w	ζ'_w	f''_w	$\frac{\zeta'_w}{\zeta'_w(\beta=1)}$	Δ^*_{ir}
0	0.3153	0.2286	0.3153	0.9039	0.5135
.5	.3391	.2439	.4163	.9646	.3279
1.0	.3530	.2528	.4862	1.000	.2329
1.4	.3611	.2580	.5312	1.020	.1825
1.8	.3675	.2621	.5701	1.037	.1445
2.2	.3729	.2655	.6047	1.050	.1147
2.6	.3775	.2684	.6359	1.062	.09034
3.0	.3815	.2710	.6645	1.072	.06999
3.4	.3849	.2732	.6909	1.080	.05264

Case 31:

$t_s=1$; $\frac{t_e}{t_s}=0.2$; $t_E=1$; $V_\infty=20{,}400$ fps; $\zeta_w=0.03$; $\frac{h_w}{h_E}=0.03$;

$N_{Pr,f,w}=0.680$; $\frac{\rho_e\mu_e}{\rho_w\mu_w}=0.5048$

β	g'_w	ζ'_w	f''_w	$\frac{\zeta'_w}{\zeta'_w(\beta=1)}$	Δ^*_{ir}
0	0.3263	0.2298	0.3263	0.9052	1.085
.5	.3500	.2446	.4146	.9633	.7834
1.0	.3649	.2539	.4778	1.000	.6175
1.4	.3738	.2595	.5189	1.022	.5274
1.8	.3811	.2640	.5546	1.040	.4589
2.2	.3872	.2678	.5865	1.055	.4044
2.6	.3925	.2712	.6153	1.068	.3597
3.0	.3972	.2741	.6417	1.080	.3222
3.4	.4013	.2767	.6663	1.090	.2901
3.5	.4023	.2773	.6721	1.092	.2825

Case 32:

$t_s=1$; $\frac{t_e}{t_s}=0.8$; $t_E=1$; $V_\infty=20{,}400$ fps; $\zeta_w=0.10$; $\frac{h_w}{h_E}=0.10$;

$N_{Pr,f,w}=0.768$; $\frac{\rho_e\mu_e}{\rho_w\mu_w}=0.4932$

β	g'_w	ζ'_w	f''_w	$\frac{\zeta'_w}{\zeta'_w(\beta=1)}$	Δ^*_{ir}
0	0.3671	0.2955	0.3671	0.8918	0.3574
.5	.3994	.3191	.5377	.9631	.1925
1.0	.4163	.3314	.6530	1.000	.1173
1.4	.4257	.3381	.7276	1.020	.07915
1.8	.4330	.3433	.7925	1.036	.05101
2.2	.4390	.3476	.8504	1.049	.02909
2.6	.4440	.3512	.9032	1.060	.01142
3.0	.4483	.3542	.9519	1.069	−.003251
3.3	.4512	.3563	.9862	1.075	----------

TABLE III.—TABLES OF SIMILAR SOLUTIONS FOR EQUILIBRIUM DISSOCIATED AIR, $F=0$ ($N_{Le}=1$)—Con.

(a) Heat-transfer cases—Continued

Case 33:

$t_s=1$; $\frac{t_e}{t_s}=0.6$; $t_B=1$; $V_\infty=20{,}400$ fps; $\zeta_w=0.10$; $\frac{h_w}{h_B}=0.10$;

$N_{Pr,f,w}=0.768$; $\frac{\rho_e\mu_e}{\rho_w\mu_w}=0.5440$

β	g'_w	ζ'_w	f''_w	$\frac{\zeta'_w}{\zeta'_w(\beta=1)}$	Δ^*_{tr}
0	0.3747	0.2916	0.3747	0.8952	0.5075
.5	.4067	.3137	.5330	.9632	.3092
1.0	.4242	.3257	.6419	1.000	.2142
1.4	.4341	.3324	.7125	1.021	.1652
1.8	.4419	.3377	.7740	1.037	.1288
2.2	.4483	.3420	.8291	1.050	.1003
2.6	.4537	.3457	.8792	1.061	.07718
3.0	.4584	.3489	.9255	1.071	.05799
3.4	.4625	.3517	.9686	1.080	--------

Case 34:

$t_s=1$; $\frac{t_e}{t_s}=0.4$; $t_B=1$; $V_\infty=20{,}400$ fps; $\zeta_w=0.10$; $\frac{h_w}{h_B}=0.10$;

$N_{Pr,f,w}=0.768$; $\frac{\rho_e\mu_e}{\rho_w\mu_w}=0.6249$

β	g'_w	ζ'_w	f''_w	$\frac{\zeta'_w}{\zeta'_w(\beta=1)}$	Δ^*_{tr}
0	0.3840	0.2891	0.3840	0.8980	0.7976
.5	.4156	.3099	.5280	.9628	.5376
1.0	.4340	.3219	.6291	1.000	.4062
1.4	.4445	.3288	.6951	1.021	.3369
1.8	.4530	.3342	.7528	1.038	.2850
2.2	.4600	.3388	.8044	1.053	.2441
2.6	.4660	.3427	.8514	1.065	.2108
3.0	.4712	.3461	.8948	1.075	.1829
3.4	.4758	.3491	.9353	1.085	.1593
3.5	.4769	.3498	.9450	1.087	.1539

Case 35:

$t_s=1$; $\frac{t_e}{t_s}=0.2$; $t_B=1$; $V_\infty=20{,}400$ fps; $\zeta_w=0.10$; $\frac{h_w}{h_B}=0.10$;

$N_{Pr,f,w}=0.768$; $\frac{\rho_e\mu_e}{\rho_w\mu_w}=0.7931$

β	g'_w	ζ'_w	f''_w	$\frac{\zeta'_w}{\zeta'_w(\beta=1)}$	Δ^*_{tr}
0	0.3965	0.2889	0.3965	0.9002	1.613
.5	.4276	.3086	.5218	.9616	1.192
1.0	.4471	.3209	.6126	1.000	.9635
1.4	.4588	.3283	.6725	1.023	.8393
1.8	.4684	.3343	.7250	1.042	.7449
2.2	.4764	.3394	.7721	1.058	.6700
2.6	.4833	.3438	.8152	1.071	.6086
3.0	.4891	.3476	.8549	1.083	.5571
3.4	.4948	.3510	.8920	1.094	.5131
3.5	.4961	.3518	.9009	1.096	.5030

Case 36:

$t_s=1$; $\frac{t_e}{t_s}=1$; $t_B=0.5$; $V_\infty=29{,}000$ fps; $\zeta_w=0.0076$; $\frac{h_w}{h_B}=0.0152$;

$N_{Pr,f,w}=0.709$; $\frac{\rho_e\mu_e}{\rho_w\mu_w}=0.1835$

β	g'_w	ζ'_w	f''_w	$\frac{\zeta'_w}{\zeta'_w(\beta=1)}$	Δ^*_{tr}
0	0.2362	0.2036	0.2362	0.8978	0.1117
.5	.2556	.2190	.3357	.9656	.03141
1.0	.2655	.2268	.4008	1.000	−.004481
1.4	.2709	.2310	.4421	1.019	−.02255
1.8	.2751	.2343	.4775	1.033	−.03582
2.2	.2786	.2369	.5088	1.045	−.04613
2.6	.2815	.2392	.5370	1.055	−.05443
3.0	.2839	.2410	.5627	1.063	−.06133
3.4	.2860	.2427	.2865	1.070	--------
∞	.3440	.2855	-------	1.259	--------

Case 37:

$t_s=1$; $\frac{t_e}{t_s}=1$; $t_B=0.5$; $V_\infty=29{,}000$ fps; $\zeta_w=0.02$; $\frac{h_w}{h_B}=0.04$;

$N_{Pr,f,w}=0.687$; $\frac{\rho_e\mu_e}{\rho_w\mu_w}=0.2569$

β	g'_w	ζ'_w	f''_w	$\frac{\zeta'_w}{\zeta'_w(\beta=1)}$	Δ^*_{tr}
0	0.2778	0.2293	0.2778	0.8962	0.1462
.5	.3010	.2469	.3994	.9651	.04882
1.0	.3128	.2558	.4794	1.000	.005505
1.4	.3193	.2607	.5303	1.019	−.01631
1.8	.3243	.2644	.5742	1.034	−.03227
2.2	.3284	.2674	.6132	1.045	−.04468
2.6	.3318	.2700	.6484	1.055	−.05466
3.0	.3347	.2721	.6807	1.064	−.06295
3.4	.3373	.2740	.7105	1.071	−.06998
3.5	.3379	.2744	.7177	1.073	--------

Case 38:

$t_s=1$; $\frac{t_e}{t_s}=1$; $t_B=0.5$; $V_\infty=29{,}000$ fps; $\zeta_w=0.05$; $\frac{h_w}{h_B}=0.10$;

$N_{Pr,f,w}=0.768$; $\frac{\rho_e\mu_e}{\rho_w\mu_w}=0.3613$

β	g'_w	ζ'_w	f''_w	$\frac{\zeta'_w}{\zeta'_w(\beta=1)}$	Δ^*_{tr}
0	0.3257	0.2918	0.3257	0.8930	0.2057
.5	.3539	.3150	.4784	.9642	.08436
1.0	.3682	.3267	.5798	1.000	.03085
1.4	.3760	.3331	.6448	1.019	.004021
1.8	.3820	.3380	.7012	1.034	−.01565
2.2	.3869	.3419	.7513	1.046	−.03090
2.6	.3911	.3452	.7969	1.057	−.04321
3.0	.3946	.3480	.8388	1.065	−.05335
3.4	.3977	.3505	.8778	1.073	−.06196
3.5	.3984	.3511	.8872	1.074	−.06394
∞	.4838	.4163	-------	1.274	--------

Case 39:

$t_s=1$; $\frac{t_e}{t_s}=0.8$; $t_B=0.5$; $V_\infty=29{,}000$ fps; $\zeta_w=0.05$; $\frac{h_w}{h_B}=0.10$;

$N_{Pr,f,w}=0.768$; $\frac{\rho_e\mu_e}{\rho_w\mu_w}=0.3897$

β	g'_w	ζ'_w	f''_w	$\frac{\zeta'_w}{\zeta'_w(\beta=1)}$	Δ^*_{tr}
0	0.3317	0.2871	0.3317	0.8971	0.2713
.5	.3595	.3087	.4745	.9646	.1342
1.0	.3742	.3201	.5710	1.000	.07082
1.4	.3824	.3263	.6331	1.020	.03855
1.8	.3888	.3312	.6869	1.035	.01470
2.2	.3940	.3351	.7349	1.047	−.00391
2.6	.3984	.3385	.7785	1.057	−.01894
3.0	.4022	.3413	.8185	1.066	−.03146
3.2	.4039	.3426	.8375	1.070	--------

Case 40:

$t_s=1$; $\frac{t_e}{t_s}=0.6$; $t_B=0.5$; $V_\infty=29{,}000$ fps; $\zeta_w=0.05$; $\frac{h_w}{h_B}=0.10$;

$N_{Pr,f,w}=0.768$; $\frac{\rho_e\mu_e}{\rho_w\mu_w}=0.4297$

β	g'_w	ζ'_w	f''_w	$\frac{\zeta'_w}{\zeta'_w(\beta=1)}$	Δ^*_{tr}
0	0.3388	0.2829	0.3389	0.9006	0.3907
.5	.3663	.3031	.4710	.9648	.2277
1.0	.3815	.3142	.5617	1.000	.1484
1.4	.3901	.3204	.6204	1.020	.1073
1.8	.3970	.3253	.6713	1.035	.07664
2.2	.4026	.3293	.7167	1.048	.05255
2.6	.4073	.3327	.7580	1.059	.03300
3.0	.4115	.3357	.7960	1.069	.01671
3.4	.4151	.3383	.8313	1.077	--------

TABLE III.—TABLES OF SIMILAR SOLUTIONS FOR EQUILIBRIUM DISSOCIATED AIR, $F=0$ ($N_{Le}=1$)—Con.

(a) Heat-transfer cases—Continued

Case 41:

$t_s=1$; $\frac{t_s}{t_s}=0.4$; $t_E=0.5$; $V_\infty=29{,}000$ fps; $\zeta_w=0.05$; $\frac{h_w}{h_E}=0.10$;

$N_{Pr,f,w}=0.768$; $\frac{\rho_e\mu_e}{\rho_w\mu_w}=0.4932$

β	g'_w	ζ'_w	f''_w	$\frac{\zeta'_w}{\zeta'_w(\beta=1)}$	Δ^*_{tr}
0	0.3477	0.2800	0.3477	0.9036	0.6235
.5	.3748	.2988	.4672	.9645	.4121
1.0	.3907	.3098	.5511	1.000	.3034
1.4	.3999	.3162	.6057	1.021	.2458
1.8	.4073	.3213	.6532	1.037	.2024
2.2	.4134	.3256	.6957	1.051	.1681
2.6	.4187	.3292	.7343	1.062	.1401
3.0	.4233	.3324	.7698	1.073	.1167
3.4	.4273	.3351	.8028	1.082	.09678

Case 42:

$t_s=1$; $\frac{t_e}{t_s}=0.2$; $t_E=0.5$; $V_\infty=29{,}000$ fps; $\zeta_w=0.05$; $\frac{h_w}{h_E}=0.10$;

$N_{Pr,f,w}=0.768$; $\frac{\rho_e\mu_e}{\rho_w\mu_w}=0.6249$

β	g'_w	ζ'_w	f''_w	$\frac{\zeta'_w}{\zeta'_w(\beta=1)}$	Δ^*_{tr}
0	0.3595	0.2794	0.3595	0.9060	1.268
.5	.3860	.2971	.4623	.9634	.9341
1.0	.4028	.3084	.5369	1.000	.7491
1.4	.4129	.3152	.5860	1.022	.6478
1.8	.4212	.3208	.6291	1.040	.5704
2.2	.4283	.3255	.6676	1.055	.5087
2.6	.4344	.3296	.7027	1.069	.4580
3.0	.4398	.3332	.7351	1.081	.4153
3.4	.4446	.3365	.7652	1.091	.3788
3.5	.4457	.3373	.7724	1.094	.3704

Case 43:

$t_s=0.333$; $\frac{t_e}{t_s}=1$; $t_E=21.9$; $V_\infty=3{,}600$ fps; $\zeta_w=0.3333$; $\frac{h_w}{h_E}=0.0152$;

$N_{Pr,f,w}=0.709$; $\frac{\rho_e\mu_e}{\rho_w\mu_w}=1.000$

β	g'_w	ζ'_w	f''_w	$\frac{\zeta'_w}{\zeta'_w(\beta=1)}$	Δ^*_{tr}
0	0.4540	0.2256	0.4540	0.7735	2.055
.5	.5476	.2725	1.053	.9344	1.368
1.0	.5858	.2917	1.426	1.000	1.138
1.4	.6053	.3014	1.662	1.033	1.032
1.8	.6199	.3087	1.867	1.059	.9577
2.2	.6314	.3145	2.049	1.078	.9017
2.6	.6409	.3192	2.214	1.095	.8578
3.0	.6489	.3232	2.366	1.108	.8222
3.4	.6558	.3267	2.508	1.120	.7926
3.5	.6574	.3275	2.542	1.123	.7859
∞	.8271	.4096	------	1.404	----------

Case 44:

$t_s=0.333$; $\frac{t_e}{t_s}=1$; $t_E=21.9$; $V_\infty=3{,}600$ fps; $\zeta_w=1.000$; $\frac{h_w}{h_E}=0.0456$;

$N_{Pr,f,w}=0.693$; $\frac{\rho_e\mu_e}{\rho_w\mu_w}=1.475$

β	g'_w	ζ'_w	f''_w	$\frac{\zeta'_w}{\zeta'_w(\beta=1)}$	Δ^*_{tr}
0	0.4944	−0.05294	0.4944	0.8031	5.645
.5	.6634	−.06279	1.820	.9525	3.708
1.0	.7231	−.06592	2.635	1.000	3.190
1.4	.7528	−.06736	3.156	1.022	2.961
1.8	.7748	−.06836	3.610	1.037	2.803
2.2	.7921	−.06910	4.016	1.048	2.686
2.6	.8062	−.06968	4.387	1.057	2.596
3.0	.8180	−.07014	4.731	1.064	2.523
3.3	.8258	−.07043	4.974	1.069	----------

Case 45:

$t_s=0.333$; $\frac{t_s}{t_s}=1$; $t_E=21.9$; $V_\infty=3{,}600$ fps; $\zeta_w=2.193$; $\frac{h_w}{h_E}=0.100$;

$N_{Pr,f,w}=0.768$; $\frac{\rho_e\mu_e}{\rho_w\mu_w}=1.969$

β	g'_w	ζ'_w	f''_w	$\frac{\zeta'_w}{\zeta'_w(\beta=1)}$	Δ^*_{tr}
0	0.5163	−0.6410	0.5163	0.6430	10.70
.5	.7584	−.9120	2.687	.9148	6.731
1.0	.8352	−.9969	3.994	1.000	5.843
1.4	.8729	−1.038	4.830	1.041	5.461
1.8	.9005	−1.068	5.557	1.071	5.202
2.2	.9221	−1.091	6.209	1.095	5.012
2.6	.9396	−1.110	6.804	1.114	4.866
3.0	.9543	−1.126	7.355	1.129	3.383
3.1	.9576	−1.129	7.487	1.133	----------

Case 46:

$t_s=0.333$; $\frac{t_e}{t_s}=1$; $t_E=3.333$; $V_\infty=11{,}000$ fps; $\zeta_w=0.05066$; $\frac{h_w}{h_E}=0.0152$;

$N_{Pr,f,w}=0.709$; $\frac{\rho_e\mu_e}{\rho_w\mu_w}=0.5122$

β	g'_w	ζ'_w	f''_w	$\frac{\zeta'_w}{\zeta'_w(\beta=1)}$	Δ^*_{tr}
0	0.3479	0.2587	0.3479	0.8356	0.7060
.5	.3960	.2939	.6089	.9492	.4387
1.0	.4176	.3096	.7703	1.000	.3359
1.4	.4288	.3178	.8708	1.014	.2869
1.8	.4374	.3240	.9564	1.046	.2519
2.2	.4442	.3290	1.032	1.054	.2254
2.6	.4498	.3330	1.099	1.069	.2044
3.0	.4545	.3365	1.161	1.081	.1872
3.3	.4576	.3387	1.204	1.094	----------
∞	.5595	.4098	---------	1.324	----------

Case 47:

$t_s=0.333$; $\frac{t_e}{t_s}=1$; $t_E=3.333$; $V_\infty=11{,}000$ fps; $\zeta_w=0.15$; $\frac{h_w}{h_E}=0.045$;

$N_{Pr,f,w}=0.693$; $\frac{\rho_e\mu_e}{\rho_w\mu_w}=0.7513$

β	g'_w	ζ'_w	f''_w	$\frac{\zeta'_w}{\zeta'_w(\beta=1)}$	Δ^*_{tr}
0	0.4054	0.2584	0.4054	0.8155	1.142
.5	.4699	.2992	.7910	.9440	.7460
1.0	.4980	.3169	1.035	1.000	.6000
1.4	.5126	.3261	1.189	1.029	.5310
1.8	.5237	.3331	1.323	1.051	.4820
2.2	.5326	.3386	1.442	1.068	.4450
2.6	.5398	.3432	1.550	1.083	.4156
3.0	.5460	.3470	1.649	1.095	.3918
3.4	.5513	.3503	1.742	1.106	----------
∞	.6867	.4324	-------	1.364	----------

Case 48:

$t_s=0.333$; $\frac{t_e}{t_s}=1$; $t_E=3.333$; $V_\infty=11{,}000$ fps; $\zeta_w=0.3333$; $\frac{h_w}{h_E}=0.100$;

$N_{Pr,f,w}=0.768$; $\frac{\rho_e\mu_e}{\rho_w\mu_w}=1.009$

β	g'_w	ζ'_w	f''_w	$\frac{\zeta'_w}{\zeta'_w(\beta=1)}$	Δ^*_{tr}
0	0.4490	0.2386	0.4490	0.7881	1.778
.5	.5335	.2838	.9965	.9374	1.191
1.0	.5690	.3027	1.345	1.000	.9860
1.4	.5874	.3125	1.568	1.032	.8907
1.8	.6012	.3199	1.761	1.057	.8235
2.2	.6121	.3258	1.935	1.076	.7728
2.6	.6212	.3306	2.093	1.092	.7329
3.0	.6289	.3347	2.240	1.105	.7003
3.4	.6355	.3382	2.376	1.112	----------

TABLE III.—TABLES OF SIMILAR SOLUTIONS FOR EQUILIBRIUM DISSOCIATED AIR, $F=0$ ($N_{Le}=1$)—Con.

(a) Heat-transfer cases—Continued

Case 49:

$t_s=0.333$; $\frac{t_e}{t_s}=0.8$; $t_E=3.333$; $V_\infty=11{,}000$ fps; $\zeta_w=0.05066$; $\frac{h_w}{h_E}=0.0152$; $N_{Pr,f,w}=0.709$; $\frac{\rho_e\mu_e}{\rho_w\mu_w}=0.5537$

β	g'_w	ζ'_w	f''_w	$\frac{\zeta'_w}{\zeta'_w(\beta=1)}$	Δ^*_{tr}
0	0.3517	0.2591	0.3517	0.8347	0.9348
.5	.4007	.2942	.6074	.9479	.6055
1.0	.4234	.3104	.7675	1.000	.4735
1.4	.4354	.3189	.8674	1.027	.4097
1.8	.4446	.3254	.9526	1.048	.3639
2.2	.4519	.3306	1.027	1.065	.3289
2.6	.4580	.3349	1.095	1.079	.3012
3.0	.4631	.3385	1.156	1.090	.2785
3.4	.4676	.3416	1.212	1.101	.2596
3.5	.4686	.3423	1.226	1.103	.2553

Case 50:

$t_s=0.333$; $\frac{t_e}{t_s}=0.6$; $t_E=3.333$; $V_\infty=11{,}000$ fps; $\zeta_w=0.05066$; $\frac{h_w}{h_E}=0.0152$; $N_{Pr,f,w}=0.709$; $\frac{\rho_e\mu_e}{\rho_w\mu_w}=0.6125$

β	g'_w	ζ'_w	f''_w	$\frac{\zeta'_w}{\zeta'_w(\beta=1)}$	Δ^*_{tr}
0	0.3563	0.2597	0.3563	0.8333	1.299
.5	.4065	.2948	.6065	.9462	.8682
1.0	.4307	.3116	.7656	1.000	.6881
1.4	.4437	.3206	.8655	1.029	.5995
1.8	.4537	.3275	.9506	1.051	.5355
2.2	.4618	.3330	1.026	1.069	.4865
2.6	.4686	.3376	1.093	1.083	.4474
3.0	.4743	.3415	1.154	1.096	.4153
3.3	.4781	.3441	1.197	1.104	.3947

Case 51:

$t_s=0.333$; $\frac{t_e}{t_s}=0.4$; $t_E=3.333$; $V_\infty=11{,}000$ fps; $\zeta_w=0.05066$; $\frac{h_w}{h_E}=0.0152$; $N_{Pr,f,w}=0.7085$; $\frac{\rho_e\mu_e}{\rho_w\mu_w}=0.7067$

β	g'_w	ζ'_w	f''_w	$\frac{\zeta'_w}{\zeta'_w(\beta=1)}$	Δ^*_{tr}
0	0.3620	0.2605	0.3620	0.8296	1.283
.5	.4143	.2963	.6091	.9434	.8807
1.0	.4408	.3140	.7690	1.000	.7056
1.4	.4553	.3237	.8699	1.031	.6182
1.8	.4666	.3312	.9561	1.055	.5546
2.2	.4759	.3373	1.032	1.074	.5056
2.6	.4836	.3424	1.100	1.090	.4661
3.0	.4902	.3468	1.163	1.104	.4341
3.2	.4932	.3488	1.192	1.111	.4199

Case 52:

$t_s=0.333$; $\frac{t_e}{t_s}=0.2$; $t_E=3.333$; $V_\infty=11{,}000$ fps; $\zeta_w=0.05066$; $\frac{h_w}{h_E}=0.0152$; $N_{Pr,f,w}=0.709$; $\frac{\rho_e\mu_e}{\rho_w\mu_w}=0.9054$

β	g'_w	ζ'_w	f''_w	$\frac{\zeta'_w}{\zeta'_w(\beta=1)}$	Δ^*_{tr}
0	0.3695	0.2620	0.3695	0.8130	4.972
.5	.4298	.3020	.6360	.9371	3.422
1.0	.4611	.3222	.8083	1.000	2.750
1.4	.4786	.3335	.9170	1.035	2.415
1.8	.4923	.3423	1.010	1.062	2.171
2.2	.5036	.3495	1.092	1.085	1.984
2.6	.5132	.3556	1.166	1.103	1.834
3.0	.5215	.3608	1.233	1.120	1.711
3.1	.5234	.3620	1.249	1.123	----------

Case 53:

$t_s=0.333$; $\frac{t_e}{t_s}=1$; $t_E=3.333$; $V_\infty=25{,}100$ fps; $\zeta_w=0.01013$; $\frac{h_w}{h_E}=0.0152$; $N_{Pr,f,w}=0.709$; $\frac{\rho_e\mu_e}{\rho_w\mu_w}=0.2940$

β	g'_w	ζ'_w	f''_w	$\frac{\zeta'_w}{\zeta'_w(\beta=1)}$	Δ^*_{tr}
0	0.2683	0.2058	0.2683	0.8391	0.4915
.5	.3042	.2329	.4621	.9497	.2990
1.0	.3206	.2452	.5828	1.000	.2240
1.4	.3293	.2517	.6581	1.026	.1879
1.8	.3358	.2566	.7221	1.046	.1621
2.2	.3411	.2605	.7784	1.062	.1424
2.6	.3454	.2637	.8288	1.075	.1268
3.0	.3491	.2665	.8747	1.087	.1141
3.4	.3522	.2688	.9170	1.096	.1034
3.5	.3530	.3014	.9271	1.098	.1010
∞	.4314	.3261	--------	1.330	----------

Case 54:

$t_s=0.333$; $\frac{t_e}{t_s}=1$; $t_E=3.333$; $V_\infty=25{,}100$ fps; $\zeta_w=0.040$; $\frac{h_w}{h_E}=0.060$; $N_{Pr,f,w}=0.711$; $\frac{\rho_e\mu_e}{\rho_w\mu_w}=0.483$

β	g'_w	ζ'_w	f''_w	$\frac{\zeta'_w}{\zeta'_w(\beta=1)}$	Δ^*_{tr}
0	0.3383	0.2511	0.3383	0.8331	0.7059
.5	.3857	.2858	.6059	.9482	.4419
1.0	.4072	.3014	.7747	1.000	.3404
1.4	.4184	.3096	.8811	1.027	.2919
1.8	.4270	.3158	.9724	1.048	.2572
2.2	.4338	.3208	1.053	1.064	.2308
2.6	.4395	.3229	1.126	1.078	.2099
3.0	.4443	.3283	1.193	1.089	.1928
3.4	.4484	.3313	1.255	1.099	----------

Case 55:

$t_s=0.333$; $\frac{t_e}{t_s}=1$; $t_E=0.667$; $V_\infty=25{,}100$ fps; $\zeta_w=0.06667$; $\frac{h_w}{h_E}=0.100$; $N_{Pr,f,w}=0.761$; $\frac{\rho_e\mu_e}{\rho_w\mu_w}=0.5790$

β	g'_w	ζ'_w	f''_w	$\frac{\zeta'_w}{\zeta'_w(\beta=1)}$	Δ^*_{tr}
0	0.3663	0.2848	0.3663	0.8285	0.8324
.5	.4194	.3255	.6738	.9470	.5292
1.0	.4433	.3438	.8089	1.000	.4137
1.4	.4558	.3533	.9925	1.028	.3587
1.8	.4652	.3605	1.099	1.049	.3194
2.2	.4728	.3663	1.193	1.065	.2895
2.6	.4791	.3710	1.279	1.079	.2658
3.0	.4844	.3750	1.357	1.091	.2465
3.4	.4890	.3785	1.430	1.101	.2302
3.5	.4901	.3793	1.448	1.103	.2266
∞	.6077	.4658	--------	1.355	----------

Case 56:

$t_s=0.333$; $\frac{t_e}{t_s}=0.8$; $t_E=0.667$; $V_\infty=25{,}100$ fps; $\zeta_w=0.040$; $\frac{h_w}{h_E}=0.060$; $N_{Pr,f,w}=0.711$; $\frac{\rho_e\mu_e}{\rho_w\mu_w}=0.5213$

β	g'_w	ζ'_w	f''_w	$\frac{\zeta'_w}{\zeta'_w(\beta=1)}$	Δ^*_{tr}
0	0.3421	0.2512	0.3421	0.8345	0.8919
.5	.3895	.2852	.5987	.9472	.5836
1.0	.4119	.3010	.7632	1.000	.4587
1.4	.4238	.3095	.8674	1.028	.3980
1.8	.4329	.3159	.9569	1.049	.3542
2.2	.4403	.3210	1.036	1.067	.3207
2.6	.4464	.3254	1.108	1.081	.2941
3.0	.4516	.3290	1.173	1.093	.2721
3.1	.4528	.3299	1.189	1.096	.2673

TABLE III.—TABLES OF SIMILAR SOLUTIONS FOR EQUILIBRIUM DISSOCIATED AIR, $F=0$ ($N_{Le}=1$)—Con.

(a) Heat-transfer cases—Continued

Case 57:

$t_s=0.333$; $\frac{t_e}{t_s}=0.6$; $t_E=0.667$; $V_\infty=25{,}100$ fps; $\zeta_w=0.040$; $\frac{h_w}{h_E}=0.060$;

$N_{Pr,f,w}=0.711$; $\frac{\rho_e\mu_e}{\rho_w\mu_w}=0.5754$

β	g'_w	ζ'_w	f''_w	$\frac{\zeta'_w}{\zeta'_w(\beta=1)}$	Δ^*_{tr}
0	0.3464	0.2517	0.3464	0.8359	1.192
.5	.3937	.2848	.5900	.9460	.8149
1.0	.4171	.3011	.7495	1.000	.6529
1.4	.4299	.3099	.8510	1.029	.5724
1.8	.4397	.3167	.9385	1.052	.5137
2.2	.4477	.3222	1.016	1.070	.4685
2.6	.4544	.3268	1.086	1.085	.4324
3.0	.4602	.3307	1.150	1.098	.4028
3.2	.4627	.3325	1.180	1.104	----------

Case 58:

$t_s=0.333$; $\frac{t_e}{t_s}=0.4$; $t_E=0.667$; $V_\infty=25{,}100$ fps; $\zeta_w=0.040$; $\frac{h_w}{h_E}=0.060$;

$N_{Pr,f,w}=0.711$; $\frac{\rho_e\mu_e}{\rho_w\mu_w}=0.8134$

β	g'_w	ζ'_w	f''_w	$\frac{\zeta'_w}{\zeta'_w(\beta=1)}$	Δ^*_{tr}
0	0.3515	0.2527	0.3515	0.8376	1.767
.5	.3983	.2849	.5788	.9443	1.264
1.0	.4231	.3017	.7318	1.000	1.032
1.4	.4369	.3110	.8299	1.031	.9138
1.8	.4477	.3184	.9148	1.055	.8266
2.2	.4567	.3243	.9902	1.075	.7588
2.6	.4642	.3294	1.058	1.092	.7040
3.0	.4707	.3337	1.121	1.106	.6588
3.3	.4750	.3366	1.165	1.116	----------

Case 59:

$t_s=0.333$; $\frac{t_e}{t_s}=0.2$; $t_E=0.667$; $V_\infty=25{,}100$ fps; $\zeta_w=0.040$; $\frac{h_w}{h_E}=0.060$;

$N_{Pr,f,w}=0.711$; $\frac{\rho_e\mu_e}{\rho_w\mu_w}=0.9173$

β	g'_w	ζ'_w	f''_w	$\frac{\zeta'_w}{\zeta'_w(\beta=1)}$	Δ^*_{tr}
0	0.3578	0.2545	0.3578	0.8398	3.423
.5	.4037	.2854	.5628	.9420	2.574
1.0	.4301	.3030	.7062	1.000	2.146
1.4	.4454	.3132	.7994	1.033	1.920
1.8	.4577	.3213	.8806	1.060	1.750
2.2	.4680	.3281	.9531	1.083	1.616
2.6	.4768	.3339	1.019	1.102	1.507
3.0	.4845	.3390	1.079	1.119	1.416

Case 60:

$t_s=0.333$; $\frac{t_e}{t_s}=1$; $t_E=0.333$; $V_\infty=35{,}600$ fps; $\zeta_w=0.005066$; $\frac{h_w}{h_E}=0.0152$;

$N_{Pr,f,w}=0.709$; $\frac{\rho_e\mu_e}{\rho_w\mu_w}=0.2321$

β	g'_w	ζ'_w	f''_w	$\frac{\zeta'_w}{\zeta'_w(\beta=1)}$	Δ^*_{tr}
0	0.2391	0.1858	0.2391	0.8405	0.4310
.5	.2709	.2100	.4113	.9500	.2617
1.0	.2855	.2210	.5191	1.000	.1955
1.4	.2932	.2269	.5864	1.026	.1636
1.8	.2990	.2313	.6439	1.046	.1408
2.2	.3037	.2348	.6944	1.062	.1234
2.6	.3075	.2377	.7398	1.075	.1096
3.0	.3108	.2401	.7811	1.086	.0983
3.1	.3116	.2407	.7909	1.089	----------
∞	.3852	.2942	-------	1.331	----------

Case 61:

$t_s=0.333$; $\frac{t_e}{t_s}=1$; $t_E=0.333$; $V_\infty=35{,}600$ fps; $\zeta_w=0.015$; $\frac{h_w}{h_E}=0.045$;

$N_{Pr,f,w}=0.693$; $\frac{\rho_e\mu_e}{\rho_w\mu_w}=0.3405$

β	g'_w	ζ'_w	f''_w	$\frac{\zeta'_w}{\zeta'_w(\beta=1)}$	Δ^*_{tr}
0	0.2878	0.2162	0.2878	0.8385	0.5445
.5	.3267	.2448	.5023	.9495	.3348
1.0	.3445	.2578	.6372	1.000	.2530
1.4	.3538	.2646	.7219	1.027	.2138
1.8	.3609	.2698	.7944	1.047	.1857
2.2	.3666	.2739	.8583	1.063	.1642
2.6	.3713	.2773	.9159	1.076	.1472
3.0	.3753	.2803	.9685	1.087	.1333
3.3	.3779	.2821	1.005	1.094	----------

Case 62:

$t_s=0.333$; $\frac{t_e}{t_s}=1$; $t_E=0.333$; $V_\infty=35{,}600$ fps; $\zeta_w=0.03333$; $\frac{h_w}{h_E}=0.100$;

$N_{Pr,f,w}=0.768$; $\frac{\rho_e\mu_e}{\rho_w\mu_w}=0.4571$

β	g'_w	ζ'_w	f''_w	$\frac{\zeta'_w}{\zeta'_w(\beta=1)}$	Δ^*_{tr}
0	0.3305	0.2696	0.3305	0.8352	0.6711
.5	.3762	.3063	.5890	.9487	.4189
1.0	.3970	.3228	.7526	1.000	.3214
1.4	.4079	.3315	.8559	1.027	.2747
1.8	.4162	.3381	.9446	1.047	.2413
2.2	.4229	.3433	1.023	1.064	.2159
2.6	.4284	.3477	1.094	1.077	.1957
3.0	.4330	.3514	1.159	1.088	.1791
3.4	.4371	.3545	1.219	1.096	.1686
∞	.5414	.4341	-------	1.345	----------

Case 63:

$t_s=0.333$; $\frac{t_e}{t_s}=0.8$; $t_E=0.333$; $V_\infty=35{,}600$ fps; $\zeta_w=0.03333$; $\frac{h_w}{h_E}=0.100$;

$N_{Pr,f,w}=0.768$; $\frac{\rho_e\mu_e}{\rho_w\mu_w}=0.4932$

β	g'_w	ζ'_w	f''_w	$\frac{\zeta'_w}{\zeta'_w(\beta=1)}$	Δ^*_{tr}
0	0.3342	0.2692	0.3342	0.8372	0.8459
.5	.3798	.3049	.5813	.9479	.5532
1.0	.4015	.3216	.7404	1.000	.4340
1.4	.4130	.3305	.8413	1.028	.3759
1.8	.4219	.3373	.9281	1.049	.3339
2.2	.4290	.3428	1.005	1.066	.3018
2.6	.4349	.3474	1.074	1.080	.2763
3.0	.4400	.3512	1.138	1.092	.2553
3.1	.4411	.3521	1.153	1.095	----------

Case 64:

$t_s=0.333$; $\frac{t_e}{t_s}=0.6$; $t_E=0.333$; $V_\infty=35{,}600$ fps; $\zeta_w=0.03333$; $\frac{h_w}{h_E}=0.100$;

$N_{Pr,f,w}=0.768$; $\frac{\rho_e\mu_e}{\rho_w\mu_w}=0.5440$

β	g'_w	ζ'_w	f''_w	$\frac{\zeta'_w}{\zeta'_w(\beta=1)}$	Δ^*_{tr}
0	0.3385	0.2693	0.3385	0.8393	1.125
.5	.3838	.3038	.5719	.9469	.7708
1.0	.4064	.3203	.7256	1.000	.6173
1.4	.4187	.3301	.8235	1.029	.5409
1.8	.4283	.3373	.9080	1.051	.4852
2.2	.4360	.3430	.9830	1.069	.4422
2.6	.4425	.3479	1.051	1.084	.4078
3.0	.4481	.3520	1.113	1.097	.3794
3.3	.4518	.3548	1.157	1.106	----------

TABLE III.—TABLES OF SIMILAR SOLUTIONS FOR EQUILIBRIUM DISSOCIATED AIR, $F=0$ ($N_{Le}=1$)—Con.

(a) Heat-transfer cases—Continued

Case 65:

$t_s=0.333$; $\frac{t_e}{t_s}=0.4$; $t_R=0.333$; $V_\infty=35{,}600$ fps; $\zeta_w=0.03333$; $\frac{h_w}{h_R}=0.100$;

$N_{Pr,f,w}=0.768$; $\frac{\rho_e\mu_e}{\rho_w\mu_w}=0.6248$

β	g'_w	ζ'_w	f''_w	$\frac{\zeta'_w}{\zeta'_w(\beta=1)}$	Δ^*_{ir}
0	0.3435	0.2699	0.3435	0.8419	1.652
.5	.3880	.3031	.5594	.9455	1.188
1.0	.4117	.3206	.7056	1.000	.9712
1.4	.4250	.3303	.7998	1.030	.8605
1.8	.4355	.3380	.8813	1.054	.7784
2.2	.4441	.3442	.9538	1.074	.7146
2.6	.4514	.3495	1.019	1.090	.6631
3.0	.4576	.3541	1.080	1.105	.6205
3.4	.4632	.3580	1.136	1.117	.5844
3.5	.4645	.3590	1.149	1.120	.5762

Case 66:

$t_s=0.333$; $\frac{t_e}{t_s}=0.2$; $t_R=0.333$; $V_\infty=35{,}600$ fps; $\zeta_w=0.03333$; $\frac{h_w}{h_R}=0.100$;

$N_{Pr,f,w}=0.768$; $\frac{\rho_e\mu_e}{\rho_w\mu_w}=0.7931$

β	g'_w	ζ'_w	f''_w	$\frac{\zeta'_w}{\zeta'_w(\beta=1)}$	Δ^*_{ir}
0	0.3496	0.2714	0.3496	0.8468	3.093
.5	.3922	.3025	.5395	.9439	2.352
1.0	.4172	.3205	.6739	1.000	1.970
1.4	.4317	.3310	.7618	1.033	1.767
1.8	.4435	.3394	.8386	1.059	1.613
2.2	.4534	.3464	.9072	1.081	1.491
2.6	.4618	.3525	.9695	1.100	1.392
3.0	.4693	.3578	1.027	1.116	1.309
3.4	.4758	.3624	1.080	1.131	1.239
3.5	.4774	.3635	1.093	1.134	1.222

Case 67:

$t_s=0.1$; $\frac{t_e}{t_s}=1.0$; $t_R=6.58$; $V_\infty=7{,}600$ fps; $\zeta_w=0.10$; $\frac{h_w}{h_R}=0.0152$;

$N_{Pr,f,w}=0.709$; $\frac{\rho_e\mu_e}{\rho_w\mu_w}=1.0$

β	g'_w	ζ'_w	f''_w	$\frac{\zeta'_w}{\zeta'_w(\beta=1)}$	Δ^*_{ir}
0	0.4070	0.2732	0.4070	0.6693	4.868
.5	.5559	.3742	1.412	.9167	3.133
1.0	.6060	.4082	1.982	1.000	2.684
1.4	.6304	.4247	2.329	1.041	2.488
1.8	.6482	.4368	2.623	1.070	2.354
2.2	.6621	.4462	2.878	1.093	2.256
2.6	.6733	.4538	3.107	1.112	2.180
3.0	.6826	.4601	3.315	1.127	2.119
3.3	.6887	.4642	3.460	1.137	-----
∞	.8679	.5817	-------	1.425	-----

Case 68:

$t_s=0.1$; $\frac{t_e}{t_s}=1.0$; $t_R=6.58$; $V_\infty=7{,}600$ fps; $\zeta_w=0.30$; $\frac{h_w}{h_R}=0.0456$;

$N_{Pr,f,w}=0.693$; $\frac{\rho_e\mu_e}{\rho_w\mu_w}=1.475$

β	g'_w	ζ'_w	f''_w	$\frac{\zeta'_w}{\zeta'_w(\beta=1)}$	Δ^*_{ir}
0	0.4599	0.2198	0.4599	0.6194	8.345
.5	.6659	.3222	2.102	.9080	5.264
1.0	.7313	.3548	3.057	1.000	4.554
1.4	.7632	.3707	3.655	1.045	4.248
1.8	.7865	.3823	4.167	1.078	4.040
2.2	.8046	.3914	4.622	1.103	3.887
2.6	.8192	.3987	5.034	1.124	3.770
3.0	.8315	.4048	5.412	1.141	3.676
3.3	.8394	.4088	5.677	1.152	-----
∞	1.082	.5279	-------	1.488	-----

Case 69:

$t_s=0.1$; $\frac{t_e}{t_s}=1.0$; $t_R=6.58$; $V_\infty=7{,}600$ fps; $\zeta_w=0.6579$; $\frac{h_w}{h_R}=0.10$;

$N_{Pr,f,w}=0.768$; $\frac{\rho_e\mu_e}{\rho_w\mu_w}=1.969$

β	g'_w	ζ'_w	f''_w	$\frac{\zeta'_w}{\zeta'_w(\beta=1)}$	Δ^*_{ir}
0	0.4934	0.09331	0.4934	0.5393	13.21
.5	.7609	.1544	2.915	.8927	8.065
1.0	.8410	.1730	4.326	1.000	7.014
1.4	.8797	.1821	5.218	1.052	6.567
1.8	.9079	.1888	5.988	1.091	6.265
2.2	.9298	.1940	6.673	1.121	6.045
2.6	.9476	.1982	7.297	1.146	5.876
3.0	.9624	.2018	7.871	1.166	5.741
3.1	.9657	.2026	8.009	1.171	------

Case 70:

$t_s=0.1$; $\frac{t_e}{t_s}=1.0$; $t_R=1.73$; $V_\infty=15{,}500$ fps; $\zeta_w=0.0262$; $\frac{h_w}{h_R}=0.0152$;

$N_{Pr,f,w}=0.709$; $\frac{\rho_e\mu_e}{\rho_w\mu_w}=0.6199$

β	g'_w	ζ'_w	f''_w	$\frac{\zeta'_w}{\zeta'_w(\beta=1)}$	Δ^*_{ir}
0	0.3293	0.2410	0.3293	0.7318	2.229
.5	.4171	.3054	.8577	.9273	1.463
1.0	.4497	.3293	1.162	1.000	1.232
1.4	.4660	.3412	1.348	1.036	1.128
1.8	.4779	.3500	1.504	1.063	1.056
2.2	.4873	.3568	1.640	1.084	1.003
2.6	.4949	.3624	1.761	1.100	.9616
3.0	.5013	.3671	1.871	1.114	.9282
3.4	.5068	.3710	1.971	1.127	------
3.5	.5080	.3719	1.995	1.129	.8944

Case 71:

$t_s=0.1$; $\frac{t_e}{t_s}=0.75$; $t_R=1.73$; $V_\infty=15{,}500$ fps; $\zeta_w=0.0262$; $\frac{h_w}{h_R}=0.0152$;

$N_{Pr,f,w}=0.709$; $\frac{\rho_e\mu_e}{\rho_w\mu_w}=0.6861$

β	g'_w	ζ'_w	f''_w	$\frac{\zeta'_w}{\zeta'_w(\beta=1)}$	Δ^*_{ir}
0	0.3317	0.2417	0.3317	0.7259	3.019
.5	.4223	.3074	.8606	.9234	2.001
1.0	.4576	.3330	1.173	1.000	1.676
1.4	.4755	.3459	1.364	1.039	1.526
1.8	.4889	.3554	1.526	1.068	1.422
2.2	.4994	.3630	1.667	1.090	1.343
2.6	.5081	.3692	1.793	1.109	1.282
3.0	.5153	.3744	1.907	1.124	1.232
3.1	.5170	.3755	1.934	1.128	-----

Case 72:

$t_s=0.1$; $\frac{t_e}{t_s}=0.50$; $t_R=1.73$; $V_\infty=15{,}500$ fps; $\zeta_w=0.0262$; $\frac{h_w}{h_R}=0.0152$;

$N_{Pr,f,w}=0.709$; $\frac{\rho_e\mu_e}{\rho_w\mu_w}=0.7924$

β	g'_w	ζ'_w	f''_w	$\frac{\zeta'_w}{\zeta'_w(\beta=1)}$	Δ^*_{ir}
0	0.3346	0.2425	0.3346	0.7158	4.769
.5	.4301	.3111	.8763	.9182	3.536
1.0	.4692	.3388	1.204	1.000	2.940
1.4	.4895	.3531	1.407	1.042	2.659
1.8	.5049	.3639	1.579	1.074	2.460
2.2	.5171	.3725	1.730	1.099	2.309
2.6	.5273	.3796	1.864	1.120	2.189
3.0	.5359	3856	1.986	1.138	2.092
3.3	.5415	.3895	2.071	1.150	-----

TABLE III.—TABLES OF SIMILAR SOLUTIONS FOR EQUILIBRIUM DISSOCIATED AIR, $F=0$ ($N_{Le}=1$)—Con.

(a) Heat-transfer cases—Continued

Case 73:

$t_s=0.1$; $\frac{t_e}{t_s}=0.262$; $t_E=1.73$; $V_\infty=15{,}000$ fps; $\zeta_w=0.0262$; $\frac{h_w}{h_E}=0.0152$;

$N_{Pr,f,w}=0.709$; $\frac{\rho_e\mu_e}{\rho_w\mu_w}=1.0$

β	g'_w	ζ'_w	f''_w	$\frac{\zeta'_w}{\zeta'_w(\beta=1)}$	Δ^*_{tr}
0	0.3377	0.2435	0.3377	0.6848	11.74
.5	.4505	.3232	.9709	.9090	7.567
1.0	.4973	.3556	1.353	1.000	6.154
1.4	.5222	.3727	1.591	1.048	5.481
1.8	.5414	.3858	1.794	1.085	5.001
2.2	.5570	.3964	1.971	1.115	4.636
2.6	.5701	.4053	2.129	1.140	4.349
3.0	.5813	.4183	2.274	1.161	4.114
3.3	.5888	.4179	2.374	1.175	-----

Case 74:

$t_s=0.1$; $\frac{t_e}{t_s}=1.0$; $t_E=1.0$; $V_\infty=20{,}400$ fps; $\zeta_w=0.0152$; $\frac{h_w}{h_E}=0.0152$;

$N_{Pr,f,w}=0.709$; $\frac{\rho_e\mu_e}{\rho_w\mu_w}=0.5122$

β	g'_w	ζ'_w	f''_w	$\frac{\zeta'_w}{\zeta'_w(\beta=1)}$	Δ^*_{tr}
0	0.3012	0.2221	0.3012	0.7397	1.876
.5	.3780	.2788	.7588	.9286	1.233
1.0	.4070	.3003	1.024	1.000	1.035
1.4	.4215	.3110	1.186	1.036	.9453
1.8	.4323	.3189	1.322	1.062	.8833
2.2	.4407	.3251	1.441	1.082	.8371
2.6	.4475	.3301	1.547	1.099	.8012
3.0	.4533	.3343	1.643	1.113	.7722
3.4	.4582	.3379	1.731	1.125	.7483
3.5	.4593	.3387	1.752	1.128	-----
∞	.5688	.4173	------	-----	1.390

Case 75:

$t_s=0.1$; $\frac{t_e}{t_s}=1.0$; $t_E=1.0$; $V_\infty=20{,}400$ fps; $\zeta_w=0.05$; $\frac{h_w}{h_E}=0.05$;

$N_{Pr,f,w}=0.699$; $\frac{\rho_e\mu_e}{\rho_w\mu_w}=0.7833$

β	g'_w	ζ'_w	f''_w	$\frac{\zeta'_w}{\zeta'_w(\beta=1)}$	Δ^*_{tr}
0	0.3649	0.2537	0.3649	0.7306	2.540
.5	.4626	.3218	.9785	.9268	1.676
1.0	.4990	.3472	1.339	1.000	1.416
1.4	.5172	.3599	1.563	1.037	1.299
1.8	.5307	.3693	1.752	1.064	1.218
2.2	.5412	.3766	1.919	1.084	1.157
2.6	.5498	.3826	2.068	1.102	1.110
3.0	.5571	.3876	2.204	1.116	1.073
3.4	.5632	.3919	2.330	1.129	-----

Case 76:

$t_s=0.1$; $\frac{t_e}{t_s}=1.0$; $t_E=1.0$; $V_\infty=20{,}400$ fps; $\zeta_w=0.10$; $\frac{h_w}{h_E}=0.10$;

$N_{Pr,f,w}=0.768$; $\frac{\rho_e\mu_e}{\rho_w\mu_w}=1.009$

β	g'_w	ζ'_w	f''_w	$\frac{\zeta'_w}{\zeta'_w(\beta=1)}$	Δ^*_{tr}
0	0.4052	0.2903	0.4052	0.7198	3.169
.5	.5196	.3729	1.159	.9246	2.093
1.0	.5617	.4034	1.607	1.000	1.778
1.4	.5828	.4185	1.886	1.038	1.636
1.8	.5983	.4297	2.125	1.065	1.539
2.2	.6105	.4385	2.336	1.087	1.466
2.6	.6204	.4456	2.527	1.105	1.410
3.0	.6287	.4516	2.701	1.120	1.364
3.4	.6358	.4567	2.863	1.132	-----
∞	.8034	.5747	------	1.425	-----

Case 77:

$t_s=0.1$; $\frac{t_e}{t_s}=0.8$; $t_E=1.0$; $V_\infty=20{,}400$ fps; $\zeta_w=0.10$; $\frac{h_w}{h_E}=0.10$;

$N_{Pr,f,w}=0.768$; $\frac{\rho_e\mu_e}{\rho_w\mu_w}=1.090$

β	g'_w	ζ'_w	f''_w	$\frac{\zeta'_w}{\zeta'_w(\beta=1)}$	Δ^*_{tr}
0	0.4073	0.2908	0.4073	0.7177	3.944
.5	.5231	.3736	1.149	.9220	2.641
1.0	.5675	.4052	1.597	1.000	2.238
1.4	.5900	.4211	1.878	1.039	2.054
1.8	.6068	.4330	2.119	1.069	1.925
2.2	.6200	.4424	2.332	1.092	1.830
2.6	.6309	.4501	2.525	1.111	1.754
3.0	.6400	.4565	2.701	1.127	1.694

Case 78:

$t_s=0.1$; $\frac{t_e}{t_s}=0.6$; $t_E=1.0$; $V_\infty=20{,}400$ fps; $\zeta_w=0.10$; $\frac{h_w}{h_E}=0.10$;

$N_{Pr,f,w}=0.768$; $\frac{\rho_e\mu_e}{\rho_w\mu_w}=1.206$

β	g'_w	ζ'_w	f''_w	$\frac{\zeta'_w}{\zeta'_w(\beta=1)}$	Δ^*_{tr}
0	0.4096	0.2913	0.4096	0.7149	5.211
.5	.5270	.3744	1.139	.9187	3.539
1.0	.5743	.4075	1.589	1.000	2.987
1.4	.5987	.4246	1.873	1.042	2.729
1.8	.6171	.4374	2.117	1.073	2.548
2.2	.6318	.4476	2.334	1.098	2.411
2.6	.6439	.4559	2.529	1.119	2.303
3.0	.6541	.4630	2.708	1.136	2.215
3.4	.6630	.4691	2.874	1.151	-----

Case 79:

$t_s=0.1$; $\frac{t_e}{t_s}=0.4$; $t_E=1.0$; $V_\infty=20{,}400$ fps; $\zeta_w=0.10$; $\frac{h_w}{h_E}=0.10$;

$N_{Pr,f,w}=0.768$; $\frac{\rho_e\mu_e}{\rho_w\mu_w}=1.392$

β	g'_w	ζ'_w	f''_w	$\frac{\zeta'_w}{\zeta'_w(\beta=1)}$	Δ^*_{tr}
0	0.4123	0.2920	0.4123	0.7098	7.815
.5	.5324	.3760	1.134	.9143	5.364
1.0	.5835	.4113	1.590	1.000	4.507
1.4	.6106	.4298	1.882	1.045	4.097
1.8	.6313	.4440	2.133	1.079	3.803
2.2	.6480	.4553	2.356	1.107	3.579
2.6	.6620	.4648	2.558	1.130	3.402
3.0	.6738	.4728	2.743	1.149	3.257
3.4	.6842	.4797	2.914	1.166	-----

Case 80:

$t_s=0.1$; $\frac{t_e}{t_s}=0.2$; $t_E=1.0$; $V_\infty=20{,}400$ fps; $\zeta_w=0.10$; $\frac{h_w}{h_E}=0.10$;

$N_{Pr,f,w}=0.768$; $\frac{\rho_e\mu_e}{\rho_w\mu_w}=1.783$

β	g'_w	ζ'_w	f''_w	$\frac{\zeta'_w}{\zeta'_w(\beta=1)}$	Δ^*_{tr}
0	0.4155	0.2927	0.4155	0.6919	17.50
.5	.5471	.3837	1.186	.9069	11.92
1.0	.6054	.4231	1.681	1.000	9.897
1.4	.6372	.4443	2.000	1.050	8.907
1.8	.6620	.4608	2.276	1.089	8.190
2.2	.6823	.4743	2.522	1.121	7.638
2.6	.6995	.4856	2.745	1.148	7.195
3.0	.7144	.4953	2.950	1.171	6.833
3.1	.7178	.4976	2.999	1.176	-----

TABLE III.—TABLES OF SIMILAR SOLUTIONS FOR EQUILIBRIUM DISSOCIATED AIR, $F=0$ ($N_{Le}=1$)—Con.

(a) Heat-transfer cases—Continued

Case 81:

$t_s=0.1$; $\frac{t_e}{t_s}=1.0$; $t_R=0.333$; $V_\infty=35{,}600$ fps; $\zeta_w=0.005066$; $\frac{h_w}{h_R}=0.0152$;

$N_{Pr,f,w}=0.709$; $\frac{\rho_e\mu_e}{\rho_w\mu_w}=0.3503$

β	g'_w	ζ'_w	f''_w	$\frac{\zeta'_w}{\zeta'_w(\beta=1)}$	Δ^*_{tr}
0	0.2510	0.1871	0.2510	0.7485	1.423
.5	.3119	.2325	.6117	.9301	.9359
1.0	.3353	.2500	.8226	1.000	.7822
1.4	.3471	.2587	.9520	1.035	.7125
1.8	.3558	.2652	1.061	1.061	.6639
2.2	.3626	.2703	1.156	1.081	.6278
2.6	.3682	.2744	1.241	1.098	.5995
3.0	.3729	.2779	1.318	1.112	.5768
3.4	.3769	.2809	1.389	1.124	.5578
3.5	.3779	.2816	1.406	1.126	.5536
∞	.4699	.3482	-----	1.393	-------

Case 82:

$t_s=0.1$; $\frac{t_e}{t_s}=1.0$; $t_R=0.333$; $V_\infty=35{,}600$ fps; $\zeta_w=0.015$; $\frac{h_w}{h_R}=0.045$;

$N_{Pr,f,w}=0.693$; $\frac{\rho_e\mu_e}{\rho_w\mu_w}=0.5138$

β	g'_w	ζ'_w	f''_w	$\frac{\zeta'_w}{\zeta'_w(\beta=1)}$	Δ^*_{tr}
0	0.3020	0.2174	0.3020	0.7460	1.776
.5	.3762	.2709	.7503	.9297	1.169
1.0	.4047	.2914	1.014	1.000	.9796
1.4	.4189	.3017	1.177	1.035	.8937
1.8	.4295	.3093	1.314	1.061	.8341
2.2	.4378	.3152	1.435	1.082	.7895
2.6	.4446	.3201	1.593	1.099	.7548
3.0	.4503	.3242	1.641	1.113	.7268
3.4	.4552	.3277	1.731	1.125	.7036
3.5	.4563	.3285	1.753	1.127	------

Case 83:

$t_s=0.1$; $\frac{t_e}{t_s}=1.0$; $t_R=0.333$; $V_\infty=35{,}600$ fps; $\zeta_w=0.03333$; $\frac{h_w}{h_R}=0.10$;

$N_{Pr,f,w}=0.768$; $\frac{\rho_e\mu_e}{\rho_w\mu_w}=0.6897$

β	g'_w	ζ'_w	f''_w	$\frac{\zeta'_w}{\zeta'_w(\beta=1)}$	Δ^*_{tr}
0	0.3463	0.2705	0.3463	0.7418	2.149
.5	.4333	.3387	.8855	.9287	1.418
1.0	.4665	.3647	1.205	1.000	1.193
1.4	.4832	.3777	1.403	1.036	1.090
1.8	.4955	.3873	1.571	1.062	1.019
2.2	.5052	.3949	1.719	1.083	.9664
2.6	.5131	.4010	1.852	1.100	.9251
3.0	.5197	.4062	1.973	1.114	.8918
3.4	.5254	.4106	2.085	1.126	------
3.5	.5267	.4116	2.111	1.129	------
∞	.6606	.5131	-------	1.407	------

Case 84:

$t_s=0.1$; $\frac{t_e}{t_s}=0.8$; $t_R=0.333$; $V_\infty=35{,}600$ fps; $\zeta_w=0.015$; $\frac{h_w}{h_R}=0.045$;

$N_{Pr,f,w}=0.693$; $\frac{\rho_e\mu_e}{\rho_w\mu_w}=0.5548$

β	g'_w	ζ'_w	f''_w	$\frac{\zeta'_w}{\zeta'_w(\beta=1)}$	Δ^*_{tr}
0	0.3037	0.2179	0.3037	0.7458	2.175
.5	.3779	.2709	.7390	.9273	1.463
1.0	.4078	.2921	1.001	1.000	1.227
1.4	.4230	.3029	1.163	1.037	1.118
1.8	.4344	.3110	1.301	1.065	1.041
2.2	.4435	.3174	1.422	1.086	.9837
2.6	.4509	.3226	1.531	1.104	.9386
3.0	.4571	.3270	1.629	1.119	.9021
3.4	.4625	.3308	1.720	1.132	.8718
3.5	.4637	.3316	1.742	1.135	.8649

Case 85:

$t_s=0.1$; $\frac{t_e}{t_s}=0.6$; $t_R=0.333$; $V_\infty=35{,}600$ fps; $\zeta_w=0.015$; $\frac{h_w}{h_R}=0.045$;

$N_{Pr,f,w}=0.693$; $\frac{\rho_e\mu_e}{\rho_w\mu_w}=0.6127$

β	g'_w	ζ'_w	f''_w	$\frac{\zeta'_w}{\zeta'_w(\beta=1)}$	Δ^*_{tr}
0	0 3056	0.2184	0.3056	0.7458	2.817
.5	.3795	.2708	.7246	.9246	1.942
1.0	.4110	.2929	.9838	1.000	1.631
1.4	.4274	.3043	1.146	1.039	1.484
1.8	.4398	.3130	1.284	1.069	1.379
2.2	.4498	.3199	1.406	1.092	1.299
2.6	.4580	.3256	1.515	1.112	1.236
3.0	.4649	.3281	1.614	1.128	1.185
3.4	.4709	.3346	1.706	1.142	1.143
3.5	.4723	.3355	1.728	1.146	1.133

Case 86:

$t_s=0.1$; $\frac{t_e}{t_s}=0.4$; $t_R=0.333$; $V_\infty=35{,}600$ fps; $\zeta_w=0.015$; $\frac{h_w}{h_R}=0.045$;

$N_{Pr,f,w}=0.693$; $\frac{\rho_e\mu_e}{\rho_w\mu_w}=0.7051$

β	g'_w	ζ'_w	f''_w	$\frac{\zeta'_w}{\zeta'_w(\beta=1)}$	Δ^*_{tr}
0	0.3076	0.2191	0.3076	0.7465	4.048
.5	.3808	.2705	.7054	.9213	2.871
1.0	.4141	.2935	.9602	1.000	2.417
1.4	.4320	.3059	1.122	1.042	2.195
1.8	.4458	.3153	1.260	1.074	2.035
2.2	.4570	.3230	1.383	1.100	1.911
2.6	.4663	.3293	1.493	1.122	1.812
3.0	.4742	.3348	1.593	1.140	1.732
3.1	.4760	.3360	1.617	1.145	-----

Case 87:

$t_s=0.1$; $\frac{t_e}{t_s}=0.2$; $t_R=0.333$; $V_\infty=35{,}600$ fps; $\zeta_w=0.015$; $\frac{h_w}{h_R}=0.045$;

$N_{Pr,f,w}=0.693$; $\frac{\rho_e\mu_e}{\rho_w\mu_w}=0.8984$

β	g'_w	ζ'_w	f''_w	$\frac{\zeta'_w}{\zeta'_w(\beta=1)}$	Δ^*_{tr}
0	0.3101	0.2200	0.3101	0.7478	7.651
.5	.3817	.2698	.6797	.9172	5.622
1.0	.4173	.2941	.9275	1.000	4.753
1.4	.4372	.3077	1.088	1.046	4.309
1.8	.4529	.3183	1.226	1.082	3.981
2.2	.4658	.3270	1.350	1.112	3.725
2.6	.4769	.3345	1.462	1.137	3.518
3.0	.4864	.3409	1.564	1.159	3.346
3.1	.4886	.3424	1.589	1.164	3.307
3.2	.4908	.3438	1.612	1.169	-----

Case 88:

$t_s=0.033$; $\frac{t_e}{t_s}=1.0$; $t_R=2.19$; $V_\infty=13{,}700$ fps; $\zeta_w=0.03333$; $\frac{h_w}{h_R}=0.0152$;

$N_{Pr,f,w}=0.709$; $\frac{\rho_e\mu_e}{\rho_w\mu_w}=1.0$

β	g'_w	ζ'_w	f''_w	$\frac{\zeta'_w}{\zeta'_w(\beta=1)}$	Δ^*_{tr}
0	0.3496	0.2507	0.3496	0.5669	10.10
.5	.5554	.3998	1.971	.9040	6.037
1.0	.6139	.4423	2.840	1.000	5.241
1.4	.6417	.4624	3.361	1.046	4.905
1.8	.6618	.4769	3.795	1.078	4.680
2.2	.6771	.4880	4.170	1.103	4.517
2.6	.6895	.4969	4.502	1.124	4.392
3.0	.6997	.5043	4.801	1.140	-----
∞	.8919	.6398	-------	1.447	-----

TABLE III.—TABLES OF SIMILAR SOLUTIONS FOR EQUILIBRIUM DISSOCIATED AIR, $F=0$ ($N_{Le}=1$)—Con.

(a) Heat-transfer cases—Continued

Case 89:

$t_s=0.033$; $\frac{t_e}{t_s}=1.0$; $t_E=2.19$; $V_\infty=13{,}700$ fps; $\zeta_w=0.10$; $\frac{h_w}{h_E}=0.0456$;

$N_{Pr,f,w}=0.693$; $\frac{\rho_e\mu_e}{\rho_w\mu_w}=1.474$

β	g'_w	ζ'_w	f''_w	$\frac{\zeta'_w}{\zeta'_w(\beta=1)}$	Δ^*_{tr}
0	0.4104	0.2630	0.4104	0.5503	13.96
.5	.6684	.4310	2.639	.9017	8.228
1.0	.7405	.4779	3.861	1.000	7.159
1.4	.7747	.5002	4.608	1.047	6.711
1.8	.7994	.5163	5.239	1.080	6.412
2.2	.8185	.5287	5.791	1.106	6.194
2.6	.8337	.5386	6.286	1.127	6.028
3.0	.8464	.5469	6.737	1.144	5.895
3.1	.8493	.5487	6.844	1.148	------
∞	1.095	.7052	------	1.476	------

Case 90:

$t_s=0.033$; $\frac{t_e}{t_s}=1.0$; $t_E=2.19$; $V_\infty=13{,}700$ fps; $\zeta_w=0.2193$; $\frac{h_w}{h_E}=0.10$;

$N_{Pr,f,w}=0.768$; $\frac{\rho_e\mu_e}{\rho_w\mu_w}=1.969$

β	g'_w	ζ'_w	f''_w	$\frac{\zeta'_w}{\zeta'_w(\beta=1)}$	Δ^*_{tr}
0	0.4546	0.2703	0.4546	0.5277	18.82
.5	.7654	.4602	3.401	.8987	10.88
1.0	.8502	.5121	5.043	1.000	9.489
1.4	.8906	.5368	6.061	1.048	8.908
1.8	.9197	.5546	6.928	1.083	8.521
2.2	.9421	.5683	7.692	1.110	------
2.6	.9602	.5794	8.382	1.131	8.025
3.0	.9752	.5885	9.014	1.149	7.854
3.1	.9785	.5906	9.165	1.153	------
∞	1.273	.7684	------	1.501	------

Case 91:

$t_s=0.033$; $\frac{t_e}{t_s}=1.0$; $t_E=0.333$; $V_\infty=35{,}600$ fps; $\zeta_w=0.005066$; $\frac{h_w}{h_E}=0.0152$;

$N_{Pr,f,w}=0.709$; $\frac{\rho_e\mu_e}{\rho_w\mu_w}=0.5122$

β	g'_w	ζ'_w	f''_w	$\frac{\zeta'_w}{\zeta'_w(\beta=1)}$	Δ^*_{tr}
0	0.2564	0.1889	0.2564	0.6440	3.852
.5	.3629	.2679	.9838	.9134	2.443
1.0	.3972	.2933	1.385	1.000	2.102
1.4	.4137	.3056	1.628	1.042	1.954
1.8	.4258	.3145	1.830	1.072	1.853
2.2	.4351	.3214	2.006	1.096	1.779
2.6	.4426	.3270	2.162	1.115	1.723
3.0	.4489	.3316	2.304	1.131	1.677
3.3	.4530	.3346	2.401	1.141	------
∞	.5700	.4191	------	1.429	------

Case 92:

$t_s=0.033$; $\frac{t_e}{t_s}=1.0$; $t_E=0.333$; $V_\infty=35{,}600$ fps; $\zeta_w=0.015$; $\frac{h_w}{h_E}=0.045$;

$N_{Pr,f,w}=0.693$; $\frac{\rho_e\mu_e}{\rho_w\mu_w}=0.7513$

β	g'_w	ζ'_w	f''_w	$\frac{\zeta'_w}{\zeta'_w(\beta=1)}$	Δ^*_{tr}
0	0.3084	0.2194	0.3084	0.6418	4.780
.5	.4379	.3121	1.211	.9131	3.031
1.0	.4794	.3418	1.712	1.000	2.609
1.4	.4995	.3562	2.016	1.042	2.427
1.8	.5141	.3667	2.272	1.072	2.304
2.2	.5254	.3747	2.494	1.096	2.213
2.6	.5345	.3813	2.693	1.115	2.143
3.0	.5421	.3867	2.872	1.131	2.088
3.2	.5455	.3891	2.957	1.138	------
∞	.6916	.4910	------	1.436	------

Case 93:

$t_s=0.033$; $\frac{t_e}{t_s}=0.8$; $t_E=0.333$; $V_\infty=35{,}600$ fps; $\zeta_w=0.015$; $\frac{h_w}{h_E}=0.045$;

$N_{Pr,f,w}=0.693$; $\frac{\rho_e\mu_e}{\rho_w\mu_w}=0.8122$

β	g'_w	ζ'_w	f''_w	$\frac{\zeta'_w}{\zeta'_w(\beta=1)}$	Δ^*_{tr}
0	0.3092	0.2197	0.3092	0.6388	5.862
.5	.4398	.3127	1.201	.9095	3.763
1.0	.4836	.3439	1.708	1.000	3.226
1.4	.5052	.3592	2.019	1.044	2.989
1.8	.5210	.3704	2.282	1.077	2.826
2.2	.5334	.3791	2.510	1.103	2.706
2.6	.5435	.3862	2.714	1.123	2.612
3.0	.5519	.3922	2.899	1.140	2.538
3.2	.5556	.3948	2.985	1.148	------

Case 94:

$t_s=0.033$; $\frac{t_e}{t_s}=0.6$; $t_E=0.333$; $V_\infty=35{,}600$ fps; $\zeta_w=0.015$; $\frac{h_w}{h_E}=0.045$;

$N_{Pr,f,w}=0.693$; $\frac{\rho_e\mu_e}{\rho_w\mu_w}=0.8984$

β	g'_w	ζ'_w	f''_w	$\frac{\zeta'_w}{\zeta'_w(\beta=1)}$	Δ^*_{tr}
0	0.3101	0.2200	0.3101	0.6352	7.658
.5	.4418	.3135	1.190	.9051	4.968
1.0	.4885	.3463	1.707	1.000	4.237
1.4	.5120	.3628	2.027	1.048	3.905
1.8	.5295	.3751	2.298	1.083	3.674
2.2	.5433	.3847	2.535	1.111	3.502
2.6	.5545	.3926	2.747	1.133	3.368
3.0	.5640	.3991	2.939	1.152	3.259
3.2	.5682	.4021	3.030	1.161	3.212

Case 95:

$t_s=0.033$; $\frac{t_e}{t_s}=0.4$; $t_E=0.333$; $V_\infty=35{,}600$ fps; $\zeta_w=0.015$; $\frac{h_w}{h_E}=0.045$;

$N_{Pr,f,w}=0.693$; $\frac{\rho_e\mu_e}{\rho_w\mu_w}=1.037$

β	g'_w	ζ'_w	f''_w	$\frac{\zeta'_w}{\zeta'_w(\beta=1)}$	Δ^*_{tr}
0	0.3110	0.2203	0.3110	0.6295	11.32
.5	.4448	.3148	1.185	.8995	7.427
1.0	.4952	.3499	1.717	1.000	6.294

Case 96:

$t_s=0.033$; $\frac{t_e}{t_s}=0.2$; $t_E=0.333$; $V_\infty=35{,}600$ fps; $\zeta_w=0.015$; $\frac{h_w}{h_E}=0.045$;

$N_{Pr,f,w}=0.693$; $\frac{\rho_e\mu_e}{\rho_w\mu_w}=1.328$

β	g'_w	ζ'_w	f''_w	$\frac{\zeta'_w}{\zeta'_w(\beta=1)}$	Δ^*_{tr}
0	0.3121	0.2207	0.3121	0.6114	24.75
.5	.4560	.3217	1.246	.8914	16.15
1.0	.5128	.3609	1.833	1.000	13.52

TABLE III.—TABLES OF SIMILAR SOLUTIONS FOR EQUILIBRIUM DISSOCIATED AIR, $F=0(N_{Le}=1)$—Con.

(a) Heat-transfer cases—Concluded

Case 97: Additional flat-plate solutions ($\beta=0$)

t_e	t_R	V_∞, fps	ζ_w	$\frac{h_w}{h_R}$	$N_{Pr,f,w}$	$\frac{\rho_e \mu_e}{\rho_w \mu_w}$	ζ'_w	f''_w
0.0476	3.131	11,300	0.0476	0.01520	0.709	1.0	0.2609	0.3683
			.1565	.04998	.699	1.529	.2591	.4326
			.3130	.09997	.768	1.969	.2387	.4695
	2.380	13,100	.0362	.01521	.708	.9056	.2527	.3522
			.238	.10	.768	1.783	.2646	.4565
	.9520	20,900	.0145	.01523	.708	.6535	.2222	.3037
			.0952	.10	.768	1.286	.2917	.4085
	.4760	29,700	.00724	.01521	.708	.5123	.1993	.2706
			.0476	.10	.768	1.009	.2815	.3708
.02173	1.430	17,000	.02173	.01520	.709	1.0	.2374	.3282
			.0715	.050	.699	1.529	.2630	.3944
			.143	.10	.768	1.969	.2887	.4345
	1.086	19,600	.0165	.01519	.709	.9052	.2279	.3136
			.109	.1004	.768	1.785	.2924	.4199
	.4346	31,100	.0066	.01519	.709	.6530	.1974	.2692
			.0435	.1001	.768	1.286	.2805	.3695
.01235	.8125	22,700	.01235	.01520	.709	1.0	.2184	.3002
			.0406	.04997	.699	1.529	.2519	.3646
			.0812	.09994	.768	1.969	.2923	.4054
	.6175	26,100	.00938	.01519	.709	.9053	.2092	.2867
			.0618	.1001	.768	1.783	.2887	.3904
.00794	.5224	28,400	.00794	.01520	.709	1.0	.2040	.2795
			.0261	.04996	.698	1.529	.2399	.3414
			.0522	.09992	.768	1.969	.2856	.3819
	.3970	32,600	.00603	.01519	.709	.9052	.1954	.2670
			.0397	.10	.768	1.783	.2790	.3670

TABLE III.—TABLES OF SIMILAR SOLUTIONS FOR EQUILIBRIUM DISSOCIATED AIR, $F=0$ ($N_{Le}=1$)—Con

(b) Insulated wall cases

β	$\bar{\tau}$	g'_w	f''_w
Case 1: $t_s=1; \frac{t_e}{t_s}=0.99; t_R=1$			
0	0.8315	0.4698	0.4698
1	.7935	.5706	1.230
Case 2: $t_s=1; \frac{t_e}{t_s}=0.95; t_R=1$			
0	0.8318	0.4706	0.4706
1	.7942	.5711	1.222
2	.7787	.6061	1.670
3	.7694	.6269	2.023
Case 3: $t_s=1; \frac{t_e}{t_s}=0.8; t_R=1$			
0	0.8331	0.4737	0.4737
1	.7974	.5731	1.188
2	.7824	.6091	1.618
3	.7733	.6307	1.956
Case 4: $t_s=1; \frac{t_e}{t_s}=0.6; t_R=1$			
0	0.8353	0.4787	0.4787
1	.8025	.5766	1.139
2	.7883	.6142	1.542
3.1	.7789	.6391	1.888
Case 5: $t_s=1; \frac{t_e}{t_s}=0.4; t_R=1$			
0	0.8378	0.4851	0.4851
1	.8082	.5811	1.082
2	.7951	.6210	1.454
3.1	.7862	.6482	1.774
Case 6: $t_s=1; \frac{t_e}{t_s}=0.2; t_R=1$			
0	0.8401	0.4937	0.4937
1	.8143	.5867	1.007
2	.8022	.6300	1.337
3	.7946	.6584	1.599
3.3	.7928	.6654	1.669
Case 7: $t_s=1; \frac{t_e}{t_s}=0.99; t_R=0.5$			
0	0.8341	0.4698	0.4698
1	.7956	.5715	1.236
Case 8: $t_s=1; \frac{t_e}{t_s}=0.95; t_R=0.5$			
0	0.8327	0.4707	0.4707
1	.7944	.5720	1.226
2	.7788	.6071	1.677
2.7	.7718	.6225	1.931

β	$\bar{\tau}$	g'_w	f''_w
Case 9: $t_s=1; \frac{t_e}{t_s}=0.8; t_R=0.5$			
0	0.8281	0.4741	0.4741
1	.7907	.5738	1.189
2	.7749	.6098	1.620
2.7	.7677	.6258	1.863
Case 10: $t_s=1; \frac{t_e}{t_s}=0.6; t_R=0.5$			
0	0.8241	0.4790	0.4790
1	.7883	.5765	1.136
2	.7727	.6139	1.537
3	.7631	.6368	1.853
Case 11: $t_s=1; \frac{t_e}{t_s}=0.4; t_R=0.5$			
0	0.8222	0.4852	0.4852
1	.7892	.5799	1.074
2	.7743	.6193	1.441
3	.7650	.6441	1.730
3.3	.7628	.6501	1.808
Case 12: $t_s=1; \frac{t_e}{t_s}=0.2; t_R=0.5$			
0	0.8220	0.4933	0.4933
1	.7932	.5836	.9909
2	.7795	.6260	1.671
3	.7708	.6540	1.568
3.4	.7681	.6629	1.658
Case 13: $t_s=0.99; \frac{t_e}{t_s}=1; t_R=1$			
0	0.8316	0.4698	0.4698
1	.8447	.5711	1.236
Case 14: $t_s=0.95; \frac{t_e}{t_s}=1; t_R=1$			
0	0.8317	0.4705	0.4705
1	.8451	.5736	1.253
Case 15: $t_s=0.333; \frac{t_e}{t_s}=1; t_R=21.9$			
0	0.8194	0.4893	0.4893
1	.8418	.7070	2.474
2	.8469	.7661	3.581
3	.8498	.7994	4.436
3.5	.8509	.8116	4.810
Case 16: $t_s=0.333; \frac{t_e}{t_s}=1; t_R=3.333$			
0	0.8709	0.4888	0.4888
1	.8846	.6600	1.936

TABLE III.—TABLES OF SIMILAR SOLUTIONS FOR EQUILIBRIUM DISSOCIATED AIR, $F=0$ ($N_{Le}=1$)—Concluded

(b) Insulated wall cases—Concluded

β	$\bar{\tau}$	g'_w	f''_w
Case 17: $t_s=0.333$; $\frac{t_e}{t_s}=1$; $t_R=0.667$			
0	0.8265	0.4872	0.4872
1	.8438	.6497	1.836
2	.8485	.6981	2.604
3.2	.8516	.7301	3.306
Case 18: $t_s=0.333$; $\frac{t_e}{t_s}=0.8$; $t_R=0.667$			
0	0.8271	0.4900	0.4900
1	.8347	.6523	1.781
2	.8355	.7032	2.525
3.2	.8360	.7374	3.208
Case 19: $t_s=0.333$; $\frac{t_e}{t_s}=0.4$; $t_R=0.667$			
0	0.8282	0.4969	0.4969
1	.8218	.6571	1.634
2	.8165	.7152	2.317
3	.8129	.7506	2.852
Case 20: $t_s=0.333$; $\frac{t_e}{t_s}=0.2$; $t_R=0.667$			
0	0.8283	0.5015	0.5015
1	.8171	.6577	1.518
2	.8092	.7213	2.153
3	.8038	.7619	2.653
3.4	.8021	.7748	2.831
Case 21: $t_s=0.1$; $\frac{t_e}{t_s}=1$; $t_R=6.58$			
0	0.8503	0.5014	0.5014
1	.8764	.8828	4.929
2	.8804	.9674	7.271
3	.8826	1.014	9.060
Case 22: $t_s=0.1$; $\frac{t_e}{t_s}=1$; $t_R=1.73$			
0	0.8553	0.5006	0.5006
1	.8747	.7935	3.468
2	.8784	.8646	5.064
3.1	.8807	.9069	6.399
Case 23: $t_s=0.1$; $\frac{t_e}{t_s}=0.75$; $t_R=1.73$			
0	0.8543	0.5026	0.5026
1	.8672	.8040	3.460
2	.8681	.8820	5.080
2.9	.8685	.9223	6.211

β	$\bar{\tau}$	g'_w	f''_w
Case 24: $t_s=0.1$; $\frac{t_e}{t_s}=0.5$; $t_R=1.73$			
0	0.8528	0.5047	0.5047
1	.8588	.8210	3.512
2	.8563	.9089	5.197
3	.8546	.9598	6.496
Case 25: $t_s=0.1$; $\frac{t_e}{t_s}=0.262$; $t_R=1.73$			
0	0.8510	0.5071	0.5071
1	.8475	.8684	3.953
2	.8400	.9744	5.902
3	.8351	1.038	7.410
Case 26: $t_s=0.1$; $\frac{t_e}{t_s}=1$; $t_R=1$			
0	0.8406	0.4997	0.4997
1	.8610	.7798	3.276
2	.8651	.8488	4.773
3.2	.8678	.8928	6.127
Case 27: $t_s=0.1$; $\frac{t_e}{t_s}=0.8$; $t_R=1$			
0	0.8404	0.5012	0.5012
1	.8554	.7850	3.230
2	.8572	.8588	4.726
2.4	.8577	.8775	5.214
Case 28: $t_s=0.1$; $\frac{t_e}{t_s}=0.4$; $t_R=1$			
0	0.8393	0.5045	0.5045
1	.8433	.8003	3.158
2	.8399	.8883	4.677
3	.8373	.9402	5.853
Case 29: $t_s=0.1$; $\frac{t_e}{t_s}=0.2$; $t_R=1$			
0	0.8379	0.5067	0.5067
1	.8350	.8266	3.319
2.2	.8263	.9437	5.242
Case 30: $t_s=0.033$; $\frac{t_e}{t_s}=1$; $t_R=2.19$			
0	0.8552	0.5068	0.5068
.75	.8794	1.015	7.268

Case 31: ($\beta=0$)

Additional flat-plate solutions

t_e	t_R	$\bar{\tau}$	f''_w
0.01235	0.812	0.8315	0.5119
.01235	.618	.8243	.5065

TABLE IV.—TABLES OF SIMILAR SOLUTIONS FOR EQUILIBRIUM DISSOCIATED AIR, NONUNIT LEWIS NUMBER

(a) Heat-transfer cases

β	$\zeta'_w(F=F_1)$	$\zeta'_w(F=F^2)$	$\zeta'_w(F=F_3)$
Case 1: $t_s=1;\ \frac{t_e}{t_s}=1;\ t_R=2;\ \zeta_w=0.0304$			
0	0.2551	0.2605	0.2551
.5	.2735	.2789	.2734
1	.2829	.2884	.2828
Case 2: $t_s=1;\ \frac{t_e}{t_s}=1;\ t_R=1;\ \zeta_w=0.0152$			
0	0.2319	0.2445	0.2383
.5	.2486	.2614	.2551
1	.2572	.2701	.2638
Case 3: $t_s=1;\ \frac{t_e}{t_s}=1;\ t_R=1;\ \zeta_w=0.1$			
0	0.3150	0.3355	0.3254
.5	.3404	.3612	.3509
1	.3531	.3742	.3638
2	.3675	.3890	.3785
3	.3763	.3979	.3874
3.5	.3795	.4013	.3907
Case 4: $t_s=1;\ \frac{t_e}{t_s}=1;\ t_R=0.5;\ \zeta_w=0.05$			
0	0.2875	0.3329	0.2997
.5	.3104	.3564	.3227
1	.3219	.3684	.3342
2	.3349	.3822	.3474
3	.3427	.3905	.3553
3.5	.3457	.3936	.3583
Case 5: $t_s=0.333;\ \frac{t_e}{t_s}=1;\ t_R=3.333;\ \zeta_w=0.05066$			
0	0.2588	0.2588	0.2588
.5	.2939	.2939	.2939
1	.3097	.3097	.3097
Case 6: $t_s=0.333;\ \frac{t_e}{t_s}=1;\ t_R=3.333;\ \zeta_w=0.3333$			
0	0.2386	0.2386	0.2386
.5	.2838	.2838	.2838
1	.3027	.3027	.3027
Case 7: $t_s=0.333;\ \frac{t_e}{t_s}=1;\ t_R=0.667;\ \zeta_w=0.04$			
0	0.2598	0.2645	0.2594
.5	.2945	.2992	.2940
1	.3102	.3149	.3097
2	.3272	.3320	.3269
3	.3371	.3419	.3369
3.5	.3408	.3456	.3406

β	$\zeta'_w(F=F_1)$	$\zeta'_w(F=F_2)$	$\zeta'_w(F=F_3)$
Case 8: $t_s=0.333;\ \frac{t_e}{t_s}=1;\ t_R=0.333;\ \zeta_w=0.03333$			
0	0.2752	0.2880	0.2823
.5	.3119	.3246	.3189
1	.3286	.3413	.3355
2	.3467	.3595	.3536
3	.3572	.3702	.3642
3.5	.3612	.3742	.3681
Case 9: $t_s=0.1;\ \frac{t_e}{t_s}=1;\ t_R=6.58;\ \zeta_w=0.6579$			
0	0.09330	0.09330	0.09330
.5	.1545	.1545	.1545
1	.1730	.1730	.1730
Case 10: $t_s=0.1;\ \frac{t_e}{t_s}=1;\ t_R=1;\ \zeta_w=0.0152$			
0	0.2235	0.2238	0.2247
.5	.2802	.2805	.2814
1	.3017	.3020	.3028
Case 11: $t_s=0.1;\ \frac{t_e}{t_s}=1;\ t_R=0.333;\ \zeta_w=0.03333$			
0	0.2768	0.2816	0.2786
.5	.3451	.3500	.3467
1	.3713	.3762	.3728
2	.3979	.4029	.3996
3.2	.4152	.4178	.4170
Case 12: $t_s=0.033;\ \frac{t_e}{t_s}=1;\ t_R=2.19;\ \zeta_w=0.2193$			
0	0.2703	0.2703	0.2703
.5	.4602	.4602	.4604
1	.5121	.5121	.5123
Case 13: $t_s=0.033;\ \frac{t_e}{t_s}=1;\ t_R=0.333;\ \zeta_w=0.007066$			
0	0.1925	0.1947	0.1928
.5	.2715	.2737	.2722
1	.2971	.2994	.2984

Case 14:
Additional flat-plate solutions ($\beta=0$)

t_e	t_R	ζ_w	$\zeta'_w(F=F_1)$	$\zeta'_w(F=F_2)$	$\zeta'_w(F=F_3)$
0.01235	0.812	0.0812	0.2965	0.2977	0.2980
.01235	.618	.00938	.2121	.2130	.2126

TABLE IV.—TABLES OF SIMILAR SOLUTIONS FOR EQUILIBRIUM DISSOCIATED AIR, NONUNIT LEWIS NUMBER—Concluded

(b) Insulated wall cases

β	$\bar{r}(F=F_1)$	$\bar{r}(F=F_2)$	$\bar{r}(F=F_3)$
Case 1: $t_s=0.333$; $\frac{t_s}{t_s}=1$; $t_R=3.333$			
0	0.8137	0.7978	0.8022
1	.8312	.8158	.8220
Case 2: $t_s=0.333$; $\frac{t_s}{t_s}=1$; $t_R=0.667$			
0	0.8762	0.7346	0.8228
1	.8920	.7586	.8452
Case 3: $t_s=0.1$; $\frac{t_s}{t_s}=1$; $t_R=6.58$			
0	0.8502	0.8502	0.8502
1	.8764	.8764	.8764
Case 4: $t_s=0.1$; $\frac{t_s}{t_s}=1$; $t_R=1$			
0	0.8195	0.7660	0.7776
1	.8453	.7937	.8056
Case 5: $t_s=0.033$; $\frac{t_s}{t_s}=1$; $t_R=2.19$			
0	0.8045	0.7827	0.8142
1	.8373	.8169	.8499
Case 6: Additional flat-plate solutions ($\beta=0$)			

t_s	t_R	$\bar{r}(F=F_1)$	$\bar{r}(F=F_2)$	$\bar{r}(F=F_3)$
0.01235	0.812	0.8234	0.7545	0.7786
.01235	.618	.8489	.7390	.8022

U.S. GOVERNMENT PRINTING OFFICE: 1963